

8. SITE 541: TOE OF THE BARBADOS RIDGE COMPLEX¹

Shipboard Scientific Party²

Date occupied: 13 February 1981

Date departed: 21 February 1981

Time on hole: 7 days, 16 hr.

Position: 15°31.2'N, 58°43.7'W

Water depth (sea level; corrected m, echo-sounding): 4940

Water depth (rig floor; corrected m, echo-sounding): 4950

Bottom felt (m, drill pipe): 4961

Penetration (m): 459

Number of cores: 50

Total length of core section (m): 459

Total core recovered (m): 400.75

Core recovery (%): 87.3

Oldest sediment cored:

Depth sub-bottom (m): 459

Nature: Radiolarian mudstone

Age: early Miocene

Measured velocity (km/s): 1.70

Basement: Not reached

Principal results: Drilling at Site 541 penetrated 459 m of Quaternary to lower Miocene hemipelagic–pelagic sediment. The cored section ranges from marly calcareous ooze to barren mud to radiolarian mud with a concentration of ash beds in the Quaternary and lower Pliocene. Quaternary to Pliocene calcareous muds accumulated at or just below the lysocline, whereas upper, middle, and lower Miocene rocks were deposited principally below the CCD (calcite compensation depth). The absence of terrigenous turbidites suggests deposition of the entire section on a physiographic high.

A reverse fault and associated scaly foliation and stratal disruption occur at 276 m coincident with stratigraphic inversion of upper Miocene mud over upper Pliocene nannofossil mudstone. Smaller-scale repetitions of a sequence of nannofossil zones and ash beds suggest reverse faults at 75 to 80, 172, and 263 m. In the basal 100 m of the hole, cores show progressive development of fracturing, intense scaly foliation, and stratal disruption; these cores locally resemble fault gouge. This conspicuous zone of de-

formation may overlie a décollement separating offscraped and underthrust sediment packages.

BACKGROUND AND OBJECTIVES

The fundamental goal of Site 541, and indeed of Leg 78A, was complete penetration of the toe of the seismically defined deformation front of the Barbados Ridge (Figs. 1 and 2). Great water depth, thick sediments, and unstable hole conditions had prevented penetration into the seaward margins of Pacific subduction zones. Drilling through an active deformation zone provided an unparalleled opportunity to define stratigraphic, structural, and diagenetic sequences that can guide interpretations of similar ancient terranes.

The location of Site 541, near the intersection of seismic profiles A1D and A1E on Figure 2, minimized both the total and sub-bottom depths to basement and increased changes of a complete penetration (Fig. 3; Ngokwey et al., this volume). The shallow depth to basement at Site 541 is due to the elevated Tiburon Rise entering the subduction zone just to the east. Specific objectives of Site 541 were:

1) to determine the origin of the discontinuously reflective, possibly allochthonous unit; to establish whether it is scraped off the ocean crust or slumped from some location upslope;

2) to define the structural geology and physical properties of the acoustically chaotic unit and investigate whether folding, faulting, or stratigraphic changes account for its westward thickening;

3) to date and establish the structural nature of the prominent reflector lying below the discontinuously reflective unit;

4) to define the lithology and structural nature of the layered sequence;

5) to date the ocean crust underthrusting the deformation front; and

6) to emplace a downhole seismometer and tiltmeter in the ocean crust.

OPERATIONS

San Juan to Site 541

After the vessel was safely clear of San Juan harbor traffic, a 20-min. stop was made to test the ship's thrusters and dynamic positioning system and to "soak" positioning beacons to be used on Leg 78A.

The 500-mi. transit from Puerto Rico to Site 541 was uneventful, except that headwinds of up to 31 knots the first day were followed by swells of up to 9 ft., which persisted into the second day of site occupancy. This ad-

¹ Biju-Duval, B., Moore, J. C., et al., *Init. Repts DSDP, 78A*: Washington (U.S. Govt. Printing Office).

² Bernard Biju-Duval (Co-Chief Scientist), Institut Français du Pétrole, 92505 Rueil Malmaison, France (present address: Centre National pour l'Exploitation des Océans, 66 Avenue d'Iéna, 75116 Paris, France); J. Casey Moore (Co-Chief Scientist), Earth Sciences and Marine Studies, University of California at Santa Cruz, Santa Cruz, California; James A. Bergen, Department of Geology, Florida State University, Tallahassee, Florida; Grant Blackinton, Hawaii Institute of Geophysics, University of Hawaii at Manoa, Honolulu, Hawaii; George E. Claypool, Branch of Oil and Gas Resources, U.S. Geological Survey, Denver Federal Station, Denver, Colorado; Glenn Foss, Deep Sea Drilling Project, Scripps Institution of Oceanography, La Jolla, California; Rodolfo T. Guerra, Exploration Services Center, Mobil Exploration and Producing Services, Dallas, Texas; Christoph H. J. Hemleben, Institut und Museum für Geologie und Paläontologie, Universität Tübingen, D-7400 Tübingen 10, Federal Republic of Germany; Michael S. Marlow, U.S. Geological Survey, Menlo Park, California; James H. Natland, Deep Sea Drilling Project, Scripps Institution of Oceanography, La Jolla, California; Carol J. Pudsey, Department of Geology, University of Leicester, Leicester, United Kingdom; G. W. Renz, Deep Sea Drilling Project, Scripps Institution of Oceanography, La Jolla, California (present address: 5260 Angeles Crest, La Canada, California); Marc Tardy, Département de Sciences de la Terre, Université de Savoie, BP 1104, Chambéry, France; Douglas Wilson, Hawaii Institute of Geophysics, University of Hawaii at Manoa, Honolulu, Hawaii (present address: Department of Geophysics, Stanford University, Stanford, California); Audrey Wright, Earth Sciences and Marine Studies, University of California at Santa Cruz, Santa Cruz, California (present address: Deep Sea Drilling Project, Scripps Institution of Oceanography, La Jolla, California).

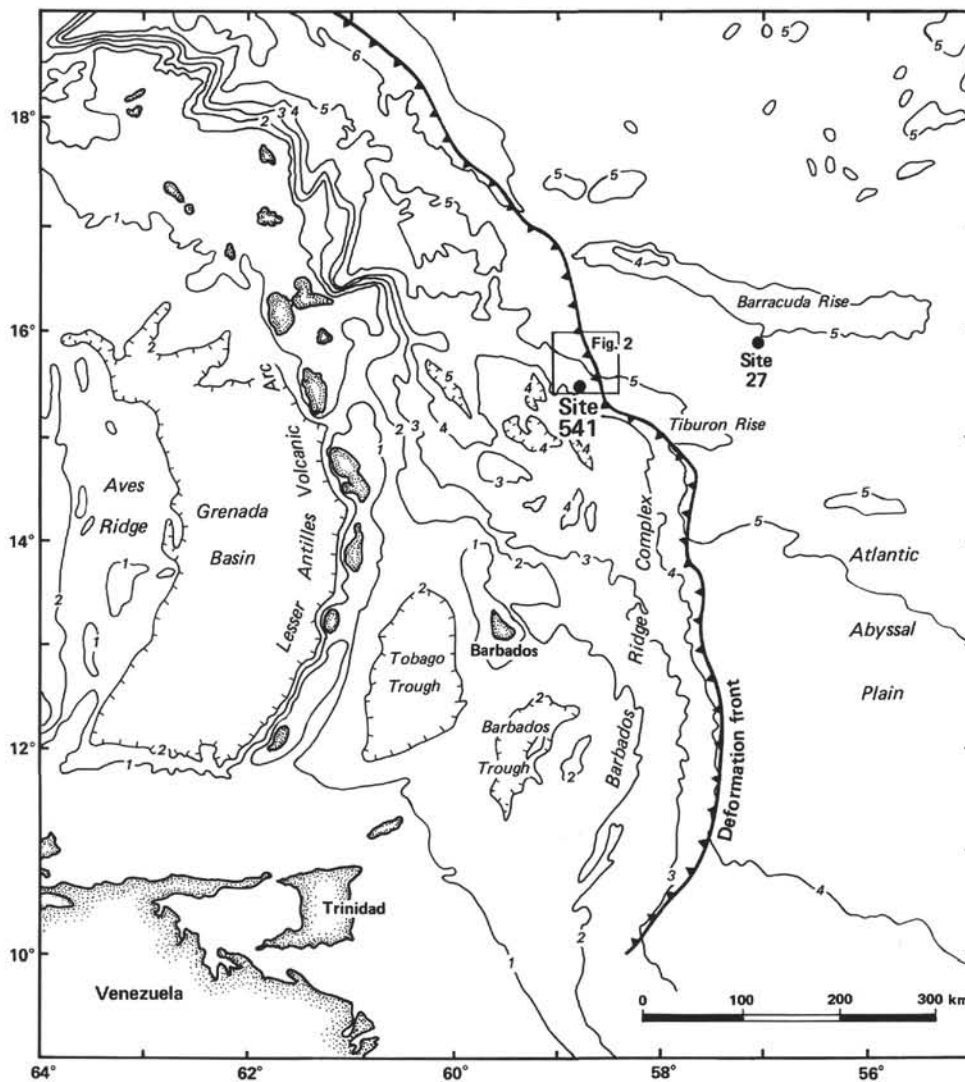


Figure 1. Regional location map. (Note position of deformation front defining eastward boundary of Barbados Ridge and Tiburon Rise underthrusting deformation front near Site 541. Leg 78A drilling area enclosed in box. Contour intervals are in kilometers.)

verse weather combination held the *Challenger's* average speed to 7.5 knots.

Following a 1.75-hr. presite survey, a positioning beacon was launched at 1404 hr. Friday, 13 February, about 135 mi. east-northeast of the Island of Martinique.

Site 541—Toe of the Barbados Ridge

Initial positioning of the vessel was complicated by divergent wind, swell, and current directions and required 2 hr. before the pipe trip could begin.

The pipe trip was lengthened by 4.5 hr. as 41 suspect joints of drill pipe (identified by the magnetic inspection in San Juan) were laid out. An inner core barrel was pumped down the pipe as the final preparation for spudding. No pressure indication of the barrel landing at the bit was noted after an appropriate interval of pumping. This indicated that the inner barrel had been stopped by a partial obstruction in the pipe or that it had been pumped out through open-ended pipe. An attempt was made to "find" the core barrel with the sand line and

overshot, but when the length of the sand line exceeded that of the drill string, we concluded that the hydraulic bit release had operated prematurely during the trip. The sand line was recovered undamaged.

The drill string was then tripped; when the drill collars had been recovered, we discovered that the outer core barrel had come unscrewed from the top sub and had been lost. A new outer core barrel assembly was made up and the drill pipe was again run to the seafloor. Hole 541 was finally spudded at 1525 hr., 15 February. Coring data for the hole are presented in Table 1.

Coring then proceeded smoothly and with excellent core recovery through about 215 m of nannofossil-rich clay, followed by about 60 m of clay. At this point a reverse fault was penetrated and the younger nannofossil clay sequence was reentered. No drilling problems were experienced until a second major deformation zone was reached at about 430 m sub-bottom. Coincident with a very low-recovery core (Core 46), high pump pressure and torquing and sticking of the drill string occurred.

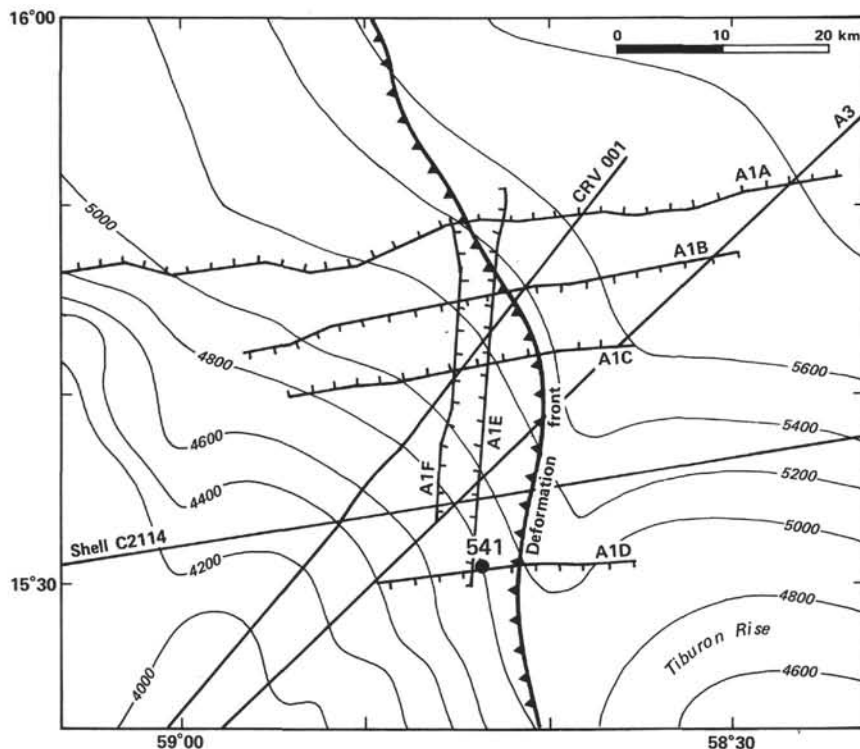


Figure 2. Detailed site location map (box, Fig. 1). (Note position of deformation front and location of seismic reflection lines used for site survey. Bathymetry is in meters. Lines A1A to A1D are from IFP/CNEXO survey [from Ngokwey et al., this volume].)

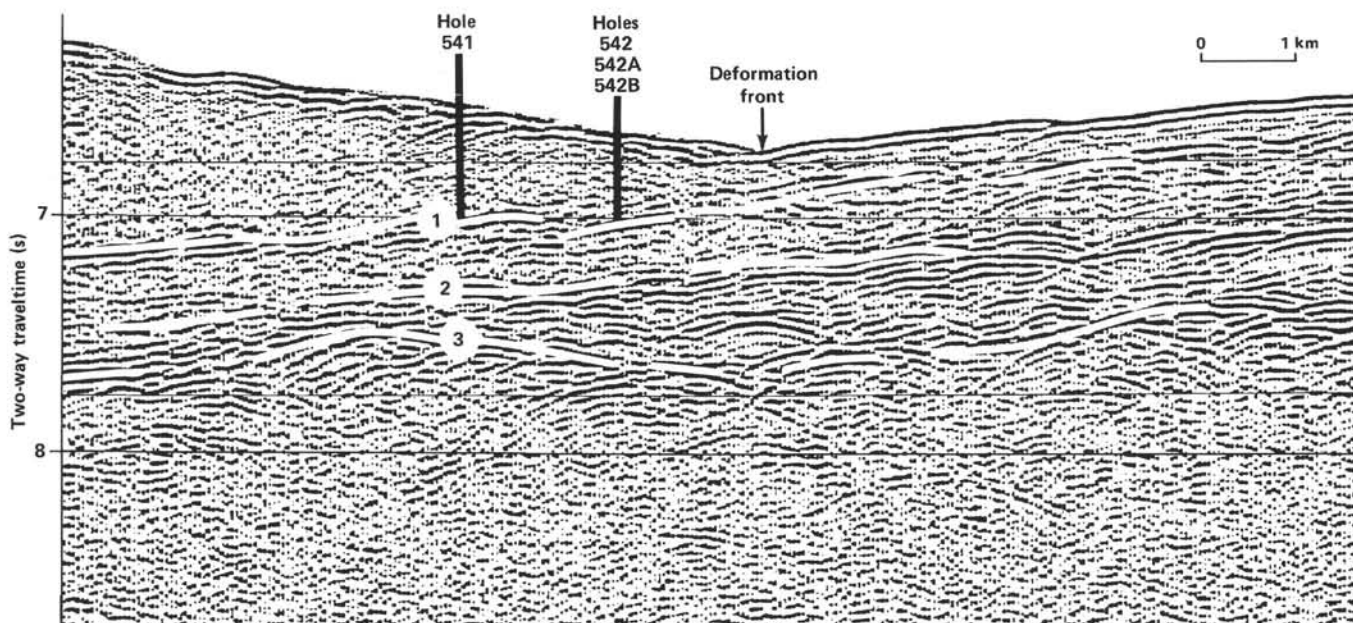


Figure 3. Seismic reflection line A1D (from Ngokwey et al., this volume.) Reflector 1 separates discontinuously reflective and acoustically layered seismic units. Reflector 2 represents a prominent horizon within the acoustically layered unit. Reflector 3 is top of oceanic crust.

The hole was flushed with mud and three additional full cores were taken. Up to 18 m of fill were encountered following the cores, despite repeated flushes, and sticking tendencies persisted on connections. Rotation could not be regained following the connection for Core 50, and it was necessary to terminate coring operations. A

short core was cut by lowering the power sub to the limit of its travel on the guide rails. The core was recovered and a hydraulic bit release go-devil was pumped down to actuate the release mechanism. About 20 min. of manipulating the drill string and pump pressure were required before the bit and associated components were

Table 1. Coring summary, Site 541.

Core no.	Date (Feb., 1981)	Time	Depth from drill floor (m)		Depth below seafloor (m)		Length cored (m)	Length recovered (m)	Amount recovered (%)
			top	bottom	top	bottom			
1	15	1635	4961-4962		0-1		1	0.82	80
2	15	1810	4962-4971.5		1-10.5		9.5	8.44	88
3	15	2005	4971.5-4981		10.5-20.0		9.5	5.66	60
4	15	2155	4981-4990.5		20-29.5		9.5	9.81	103
5	15	2350	4990.5-5000		29.5-39.0		9.5	4.04	42
6	16	0125	5000-5009.5		39-48.5		9.5	1.12	12
7	16	0550	5009.5-5019.0		48.5-58.0		9.5	9.83	103
8	16	0736	5019.0-5028.5		58.0-67.5		9.5	9.80	103
9	16	0912	5028.5-5038.0		67.5-77.0		9.5	9.82	103
10	16	1050	5038.0-5047.5		77.0-86.5		9.5	9.77	103
11	16	1216	5047.5-5057.0		86.5-96.0		9.5	6.15	65
12	16	1540	5057.0-5066.5		96.0-105.5		9.5	9.92	104
13	16	1732	5066.5-5076.0		105.5-115.0		9.5	9.88	104
14	16	1905	5076.0-5085.5		115.0-124.5		9.5	9.90	104
15	16	2040	5085.5-5095		124.5-134.0		9.5	7.85	83
16	16	2230	5095.0-5104.5		134.0-143.5		9.5	8.97	94
17	17	0243	5104.5-5114.0		143.5-153.0		9.5	9.4	98
18	17	0429	5114.0-5123.5		153.0-162.5		9.5	8.31	87
19	17	0617	5123.5-5133.0		162.5-172.0		9.5	9.52	100
20	17	0756	5133.0-5142.5		172.0-181.5		9.5	8.53	89
21	17	0945	5142.5-5152.0		181.5-191.0		9.5	4.44	46
22	17	1125	5152.0-5161.5		191.0-200.5		9.5	9.40	98
23	17	1302	5161.5-5171.0		200.5-210.0		9.5	9.40	98
24	17	1436	5171.0-5180.5		210.0-219.5		9.5*	8.64	90
25	17	1619	5180.5-5190.0		219.5-229.0		9.5	9.84	104
26	17	1808	5190.0-5199.5		229.0-238.5		9.5	7.88	83
27	17	1958	5199.5-5209.0		238.5-248.0		9.5	9.89	104
28	17	2150	5209.0-5218.5		248.0-257.5		9.5	9.92	104
29	17	2345	5218.5-5228.0		257.5-267.0		9.5	9.04	95
30	18	0133	5228.0-5237.5		267.0-276.5		9.5	9.89	104
31	18	0312	5237.5-5247.0		276.5-286.0		9.5	9.94	105
32	18	0503	5247.0-5256.5		286.0-295.5		9.5	9.27	98
33	18	0640	5256.5-5266.0		295.5-305.0		9.5	10.14	106
34	18	0830	5266.0-5275.5		305.0-314.5		9.5	9.10	96
35	18	1014	5275.5-5285.0		314.5-324.0		9.5	10.03	106
36	18	1155	5285.0-5294.5		324.0-333.5		9.5	2.32	24
37	18	1418	5294.5-5304.0		333.5-343.0		9.5	9.80	103
38	18	1555	5304.0-5313.5		343.0-352.5		9.5	9.53	100
39	18	1759	5313.5-5323.0		352.5-362.0		9.5	4.46	47
40	18	1943	5323.0-5332.5		362.0-371.5		9.5	9.83	103
41	18	2137	5332.5-5342.0		371.5-381.0		9.5	9.01	95
42	18	2320	5342.0-5351.5		381.0-390.5		9.5	9.72	102
43	19	0115	5351.5-5361.0		390.5-400.0		9.5	8.98	95
44	19	0250	5361.0-5370.5		400.0-409.5		9.5	9.83	103
45	19	0430	5370.5-5380.0		409.5-419.0		9.5	9.98	104
46	19	0740	5380.0-5389.5		419.0-428.5		9.5	0.69	7
47	18	1225	5389.5-5399.0		428.5-438.0		9.5	3.28	34
48	19	1531	5399.0-5408.5		438.0-447.5		9.5	7.89	83
49	19	1818	5408.5-5418.0		447.5-457.0		9.5	7.28	76
50	19	2320	5418.0-5428.0		457.0-467.0		4.0	3.79	39
Total							459.0	400.75	87.3

released. The pipe was then pulled until only the BHA (bottom-hole assembly) remained in the hole, and preparations were made for logging.

On the first logging attempt, temperature was being logged downward when the logging sonde was stopped by a soft clay "bridge" only 10 m beyond the end of the pipe. When attempts to work the tool past the obstruction failed, the tool was recovered and a "short trip" was made. This trip consisted of running the open-ended pipe down to the top of the hole fill at about 415 m sub-bottom and then pulling back to one stand (28.5 m) below its earlier position to keep the trouble spot behind pipe. A second logging attempt was aborted due to an electrical problem in the tool that developed about one-third of the way down the pipe. On the third attempt, the sonde logged temperature to about 18 m beyond the pipe before it again stopped in the soft clay. After numerous attempts to work the tool past the bridge, a static temperature check was made and log function was switched to the density-caliper-gamma ray mode in an attempt to log the approximately 46 m of open hole that could be exposed by raising the pipe in the derrick. Un-

fortunately, the tool had been damaged by the attempts to penetrate the bridge, and no log could be recorded.

Operations in Hole 541 were terminated at this point and the drill string was recovered, with all pipe on deck at 0600 hr., 21 February.

SEDIMENT LITHOLOGY

Lithostratigraphy

Site 541 is located in 4950 m water depth, about 3 km west of the toe of the accretionary prism. The hole was continuously cored to a sub-bottom depth of 459 m. Recovery of the cored material was excellent (87.3%, see Table 1) and provides a good record of the lithostratigraphy of the Lesser Antilles forearc accretionary prism (Fig. 4).

Two major tectonic units are present at Site 541, separated by a reverse fault at a sub-bottom depth of 276 m. Tectonic Unit A is 276 m thick and consists of Recent to upper Miocene sediments. Tectonic Unit B is 184 m thick and consists of middle Pliocene to lower Miocene sediments. A summary of the seven lithostratigraphic units cored at Site 541 is shown in Table 2. Carbonate percentages measured downhole at Site 541 were determined with the shipboard carbonate bomb (Fig. 4).

The sediments of Tectonic Unit A can be divided into four distinct, conformable lithologic units based on macroscopic core descriptions, smear slide analyses, and carbonate bomb data from the cored interval.

Lithologic Unit 1 is a relatively uniform, 65-m-thick, lower upper Pleistocene to lower Pleistocene nannofossil mud with common ash layers and disseminated ash particles that has been highly deformed by drilling. The upper 40 m of the unit is olive gray (5Y 5/3) in color, gradually changing to grayish brown (10YR 5/2) in the lower 25 m of the unit. The ash beds are predominantly dark grayish brown (10YR 3/2) to dark gray (10YR 6/1) in color.

Lithologic Unit 2 is a 70-m-thick, lower Pleistocene to upper Pliocene, bioturbated marly nannofossil ooze or marly foraminiferal ooze that has fewer discrete ash layers and a higher calcium carbonate content than is characteristic of Unit 1. It is lighter in color than Unit 1, ranging from light olive gray (5Y 6/2) to olive gray (5Y 5/2). There are only two major ash deposits in Unit 2, both closely spaced in Core 12. Although this unit has

Table 2. Lithologic units, Site 541.

Unit	Lithology	Core range (core-section, cm level)	Depth below seafloor (m)
1	Nannofossil mud with common ash layers	1 to 8	0-65
2	Marly nannofossil ooze and marly foraminifer ooze with rare ash layers	9 to 15	65-135
3	Nannofossil mud with ash layers	16 to 24-3, 50	135-215
4	Mud	24-3, 50 to 30-6	215-276
5	Nannofossil mud with ash layers	30-6 to 37	276-340
6	Mudstone	37 to 47-2, 50	340-430
7	Radiolarian mudstone	47-2, 50 to 50	430-459

been moderately to very deformed by drilling, faint bedding planes indicate that layering is horizontal. Coarse-grained, foraminifer-bearing gravity flow deposits 2 to 4 cm thick characterize the lower portions of this unit (Cores 13–15).

Lithologic Unit 3 is an 80-m-thick, upper Pliocene to upper Miocene nannofossil mud that contains common ash layers and disseminated ash particles. It has been moderately deformed by drilling. The mud ranges from gray (5Y 6/1) to olive gray (5Y 5/2) in color and contains faint, dispersed ash mottles in bioturbated intervals. The clay content of the mud increases systematically downsection, as expressed by the generally darker shades of gray characteristic of the lower cores of Unit 3. The ash layers range from dark olive gray (5Y 3/2) to dark gray (5Y 4/1) to black in color. Bases of these ash beds dip as much as 40° from horizontal.

Lithologic Unit 4 is 60 m thick and is differentiated from the overlying sediment by a distinctly lower percentage of calcareous components. It is an upper Miocene, gray (5Y 5/1) to greenish gray (5GY 5/1) mud with medium light gray burrows and mottles filled with redistributed altered ash. Drilling laminations are found throughout the section. The lower 25 m of Unit 4 contain several layers of olive gray (5Y 5/2) marly nannofossil ooze, perhaps due to fluctuating levels of the CCD associated with sea-level changes in the late Miocene. The mud is internally deformed and is characterized by variably developed slickensided fracture surfaces throughout the section. This internal deformation is associated with movement along the reverse fault that separates Unit 4 from the underlying Unit 5 of Tectonic Unit B.

The sediments of Tectonic Unit B can be divided into three distinct lithologic units based on macroscopic core descriptions, smear-slide analyses, and carbonate-bomb data from the cored interval. The boundaries between these units are somewhat arbitrarily defined.

Lithologic Unit 5 is a 65-m-thick, upper Pliocene to upper Miocene, bioturbated nannofossil mud with thin ash layers and dispersed ash particles. A major fault at 276 m sub-bottom defines the top of this unit. The nannofossil mud ranges from light gray (5Y 6/1) to gray (5Y 5/1) to olive gray (5Y 5/2) in the top portion of the unit, gradually changing to a darker grayish brown (10YR 5/2) downsection. The color change results from an increased clay content toward the base of the unit. The ash layers range from dark gray (5Y 4/1) to black in color. Bedding dips up to 40° from horizontal. The age and the lithology of Unit 5 is comparable with those of Unit 3 of Tectonic Unit A.

Lithologic Unit 6 is a 90-m-thick, brecciated, intensely fractured, upper Miocene to middle(?) Miocene mudstone with infrequent ash layers and dispersed ash particles. It is differentiated from Unit 5 by a lower percentage of calcareous components. The mudstone ranges from light gray (2.5Y 5-6/2) to olive gray (5Y 5/2) in color and consists of internally fractured drilling “biscuits” (coherent lumps of mudstone) in a matrix of smaller, extensively sheared fragments of similar lithology. These biscuits are commonly bioturbated, with larg-

er biscuits having burrows filled with dark gray (5GY 4/1) mudstone. The lower 50 m of this unit contain biscuits of considerable color variation, indicating a mixing of different lithologies. This heterogeneity could be either an artifact of caving between cores or a fault zone fabric. There are several thin layers of nannofossil and foraminifer chalk distributed throughout this unit, suggesting that the level of the CCD fluctuated during its deposition. The age and the lithology of Unit 6 are comparable with those of Unit 4.

Lithologic Unit 7 is a 30-m-thick, bioturbated, brecciated and highly sheared, light yellowish brown (10YR 6/4), middle Miocene(?) to lower Miocene radiolarian mudstone. The upper part of this unit (Core 47, Section 2 through Core 50, Section 1) also contains lumps and highly sheared zones of light olive brown (2.5Y 5/4) and greenish gray (5Y 5/1) bioturbated mudstones. These color variations indicate that several rock types have been mixed in this section of the hole. This could be the fabric of a fault zone, but hole conditions indicate a lot of caving between cores, so some of the observed mixing and heterogeneity of rock types may be artificial.

The vast majority of the sediments cored at Site 541 show no evidence of having been deposited by current action, but instead seem to have been accumulated by pelagic-hemipelagic settling. The ash beds do not appear to have been redeposited as turbidites, so they probably settled to the seafloor following volcanic eruptions on the Lesser Antilles Island arc. The thin, foraminifer-rich beds at the base of Unit 2 lack distinct grading and lamination, but are probably gravity flow deposits. An alternative explanation is that the level of the CCD fluctuated as oceanographic conditions changed, and deposition of foraminifer-rich beds occurred at times when the local CCD was depressed. This alternative is less likely, however, as such fluctuations are gradual and would not likely produce thin, well-defined foraminifer-rich layers.

The environment of deposition of sediments cored at Site 541 was in quiet, deep water adjacent to the Lesser Antilles island arc. Although it is true that terrigenous turbidites were not found in the cored section, this absence may be due to location of the site on a topographic high rather than to great distance from any terrigenous source. Common ash beds and disseminated ash particles in the cores indicate a substantial input of volcanic material from the Lesser Antilles island arc.

Comparison of the ages, thicknesses, and lithologies of Tectonic Units A and B and the distribution of ash layers in Lithologic Units 3 and 5 (see the section on Volcanic Ash, this chapter) suggest that Lithologic Units 3 and 4 above the major fault are lithologically correlative with Lithologic Units 5 and 6 below the fault. In other words, Lithologic Units 5 and 6 represent a repeated section of Lithologic Units 3 and 4. Units 5 and 6 were emplaced beneath Units 3 and 4 by movement along the fault that separates Tectonic Units A and B.

It is uncertain whether Lithologic Unit 7 should be considered a part of Tectonic Unit B or designated as the top of another, deeper Tectonic Unit C, inasmuch as evidence for shear in Unit 7 is abundant and could indi-

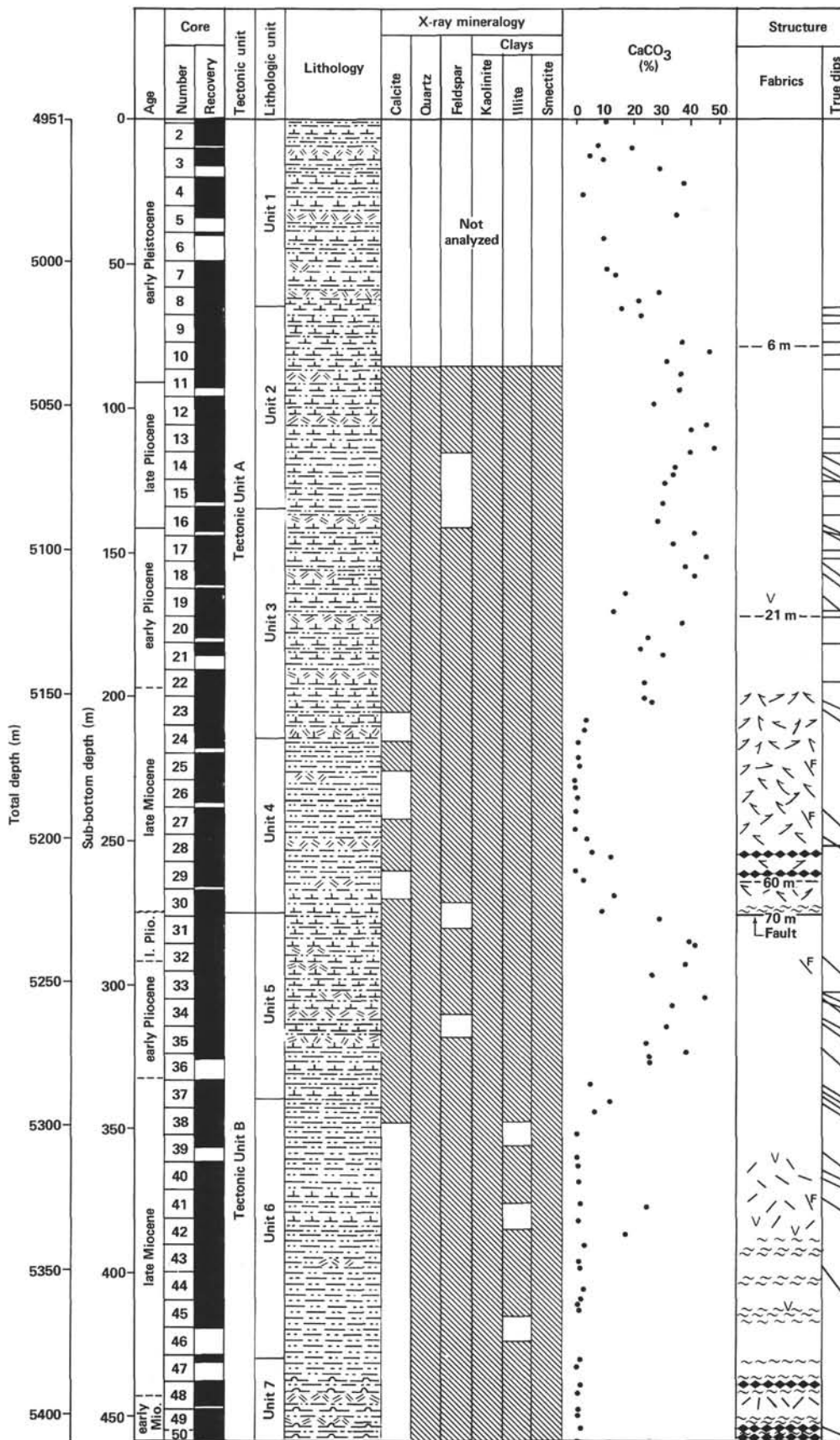


Figure 4. Summary lithology, sediment composition, structure, physical properties, and seismic stratigraphy, Site 541. (In X-Ray Mineralogy columns, blackened areas simply indicate presence. In Structure-Fabrics column, displacements are shown in meters.)

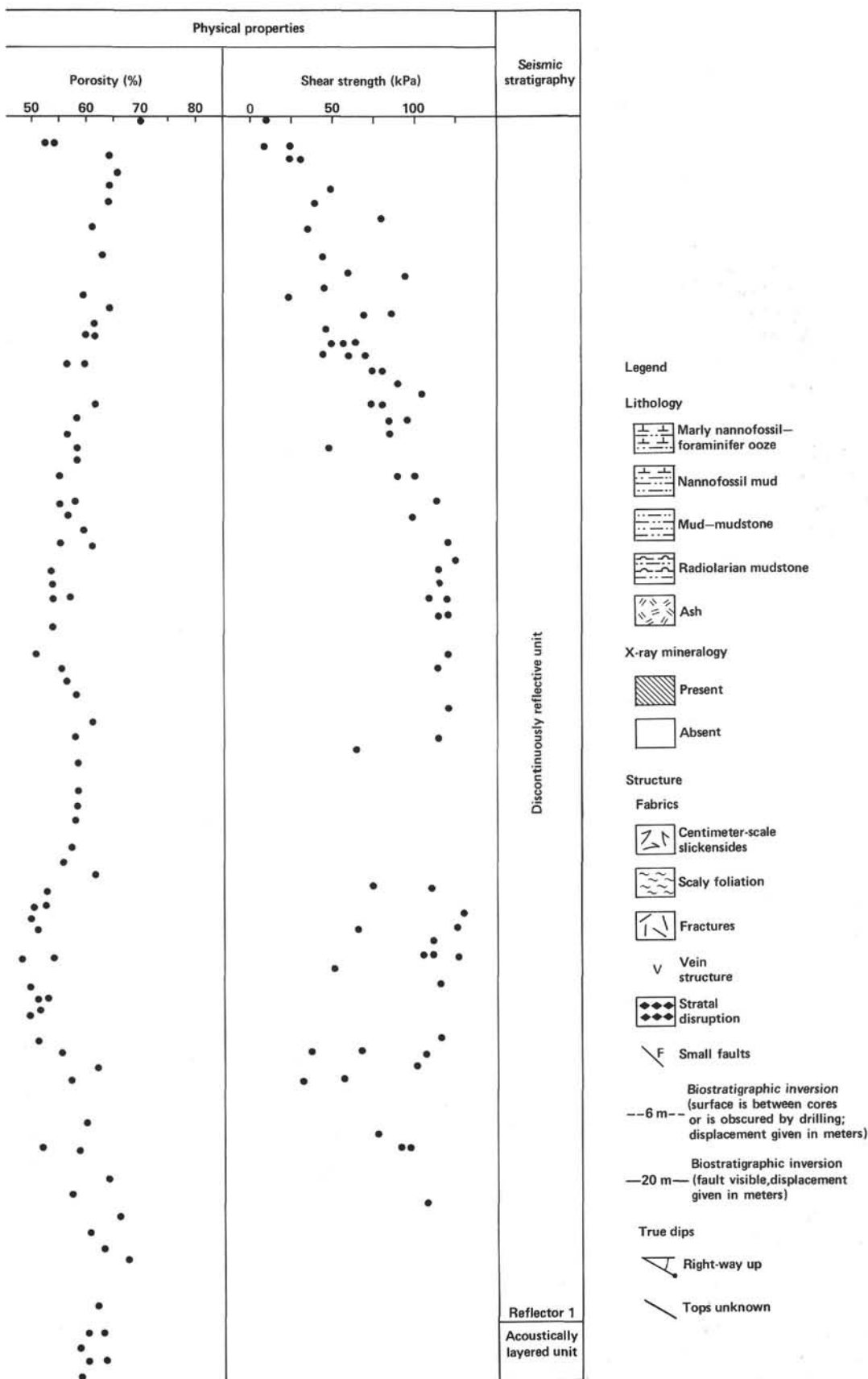


Figure 4. (Continued).

cate another fault. Geophysical profiles indicate that drilling at Site 541 may have just penetrated Reflector 1, in which case Unit 7 may represent the topmost lithology of the sedimentary section below that reflector.

Bioturbation

Probably the entire section is bioturbated, but burrowing is much more pronounced in the lithified muds of the lower tectonic unit. Bioturbation was first noted in Core 8, but no burrows could be identified due to intense drilling disturbance. The first burrowed ash bed occurs in Core 10, Section 3. Gray ash beds generally have bioturbated contacts, with gray ash carried down into olive gray mud below, and olive gray mud from above carried down into the ash bed. These occurrences provide way-up evidence. Burrow mottling occurs from Cores 10 to 18.

The first recognizable *Chondrites* appears in Core 19 and is accompanied by larger (up to 5-mm diameter) cylindrical burrows mostly oblique to bedding. Throughout the section, *Chondrites* burrows are 1 to 2 mm in diameter. Core 21 contains *Chondrites*, *Planolites*, rarer *Cylindrichnus*, and a possible *Zoophycus*. Burrow mottling was noted in Cores 22 to 35, but few ichnogenera were identified.

Core 36 was the first to be sawed in half rather than cut, and the sawed surfaces expose burrows extremely well. *Planolites* is abundant, and *Cylindrichnus*, *Chondrites*, and composite burrows also occur. A few vertical burrows resemble *Teichichnus* in shape and size but lack a meniscus fill. Cores 37 and 38 are mottled; 39 is too soupy to see burrows. Cores 40 to 45 have a well-preserved burrow assemblage as follows:

<i>Planolites</i>	— abundant
<i>Chondrites</i>	— abundant
<i>Zoophycus</i>	— common
<i>Planolites/Chondrites</i> (composite large)	— fairly common
<i>Cylindrichnus</i>	— rare

in addition to abundant nondescript near-cylindrical burrows.

The yellow brown mudstone in Core 47 contains only a few indistinct *Chondrites* burrows.

All these burrows have been previously described from many DSDP cores. They are made by deposit feeders that thoroughly rework the sediment and destroy original bedding. However, where traces of bedding remain in cores (e.g., ash beds) and also in outcrops, many burrows tend to be either flattened parallel to bedding (e.g., *Planolites*) or to occur in bedding-parallel rows (*Chondrites* and *Planolites*). This fact is important for structural measurements.

Zoophycus burrows extend across cores at a low angle to bedding (see Ekdale, 1974). It was noted at this site that the meniscus fill of *Zoophycus* is not always symmetrical about the center but tends to be offset with a long limb and a short limb (Fig. 5). The long limb is downsection. In heavily burrowed, tectonically disturbed sequences this could be the only method to detect the way up of the strata.

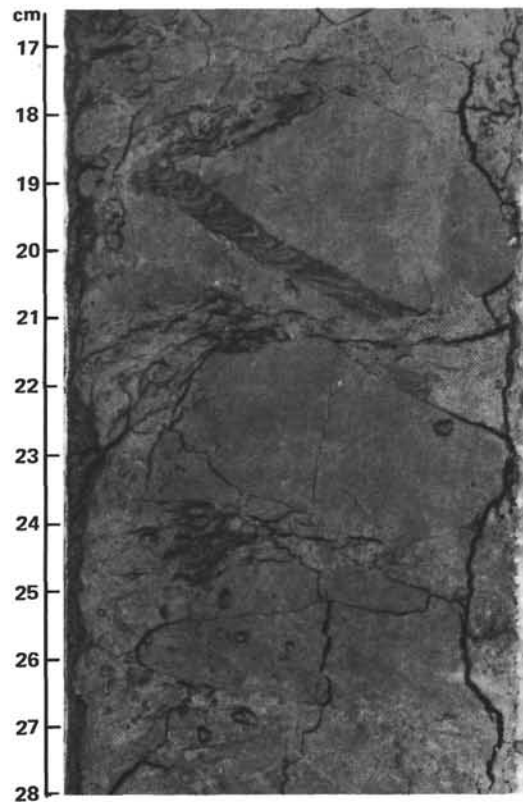


Figure 5. *Zoophycus* burrow with asymmetric meniscus fill (Sample 541-40-5, 17–28 cm). (The larger limb of the asymmetric fill is downsection.)

The intense bioturbation at this site, particularly in Cores 40 to 45, indicates a slow sedimentation rate allowing time for complete reworking. All the ichnogenera occur in a wide depth range, so the assemblage gives no definite indication of water depth.

X-Ray Mineralogy

Sixty-five samples from Cores 11 to 50 were analyzed using the shipboard X-ray diffractometer. Samples were prepared on glass slides in the same way as smear slides, then dried on a desiccating oven for at least one half hour. Each sample (one per core, plus some distinctive layers such as ashes) was X-rayed twice (oriented dry sample from $2\theta = 3^\circ$ to 35° , and glycolated, from $2\theta = 3^\circ$ to 15°). Minerals were identified by their characteristic peaks on the diffractogram (Carroll, 1970, table 12).

Minerals identified include quartz, alkali feldspar and plagioclase, calcite, and the clay minerals kaolinite, illite, and smectite. The shipboard diffractometer gives a pseudo-peak at $2\theta = 7\frac{1}{2}^\circ$, with a blank glass slide as the sample. Results are summarized in Figure 4.

Quartz is present in all samples and shows no systematic increase or decrease down the hole. One or both feldspars are present, in most samples: their proportions appear to vary widely and unsystematically. There is very little feldspar from 115 to 200 and 270 to 320 m sub-bottom (except for an ash layer at 180 m). Calcite, more accurately analyzed by the carbonate bomb meth-

od, is present from 0 to 205 and 270 to 345 m sub-bottom. Of the clays, kaolinite is present in all samples. Illite is present down to 340 m, where it decreases rather sharply (much lower peak height): this decrease corresponds to a downward increase in smectite peak height and sharpness. Of the distinctive lithologies, all the gray and black ashes have a high feldspar content and the feldspar peaks are very sharp. The bluish and greenish muds associated with the ashes are rather variable, some being feldspar-rich and others calcareous. There is little difference between gray brown and olive gray muds except that the latter may contain slightly less kaolinite: colors may result from chemical rather than mineralogical composition.

The smectite-rich interval below 380 m corresponds to the zone of pervasively sheared, scaly clays.

Volcanic Ash

The eastern slope of the Barbados Ridge is in an unusually favorable position for the preservation of ash beds derived by explosive volcanism from the Lesser Antilles arc. The sediments are almost entirely hemipelagic and lack obvious turbidites (although some redeposition of foraminifers has occurred—see the section on Paleoenvironment, this chapter); hence redeposition of ash has not occurred. Therefore, ash from individual eruptions, particularly the major eruptions, is well preserved, with bioturbation being the only disturbing sedimentological factor.

In Hole 541, recognition of volcanic ash in the upper few cores was complicated by intense core deformation during drilling. Not even the distinctive Roseau ash (e.g., Sparks et al., 1980) is recognizable in the upper few meters of Core 2, where it should occur. Throughout most of the cores below the intensely disturbed upper few meters, major ash falls are readily apparent, although minor fine ash falls have been largely redistributed by burrowing organisms. In or near tectonic shear zones (Cores 25–30 and 40–50), additional disturbance of ash beds has undoubtedly resulted from faulting. All of these factors complicate interpretation of rates, frequency, and volume of explosive Lesser Antilles volcanism in the affected intervals. The least disturbed portions of the cores are from about 60 to 200 m below the seafloor (Cores 8–23) and 290 to 330 m below the seafloor (Cores 32–36). Cores 8–23 represent a nearly stratigraphically uninterrupted sequence of marly calcareous oozes and clays ranging in age from Miocene to late Pliocene.

Ash beds in cores from Hole 541 are as much as 7 cm thick, but are clearly recognizable as ash beds even when only 1 to 2 cm thick. The thicker beds typically have sharp lower contacts and bioturbated upper contacts. All of these have a uniform grain-size distribution and no scour or internal bedding, hence are not turbidites. They are generally very dark gray, nearly black, in color, and some are rich in crystals (plagioclase, quartz, clinopyroxene, orthopyroxene, amphibole, and biotite, in order of decreasing abundance). This reflects the marked density sorting between crystals and glass that occurs in the atmosphere before the materials are deposited, with

crystals settling faster than glass (Carey and Sigurdsson, 1980). Thinner beds can be either black or gray in color, with gray colors possibly resulting from a high concentration of leucocratic minerals in the ash, high SiO₂ content of glass, or mixing with adjacent hemipelagic sediments. Very thin beds tend to have been dispersed up and down the cores for tens of centimeters by burrowing organisms. Many of these can still be recognized by the specks of almost pure ash in the burrow traces. Much of the glass in the ashes of all the cores has been extensively altered to clay minerals (illite and smectite, as revealed by X-ray diffractograms). In smear slides, the glass appears charged with moderately birefringent clays and iron hydroxides.

In all, there are 119 ash beds in the Hole 541 cores, of which 29 are major ash falls more than 2 cm thick. The upper 18 of these major ash beds range in age from late Miocene to Quaternary. The remainder occur below the distinct reverse fault in Core 30, and of these, 10 repeat major ash beds in the upper 18. In all then, 19 intact major ash falls appear to have been sampled. There are two dominant intervals of major ash-producing eruptions, one in the early Pliocene, and one in the late Pleistocene. Miocene and late Pliocene activity was more subdued.

The unusually high recovery throughout most of Hole 541 allows an interesting comparison to be made of the ash stratigraphy in age-equivalent strata above and below the fault in Core 30. Shear deformation appears to be minimal in the carbonate-rich segments of the hole, whereas it is extensive in clays and mudstones. In Cores 18 and 33 there occur two closely spaced ash falls, separated by fewer than 10 cm of hemipelagic carbonate ooze. Assuming that these are identical ash beds, comparison of core photos shows that near the pair, there are no fewer than 7 other major ash beds that occur at precisely the same depths in both groups of cores (see Natland, this volume). Cores 19 and 36 are markedly more enriched in clays than higher cores, but occur at almost exactly the same depth below the ash-bed pair both above and below the fault. For about 30 m or so, evidently, precisely correlative sequences from above and below the fault can be matched. Below this, however, in the clay-rich materials, faulting and shear deformation occur in both sequences, making it impossible to correlate ash beds. The differences in stratigraphy of these two clay-rich intervals occur because one or both of them contain faults.

STRUCTURAL GEOLOGY

The most conspicuous structure documented at Site 541 is a reverse fault at 276 m (Core 30) along which Miocene mud has been emplaced structurally above Pliocene nannofossiliferous mud. More pervasive, smaller-scale deformational features are progressively developed in the 75 m of section immediately above this fault. Three stratigraphic inversions also occur above the fault. The Pliocene section immediately below this fault is gently dipping but otherwise undeformed. Approximately 100 m above the base of the hole, fracturing and penetrative shearing are again important and probably formed

in or adjacent to another major fault zone. In this section of the Site 541 report, structural features are described in detail, proceeding from the top to the bottom of the hole. Observations are depicted graphically in Figure 4.

Horizontal layers that had not been reoriented by drilling were first noted in Core 8, below 59 m (sub-bottom depth). The first dipping layers were measured in Core 14; they have true dips of about 20°. From this point until the onset of internal fracture and flow in Core 23, alternating sections of mud and ooze 5 to 15 m thick are characterized by either horizontal attitudes or layers dipping on average 20°, but as much as 40°. In several cases, attitudes were obtained on right-way-up ash layers with sharp bottoms and bioturbated tops. Note that dips do not increase progressively downhole as would be the case if tilting had occurred during deposition. The alternation of horizontal and dipping layers indicate instead that some restricted stratigraphic intervals are either tilted or gently folded, perhaps due to gravity-driven slumping or small displacements along décollements.

The first hint of more pervasive deformation occurs in a few 10-cm intervals in Cores 23 and 24, but most of Cores 25 to 29 and the upper 130 cm of Core 30 are characterized by incipient to thorough internal disruption. Bioturbation structures (burrowing, mottling) are undistorted locally, but generally they have been obliterated. Cores are pervaded by slickensided, polished surfaces that can be broken out of drilling biscuits on a scale of 1 cm or so. These are interpreted as slip surfaces, accommodating and distributing small (<<1 mm) displacements throughout the section, but the surfaces appear not to have any preferred orientation. They are definitely less penetrative and oriented than "scaly" foliation, which is developed for about 20 cm above the fault in Section 6 of Core 30. Scaly mudstone is common in Cores 42 to 50 and is more fully described later. A 7-cm-long sharp fault, dipping 60°, with striations pitching 80° on its polished surface, occurs in Core 25, Section 5. The deformation and distortion in Cores 25 to 30 is described best as mesoscopic plastic flow accommodated in part along mesoscopically visible discontinuities (= polished surfaces). This flow has also resulted in stratal disruption, because some layers of distinctly colored mud were broken up, or disharmonically folded and swirled, sometime prior to the development of drilling laminations. Other layers, such as in Core 30, Section 6, apparently were juxtaposed along steeply dipping faults. The stratal disruption was obviously complex, but its nature is obscure because disrupted layers have been subsequently rotated along horizontal drilling fractures. We believe all of this internal deformation is related to the major fault discussed next.

This fault, emplacing Miocene structurally above Pliocene, is visible in Core 30, Section 6, from 122 to 143 cm. Pervasively sheared, scaly, dark olive gray Miocene mud is separated from lighter gray Pliocene nannofossil-rich mud by a black-stained zone up to 5 mm thick that represents the actual fault surface. Offset nannofossil zones suggest 70 m of throw across the fault. The

in situ orientation of the fault is difficult to determine because it has been reoriented drastically by rotations along drilling laminations, but its appearance in several biscuits over the interval mentioned suggests that it is either moderately to steeply dipping or perhaps folded or imbricated *in situ*. In any case, we sampled only a miniscule part of the fault and can only guess its actual orientation. It is important to note, however, that whatever its attitude, reverse dip slip must have occurred along it to emplace gently dipping older strata over younger.

In addition to the major fault at 276 m, nannoplankton biostratigraphy indicates repeated sections near the base of Core 9, at the base of Core 19, and possibly within Core 29, although the actual physical features responsible for these inversions (reverse faults, small slumps) were not observed in the cores. Two ash beds in Core 18 may be equivalent to ash beds in Core 20, and a paleomagnetic reversal event is repeated in Cores 18 and 20 (see the section on Paleomagnetism, this chapter). There is also a change in dip, corresponding with this stratigraphic inversion, from about 40° in Cores 18 and 19 to horizontal in Cores 20 to 22. Although the vertical offset across the fault at 276 m is only 70 m, similar nannofossil assemblages occur in Cores 23 and 38 (205 and 345 m), suggesting a total of about 130 m of throw. Thus the fault at 263 m apparently accommodates about 60 m of throw.

Aside from a few centimeter-scale, randomly oriented polished surfaces and a sharp steeply dipping fault in the first section of Pliocene mud below the fault at 276 m, the sediments appear to be internally undeformed in contrast to sediments above the fault. However, the section from Cores 31 to 41 is all gently to moderately dipping; 16 attitudes (5 definitely right-way-up) average 25° but range as high as 45°. A sharp, 50° fault with striations pitching 65 to 75° cuts across Core 32, Section 6. Beginning in Core 40, interval deformation is again evident and is expressed as fracturing in biscuits of coherent mudstone. Breccia is locally developed between some biscuits, probably having formed from drilling-induced disruption of fractured mudstone. The intensity of fracturing is variable in Cores 40, 41, and 42. Judging from the fine preservation of burrows, displacements along the fractures were negligible.

Core 42, Section 5 marks the first appearance of penetratively deformed, foliated, scaly mudstone. This scaliness is the mesoscopic expression of slip along innumerable closely spaced subparallel surfaces. Typical samples of affected mudstone can be disaggregated into small polished chips. The fabric of scaly mudstone in these cores strongly resembles deformed, or "sheared," mudstones and serpentinites in on-land fault zones, and there was general agreement on board that the prevalence of this feature from Cores 42 to 50 indicates that we had penetrated another major fault zone. The polished surfaces are strongly oriented and impart a definite foliation to mudstone within drilling biscuits, but the orientation of the foliation generally varies from biscuit to biscuit, possibly due to rotation during drilling. We estimate that horizontal attitudes are most abundant, especially in Cores 48 to 50. Typically, scaly mud-

stone occurs in 10- to 20-cm-thick zones separating intervals comprising biscuits of coherent or fractured burrowed mudstone, but some scaly zones are as much as 1 m thick. Some zones include lens-shaped inclusions, augen, or wispy streaks of mudstone or ash that are colored differently from the scaly matrix and thus are presumably tectonic inclusions recording modest stratal disruption and mixing in shear zones.

Some sections of Cores 49 to 50 also contain intervals comprising angular fragments of different lithologies surrounded by soupy drilling mud and breccia. Their fabric is so different from the foliated intervals that we interpret them as cavings that collected in the hole as the drill string was run up and down to prevent sticking. Some of the foliated and fractured zones undoubtedly were further disturbed by drilling, as suggested by swirling patterns in Cores 49 and 50.

One other small-scale structure was documented at Site 541. "Vein structure," or "veins," as defined on Leg 67, refers to dark 1-mm-thick planar or curvilinear discontinuities generally spaced about 1 to 5 mm apart on cut surfaces of cores. We noted very rare veins in biscuits in Cores 19, 40, 41 and 45. They appear to be oriented either vertically or horizontally. They differ from veins described on Leg 67 (Cowan, 1982), and "spaced cleavage" described on Leg 66 (Lundberg and Moore, 1982), in that individual components of sets are not subparallel but rather anastomose around a common "zone axis." The net effect is that the mud is segmented into roughly cylindrical, irregular rods, 1 to 3 mm in diameter, parallel to the zone axis, rather than thin planar or curvilinear panels. The significance of these structures is unknown, pending further investigation.

In summary, we feel that we penetrated two major zones of deformation at Site 541. One of them formed above a major fault zone that repeats the stratigraphic section. We did not detect any stratigraphic inversion or repetition in the lower deformed zone, but much of the mudstone is barren of fossils. Smectite is decidedly more abundant in the internally deformed sediments in Cores 25 to 30 and 42 to 50 (see the Lithology section, this chapter), which possibly causes the localization of deformation.

BIOSTRATIGRAPHY

The biostratigraphy described herein is based on shipboard investigations. For more complete summaries, see Bergen (nannofossils—this volume) and Renz (radiolarians—this volume).

Nannofossils

A biostratigraphic summary of Site 541 nannofossils, radiolarians, and foraminifers is plotted with depth, age, and paleomagnetism in Figure 6.

Nannofossil-bearing sediments at Site 541 range in age from late Miocene (CN9a) to early late Pleistocene. Pliocene sediments generally contain common and moderately preserved calcareous nannofossils. Miocene sediments are either barren or contain relatively few and often poorly preserved floras.

Four stratigraphic repetitions of section are recognized at Site 541. The largest of these is in Core 30, Section 6, where an upper Miocene mud (CN9a) overlies an upper Pliocene nannofossil mud (CN12a). Two smaller repetitions of section occur within the larger repeated unit. The first of these is in upper Miocene muds above Sample 541-29-4, 75–76 cm, where *Amaurolithus primus*, *A. delicatus*, *Discoaster surculus*, and *D. quinqueramus* disappear. *D. berggrenii* then enters in Sample 541-28, CC, followed by *D. surculus* and *D. quinqueramus* in the top half of Core 28. The amaurooliths are not found again until the base of Core 24. The second, small repetition occurs between Sample 541-20-1, 45–46 cm and Section 541-19, CC. At this break, sediments from the *Sphenolithus neoabies* Subzone (CN11a) are found below those of *Ceratolithus acutus* Subzone (CN10b).

A final repetition occurs in lower Pleistocene sediments from Core 9. *Cyclococcolithina macintyreii*, which is last seen in Sample 541-10-3, 75–76 cm, is found again in Core 9, Sections 5 through 2. In addition, a succession of *Gephyrocapsa* species seen in Core 10 is repeated in the top five sections of Core 9 and the bottom of Core 8. This repetition involves approximately 6 m of section.

There are two places in Hole 541 where section is missing. The first is between Samples 541-37-1, 35–36 cm (CN10b) and 541-36, CC (CN9b), where the *Triquetrorhabdulus rugosus* Subzone (CN10a) is missing. This hiatus is not seen uphole. A second hiatus is located in the upper part of Core 13. Here, only Sample 541-13-1, 75–76 cm is from the *D. pentaradiatus* Subzone (CN12c).

Core 1 contains the only upper Pleistocene, nannofossil-bearing sediments in the Leg 78A sites. *Gephyrocapsa oceanica* and *Ceratolithus cristatus* occur in this core, but not *Pseudoemiliana lacunosa* or *Emiliana huxleyi*. It is possible that the absence of *E. huxleyi* is due to deposition below the compensation depth of that species.

Samples 541-2-1, 70–72 cm through 541-11-3, 131–132 cm contain *P. lacunosa* but have no discoasters. This whole interval is placed in the lower Pleistocene. The Pliocene/Pleistocene boundary is placed at the last common occurrence of *D. brouweri* and agrees with the foraminifers. The occurrence of *Cyclococcolithina macintyreii* (up to Sample 541-10-3, 75–76 cm and in Core 9, Sections 2 to 5) places these samples in the *Cyclococcolithina macintyreii* Zone of Gartner (1977).

Samples 541-11-4, 8–9 cm through 541-16-4, 13–14 cm are assigned to the upper Pliocene, on the basis of the last occurrences of *D. brouweri* and *Reticulofenestra pseudoumbilica*. *Sphenolithus neoabies*, whose last occurrence is used in conjunction with that of *R. pseudoumbilica*, disappears after Sample 541-16-3, 13–14 cm. The upper Pliocene is divided up as follows:

- 1) Sample 541-11-4, 8–9 cm to Section 541-12, CC—*Calcidiscus macintyreii* Subzone (CN12d);
- 2) Sample 541-13-1, 30–31 cm—*Discoaster pentaradiatus* Subzone (CN12c);
- 3) Samples 541-13-2, 30–31 cm to 541-13-5, 30–31 cm—*Discoaster surculus* Subzone (CN12b); and

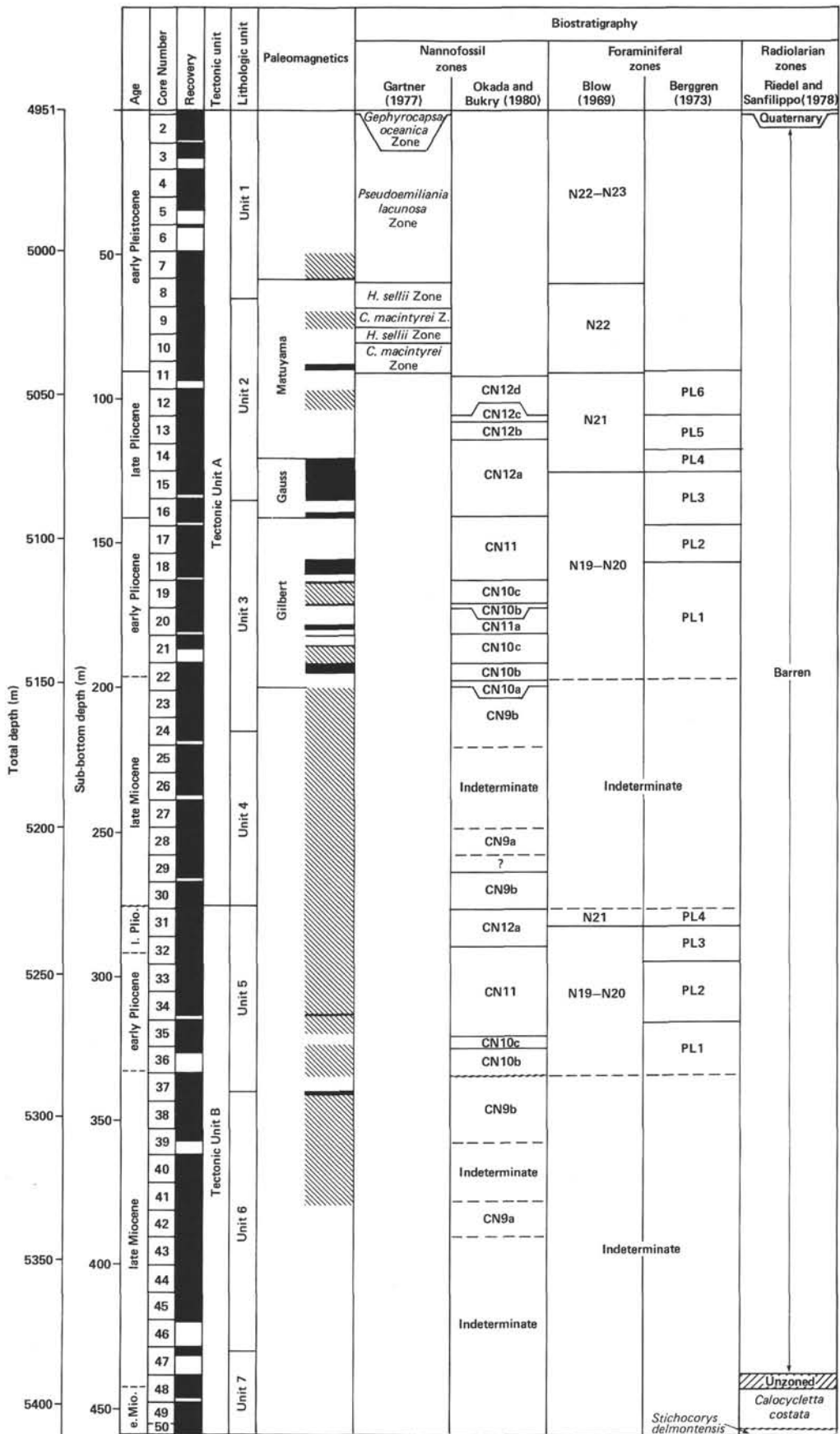


Figure 6. Summary biostratigraphy and magnetostratigraphy, Site 541. (Polarity normal intervals are black, polarity reversed intervals are white, and polarity uncertain intervals [or intervals with no data] are diagonally striped.)

4) Samples 541-13-6, 30–31 cm to 541-16-4, 13–14 cm—*Discoaster tamalis* Subzone (CN12a).

Sample 541-16-5, 13–14 cm through Sample 541-18-6, 43–44 cm are assigned to the *Reticulofenestra pseudoumbilica* Zone (CN11). *R. pseudoumbilica*, *Sphenolithus abies*, and *S. neoabies* are found throughout this interval. *Discoaster asymmetricus* becomes common by Sample 541-17-2, 40–41 cm, and this marks the beginning of its acme.

Samples 541-18, CC through 541-19-5, 60–61 cm are placed in the *Ceratolithus rugosus* Subzone (CN10c), based on the presence of *Amaurolithus tricorniculatus* and absence of *C. acutus*. *C. acutus* is present in Sample 541-19-6, 79–80 cm through Section 541-19, CC. This interval is placed in the *Ceratolithus acutus* Subzone (CN10b).

Core 20, Section 1 through Core 22, Section 2 contain approximately 21 m of section seen above Section 541-19, CC. Samples 541-20-1, 45–46 cm through 541-20-7, 4–5 cm contain *R. pseudoumbilica* and *S. neoabies* but not *A. tricorniculatus* and *D. asymmetricus*. This interval is assigned to the *Sphenolithus neoabies* Subzone (CN11a). Sections 541-20, CC to 541-21, CC contain *A. tricorniculatus* and are in the *Ceratolithus rugosus* Subzone (CN10c). The occurrence of *C. acutus* from Samples 541-22-1, 22–23 cm to 541-22-4, 22–23 cm indicates that this section is from the *Ceratolithus acutus* Subzone (CN10b). Samples 541-22-5, 22–23 cm and 541-22-6, 22–23 cm do not have *C. acutus* and *D. quinqueramus* and are placed in the *Triquetrorhabdulus rugosus* Subzone (CN10a). Sections 541-22, CC to 541-24, CC all contain *D. quinqueramus*. *A. primus* and *A. delicatus* are in only some of these samples because of poor preservation. This interval is assigned to the *Amaurolithus primus* Subzone (CN9b) of the late Miocene.

Cores 25 through 27 are barren except for sparse assemblages in Section 541-27, CC. Core 28 contains *D. berggrenii* throughout, and no amauroliths. It is assigned to the *Discoaster berggrenii* Subzone (CN9a). The top three sections of Core 29 are barren except for the occurrence of numerous discoasters in Sample 541-29-2, 75–76 cm. This sample is probably older than the *Discoaster berggrenii* Subzone (CN9a), but lacks any marker species. Samples 541-29-4, 75–76 cm to 541-30-6, 130–131 cm contain *D. surculus*, *D. quinqueramus*, *A. primus*, *A. delicatus*, but not *D. berggrenii*. This section is from the *Amaurolithus primus* Subzone (CN9b) and is younger than Core 28.

A major stratigraphic inversion occurs between Samples 541-30-6, 130–131 cm, and 541-30-6, 135–136 cm. Samples 541-30-6, 135–136 cm to 541-33-2, 58–59 cm are assigned to the late Pliocene *Discoaster tamalis* Subzone (CN12a) on the basis of occurrence of *D. tamalis* and absence of *R. pseudoumbilica*. *S. abies* and *S. neoabies* have their last occurrences in Sample 541-32-2, 69–70 cm and Sample 541-32-1, 45–46 cm, respectively.

Samples 541-33-3, 58–59 cm to 541-35-3, 69–70 cm contain *R. pseudoumbilica* and no *A. tricorniculatus*. This indicates that this section is in the *R. pseudoumbilica* Subzone (CN11). The beginning of the acme of *D.*

asymmetricus can be placed in Core 33, Section 6. Sample 541-35-4, 64–65 cm to Section 541-35, CC are placed in the *Ceratolithus rugosus* Subzone (CN10c), based on the presence of *A. tricorniculatus* and the absence of *C. acutus*. All samples from Core 36 are assigned to the *Ceratolithus acutus* Subzone (CN10b), based on the occurrence of that species alone. A hiatus is present below this as *D. quinqueramus*, *D. surculus*, and *A. primus* are found from Samples 541-37-1, 35–36 cm to 541-39-3, 21–22 cm. This interval is placed in the *Amaurolithus primus* Subzone (CN9b). Barren intervals are common in Cores 38 and 39. Cores 40 to 41, Section 2 are totally barren.

Samples 541-41-4, 34–35 cm to 541-42-5, 69–70 cm usually contain *D. berggrenii* or *D. surculus*. No amauroliths are found in this section, so it is placed in the *Discoaster berggrenii* Subzone (CN9a). The occurrence of nannofossils in this interval may suggest a small repetition of section above Sample 541-42-4, 85–86 cm, but this repetition is hard to be sure of because of poor assemblages. Section 541-42, CC contains the last nannofossils of any kind. Cores 43 to 50 are barren.

Radiolarians

Siliceous microfossils consist of only radiolarians and sponge spicules. No diatoms or silicoflagellates are seen. In Core 1 (Sections 1 and core catcher), sponge spicules are few and broken. Radiolarians are very rare with fine, thin-walled skeletons indicating considerable dissolution.

Cores 2 through 46 are barren.

In Section 541-47, CC, very few and very badly preserved radiolarian specimens occur. No speciation is possible. In Cores 48 to 50 radiolarians are very rare to abundant, occurring in moderately well preserved (with little dissolution but common breakage), diverse assemblages. Orosphaerid fragments are common. Using the zonation of Riedel and Sanfilippo (1978), emend. Sanfilippo and Riedel (in press), radiolarians range from the *Calocyclus costata* Zone to the *Stichocorys delmontensis* Zone of the early Miocene.

Samples 541-48-5, 105–107 cm through 541-50-1, 120–122 cm are assigned to the *Calocyclus costata* Zone. The following species occur (except in Samples 541-49-1, 10–12 cm through 541-49-3, 35–37 cm, where specimens are poorly preserved):

<i>Calocyclus costata</i>	<i>Stichocorys wolffii</i>
<i>Calocyclus virginis</i>	<i>Cyrtocapsella cornuta</i>
<i>Stichocorys delmontensis</i>	<i>Dorcadospyrus dentata</i>

Lychnocanoma elongata is absent.

Samples 541-50-3, 12–14 cm through Section 541-50, CC are assigned to the *Stichocorys delmontensis* Zone due to the appearance of *L. elongata* and *Dorcadospyrus ateuchus* and the disappearance of *Calocyclus costata* and *S. wolffii*. *Theocyrtis annosa* is absent. The following species dominate the assemblage:

<i>Calocyclus virginis</i>	<i>Dorcadospyrus ateuchus</i>
<i>Cyrtocapsella cornuta</i>	<i>Lychnocanoma elongata</i>
<i>Cyrtocapsella tetrapera</i>	<i>Stichocorys delmontensis</i>

Specimens of *S. delmontensis* appear almost identical with previous specimens of *S. wolffii*, differing only in a slightly more porous (>6 pores/visible half) thorax.

The *Stichocorys wolffii* Zone itself is absent, perhaps due to poor recovery in Core 50 (39%) and the resulting hiatus between Sections 1 and 3.

Foraminifers

Drilling at Site 541 provided sediments that are rich in planktonic foraminifers from the upper part of the Miocene to the Quaternary. Most of the sediments from the middle Miocene through most of the upper Miocene are barren of foraminifers. Two tectonic units (Units A and B) are recognized at Site 541. Tectonic Unit A overlies Tectonic Unit B and is separated from it by a reverse fault. Tectonic Unit A is approximately 276 m thick and consists of upper Miocene to Quaternary sediments. Tectonic Unit B is approximately 184 m thick and consists of lower Miocene to lower Pliocene sediments. Planktonic foraminifers are present only in the upper 189.5 m of Tectonic Unit A and in the upper 69 m of Tectonic Unit B.

Samples 541-1-1, 60–62 cm through 541-8-3, 68–70 cm are assigned to the Quaternary, Zones N22 to N23 of Blow (1969). *Globorotalia* (*G.*) *truncatulinoides truncatulinoides* (d'Orbigny), *Sphaeroidinella dehiscentes dehiscentes* (Parker and Jones), *Globigerinoides ruber* (d'Orbigny), *G. sacculifer* (Brady), and *Neogloboquadrina dutertrei* (d'Orbigny) are some of the dominant forms found throughout this interval. The sediments from Samples 541-8-4, 39–41 cm to 541-11-3, 131–133 cm are assigned to Zone N22 on the basis of the occurrence of *Globigerinoides obliquus obliquus* Bolli, *Globorotalia* (*T.*) *tosaensis* Takayanagi and Saito, and *G. (G.) truncatulinoides truncatulinoides*. The first occurrence of *G. (T.) tosaensis* occurs in Section 541-10, CC.

The samples from 541-11-2, 67–71 cm to 541-11-3, 131–133 cm are assigned to Zone N22 on the occurrence of *G. (G.) truncatulinoides truncatulinoides*. The first downhole occurrence (extinction datum) of *Globigerinoides obliquus extremus* Bolli and Bermuda is recorded in Sample 541-11-2, 67–71 cm. The extinction datum of *G. obliquus extremus* marks the top of Zone PL6 of Berggren (1973); Zone PL6 marks the top of the upper Pliocene, as reported by Berggren (1973). However, Blow (1969) places the Pliocene/Pleistocene boundary immediately below Zone N22. The placement of the Pliocene below Sample 541-11-3, 131–133 cm is in agreement with the nannofossil evidence (Bergen, this volume).

The interval from Core 11, Section 4 to Sample 541-14-7, 35–37 cm is assigned to the upper Pliocene Zone N21. Diagnostic foraminifers within this interval are *G. obliquus extremus*, *Globorotalia* (*T.*) *tosaensis*, *G. (G.) miocenica* Palmer, *G. (G.) multicamerata* Cushman and Jarvis, *Globoquadrina altispira altispira* Cushman and Jarvis, and *G. altispira globosa* Bolli. The extinction datum of *Globorotalia* (*G.*) *miocenica* (above Sample 541-13-1, 70–72 cm) marks the top of Zone PL5 of Berggren. The top of Berggren's Zone PL4 is placed above Sample 541-14-2, 74–76 cm on the first downhole occur-

rence of *G. (G.) multicamerata* and *Globoquadrina altispira altispira*.

Sediments assignable to the basal zone (Zone PL3 of Berggren, i.e., N19 to N20 of Blow) of the upper Pliocene are seen from Section 541-14, CC to Sample 541-16-5, 75–77 cm. *Sphaeroidinella dehiscentes dehiscentes* and *Sphaeroidinellopsis subdehiscentes paenedehiscentes* Blow are found within this interval.

The lower/upper Pliocene boundary is placed below Sample 541-16-5, 75–77 cm and above Sample 541-16-6, 75–77 cm. The extinction datum of *Globorotalia* (*G.*) *margaritae* Bolli and Bermudez above Sample 541-16-6, 75–77 cm defines the top of the lower Pliocene Zone PL2 of Berggren. The placement of the top of the lower Pliocene on the basis of the nannofossil evidence is at Sample 541-16-5, 13–14 cm.

The section from Sample 541-16-6, 75–77 cm to Sample 541-18-2, 70–72 cm is assigned to that part of Zone N19 of Blow below the *G. (G.) margaritae* extinction datum.

Sediments from Sample 541-18-3, 70–72 cm to Section 541-22, CC contain specimens of the foraminifer *Globigerina nepenthes* Todd and *Sphaeroidinellopsis subdehiscentes paenedehiscentes*. They are assignable to that part of Zone N19 (i.e., PL1 of Berggren) that occurs below the extinction datum of *G. nepenthes*.

The boundary between the upper Miocene and the lower Pliocene cannot be determined at this site with the available foraminiferal evidence. However, on the basis of the nannofossil evidence (Bergen, this volume) the Miocene/Pliocene boundary occurs at the base of Core 22, Section 4. The sediments from Cores 23 to 24 are assigned to the upper Miocene. The samples from Core 25 to Sample 541-30-6, 57–59 cm are barren of foraminifers or contain very sparse occurrences of foraminifers. This interval is no older than late Miocene.

The interval from Samples 541-30-7, 57–59 cm (top of Tectonic Unit B) to 541-31-2, 70–72 cm is assignable to the upper Pliocene Zone N21 of Blow (i.e., PL4 of Berggren) because of the occurrence of *Globorotalia* (*G.*) *multicamerata* and *Globoquadrina altispira altispira*.

The interval from Samples 541-31-3, 70–72 cm to 541-32-4, 70–72 cm is assignable to Zone N19 to N20 (i.e., PL3 of Berggren). Specimens of *Sphaeroidinellopsis subdehiscentes paenedehiscentes* and *Sphaeroidinella dehiscentes dehiscentes* are present throughout.

The lower/upper Pliocene boundary is placed above Sample 541-32-5, 85–87 cm, where rare specimens of *Globorotalia* (*G.*) *margaritae* are found. The interval from Sample 541-32-5, 85–87 cm to Core 34 is assigned to that part of Zone N19 (i.e., PL2 of Berggren) below the extinction of *G. (G.) margaritae*.

The boundary of the lower Pliocene Zones PL1/PL2 of Berggren is placed above Section 541-34, CC. *Globigerina nepenthes* is common in Section 541-34, CC. Its extinction marks the top of Zone PL1.

The interval below Section 541-34, CC to Sample 541-37-4, 70–72 cm is interpreted as upper Miocene to lower Pliocene. These sediments contain a sparse foraminiferal assemblage dominated by *G. nepenthes* and *Sphae-*

roidinellopsis subdehiscens paenedehiscens. The first definite upper Miocene sediments occur at the base of Core 36 on the basis of the nannofossil evidence (Bergen, this volume).

The sediments from Sample 541-37-5, 68–70 cm to Section 541-42, CC are barren of foraminifers or contain a sparse occurrence of foraminifers.

The sediments below Section 541-42, CC are barren of foraminifers.

PALEOENVIRONMENT

The following environmental analysis is based mainly on the occurrence and preservation of planktonic foraminifers. Calcareous nannofossils and smear slides also provided additional data. According to Wright (this volume), the calcite compensation depth (CCD) at Site 541 is around a depth of about 5200 m. The lysocline (depth of increasing dissolution) of planktonic foraminifers occurs at the estimated level of 4800 to 4850 m (Berger, 1979). Criteria for estimating the depth of deposition in relationship to the CCD level are presence above and absence below (1) surface dwellers (spinose species), (2) thin-shelled juveniles, and (3) thin-shelled (transparent) adult specimens that calcify mainly in deeper water. Criteria for dissolution effects are (1) pore widening (surface dwellers), (2) dissolved keel regions of globorotalid forms, and (3) isolated chambers or chamber pieces (Berger, 1968). According to data from recent tropical to subtropical environments (Parker and Berger, 1971; Thunell and Honjo, 1981), planktonic foraminifers can be grouped as follows:

Less resistant	More resistant
<i>Globigerina bulloides</i> / <i>G. falconensis</i>	<i>Orbulina universa</i> (thick shelled)
<i>G. aequilateralis</i>	<i>Globorotalia truncatulinoides</i> and related species
<i>Orbulina universa</i> (thin shells)	<i>Globigerinoides conglobatus</i> <i>Neogloboquadrina dutertrei</i> and related species
<i>Globigerinoides ruber</i> pink and white	<i>Pulleniatina obliquiloculata</i>
<i>G. sacculifer</i>	<i>Globorotalia crassaformis</i>
<i>Globorotalia menardii</i> (keeled globorotalids, thin shelled)	<i>G. menardii</i> (thick shelled) and related species
Juveniles of most species	<i>G. tumida</i> <i>Globigerina nepenthes</i> <i>Sphaeroidinella dehiscens</i> and related species

Most species of the less resistant to dissolution group are surface dwellers (upper 50 m of the water column) or species that may migrate as deep as 400 m for reproduction. For example, *O. universa* reproduces normally in shallow water (upper 150 m), but some of the existing population may migrate to deeper water for reproduction while they are still calcifying and thus develop thicker shells. Hardly any dissolution takes place during settlement to the lysocline (Berger, 1970). Below the lysocline, differential dissolution of the foraminifers causes assemblages of low diversity of enriched thick-shelled specimens. "Assemblages" deposited close to the CCD are nearly monospecific, consisting of *S. dehiscens* (*S. paenedehiscens*) and its fragments. Sometimes keel fragments and other indistinguishable pieces are observable.

Those samples are enriched in the more resistant benthic foraminifers.

Tectonic Unit A

Most samples from Site 541 containing calcareous fossils were deposited at or below the lysocline. Samples from Cores 1 and 2 show slight dissolution of all species in a cold-water influenced assemblage (e.g., *Globigerina bulloides*, *Globorotalia inflata*, *G. truncatulinoides*). However, the less resistant shelled *Globigerinoides ruber* are still present. The robustness of their shells highly depends on the amount of calcite they secrete just prior to reproduction (Bé, 1980). A tectonically displaced section (Sample 541-4-1, 50–70 cm) of the Pliocene characterizes a spike of a badly dissolved assemblage. A spike at the base of Core 2 seems to be caused by gravity-flow deposits. The sample contains abundant quartz grains and a mixture of rather well and poorly preserved foraminifers. The sediments immediately below contain a rather well preserved assemblage. The tropical to subtropical assemblage in Core 3 shows slightly more dissolution. Chambers and chamber fragments are common; isolated keels are absent, and *G. ruber* has lost its pinkish color (pigment has been dissolved). Similar examples of transported material by means of gravity flow can be seen in Core 4, Section 3 to Core 6 and the core catcher of Core 4. In contrast to Core 2, these samples contain more thick-shelled specimens that appear to be concentrated by differential dissolution (e.g., *Sphaeroidinella dehiscens* or thick-shelled *Orbulina universa*). Core 4, Sections 5 and 6 contain a rather well preserved tropical assemblage that seems to be deposited *in situ*. Increasing dissolution is obviously seen in Cores 5 and 6. A certain cold-water faunistic influence is observed in Core 5, Section 3, as indicated by some specimens of *Globigerina bulloides*, *Globorotalia inflata*, and small forms of *Neogloboquadrina* cf. *pachyderma*, whereas Section 541-6, CC exhibits only a few shell fragments. Thus the sediment has been deposited below the CCD.

Decreasing dissolution occurs in Cores 7 and 8 toward the end of the lower part of the Pleistocene and is followed by a sequence of cores containing rather well preserved tropical foraminiferal assemblages. The rapid decrease of dissolution in Cores 7 and 8 coincides with the boundary between lithologic Units 1 and 2. The best preservation is seen in Cores 9 through 11, indicating sedimentation above or at the lysocline level. More detailed studies reveal a fluctuating CCD relative to the seafloor and coinciding with glacial or interglacial phases (see Hemleben, this volume). A spike below the Pleistocene/Pliocene boundary appears again to be due to gravity-flow deposits indicated by a rather large amount of fragments in the fine fraction ($>63 \mu\text{m}$) and quartz grains. Core 13, Section 5 through Core 14, Section 6 show rather well preserved assemblages of a warm water (tropical) environment. Beginning with Core 17, Section 2, dissolution increases slowly with drilling depth but is interrupted by several gravity-flow deposits showing generally better preservation. Core 23 is characterized by rapidly increasing dissolution and Core 24 reaches the

CCD, which coincides with the boundary of Lithologic Units 3 and 4. Core 25 through Core 30, Section 6 are mostly barren of planktonic foraminifers and contain only fish bone debris and some shark teeth. Thus sedimentation took place below or at the level of the CCD. Core 28, Section 4 through Section 541-28, CC contain shell fragments and some highly resistant species such as *Globigerina nepenthes*. Most samples showing none or only rare fragments of planktonic foraminifers still contain some benthic shells. This clearly shows (1) the greater resistance of benthic foraminifers to dissolution, and (2) the level of sedimentation being close to the CCD. Whether the sharp increase of dissolution is influenced by the rising CCD, as Berger (1977) has suggested, or whether it is due to subsidence cannot be decided here because we need more data. In addition, the poor preservation in Lithologic Unit 3 may be influenced by bioturbation (see the section on Bioturbation, this chapter).

Tectonic Unit B

The changes in fossil preservation in sediments in Tectonic Unit B cannot be directly compared to its equivalent unit in Tectonic Unit A. The preservation in Unit B is poor in comparison to that in Unit A.

This difference may be influenced by bioturbation and compaction and by minor tectonic movements. Collapsed specimens occur more often than in Tectonic Unit A. Assemblages of Cores 31 through 34 are rather well-preserved, but the juveniles and thin-shelled specimens of most species are absent. However, Core 34, Section 2 shows an exceptional well-preserved assemblage of tropical species. Within Core 37, Section 1 the "foraminiferal CCD" has been reached. Core 39 through Core 42, Section 6 are deposited close to—either slightly above or below—the CCD, as documented by the presence or absence, respectively, of fragments and the occurrence of a few benthic foraminifers. Cores 42, Section 7 through 50 are barren of calcareous fossils and are thus deposited below the CCD. This becomes more evident as radiolarians appear in the core catcher of Core 47. Comparing Cores 22 through 30 of Unit A with Cores 37 through 42 of Unit B, it appears that the latter core sequence may have been deposited slightly deeper with respect to the CCD.

Few benthic foraminifers occur in most samples but have not been studied in detail. However, all observed specimens are deep-water (abyssal) species and normally better preserved than the planktonic foraminifers. This phenomenon was noted by Parker and Berger (1971) and Schnitker (1979) on Leg 48. Shallow-water species are only observed in one gravity-flow deposit (Cores 4–6). This observation indicates that the source of the gravity-flow deposits is not from a continental or island arc slope. These sediments may have originated from the upper part of the Barbados Rise.

In considering the depth position of the CCD several different factors must be taken into account: (1) uplift or subsidence, (2) changes in the water mass system (e.g., current system), (3) climatic changes, and (4) current transport of calcareous particles below the CCD.

However, comparing abundances of tropical and subtropical faunal composition (e.g., occurrence of *Globorotalia menardii* versus *G. truncatulinoides*), excluding gravity-flow deposits and tectonically displaced sediments, shows that the CCD fluctuated during the Quaternary, reflecting the glacial and interglacial phases. Carbonate bomb data, calcareous nannofossils, and foraminiferal abundances in the cores support the results that indicate a trend toward a rising CCD during the Miocene.

PORE-FLUID CHEMISTRY

Eleven samples were taken for pore-fluid chemistry at Site 541. Three additional samples were obtained with the *in situ* samples. The data are listed in Gieskes et al. (this volume), where they are plotted versus depth and summarized. The second *in situ* sample did not succeed in displacing the fresh water that is normally kept in the sampler core prior to sampling, hence is somewhat diluted, giving reductions in salinity and chlorinity. The major trends of the data with increasing depths are (1) a drop in alkalinity, (2) erratic salinity values despite monotonically diminishing chlorinity, and (3) a marked decrease in Mg^{2+} and a complementary increase in Ca^{2+} . The changes in alkalinity, Mg^{2+} , and Ca^{2+} result from exchange of Ca^{2+} in volcanic glass in the sediments with Mg^{2+} to form clay minerals, reactions which consume alkalinity. Other data (heat flow, physical properties, fluid pressure measurements) at both Sites 541 and 542 indicate that pore fluids may migrate along fractures and faults in the sediments from the major shear zone, or décollement, reached at Site 541. Some of the pore-fluid gradients at Site 541, therefore, may have been influenced by tectonically induced pore-fluid migration.

ORGANIC GEOCHEMISTRY

In view of the oil production on Barbados Island to the south, the hydrocarbon geochemistry of Leg 78A sites was observed with much interest and considerable caution. Total organic carbon content of Hole 541 sediments was very low, decreasing from about 0.24% in the shallowest cores to about 0.06% at total depth of about 453 m. Hydrocarbon gases were dispersed at background levels in the sediments. Concentrations of C_1 to C_6 hydrocarbons were estimated at 10 to 700 standard volumes of gas per 10^9 volumes of sediment, increasing regularly with increasing depth of burial.

In general, the low organic carbon content reflects poor organic matter productivity and preservation in the deep sea environment. Low hydrocarbon content reflects absence of hydrocarbon precursors deposited and preserved with the sediments.

PHYSICAL PROPERTIES PROCEDURES

Sonic velocity, wet-bulk density, porosity, water content (percent wet weight), shear strength, and thermal conductivity were determined (Table 3).

Compressional Acoustic Velocity

Velocities were measured using the Hamilton Frame device (Boyce, 1976). In the upper part of the hole, soft

Table 3. Summary of physical properties for Site 541.

Sample (core-section, interval in cm)	Sub-bottom depth (m)	Sonic velocity (km/s)		2-min. GRAPE				Gravimetric			Acoustic impedance ($\times 10^3$ g/cm ² s) v ^a	Shear strength (kPa)	Thermal conductivity [$\times 10^{-3}$ (cal/ cm · s · deg)]
				Wet-bulk density (g/cm ³)		Porosity (%)		Wet-bulk density (g/cm ³)	Porosity (%)	Water (%)			
		H ^a	v ^a	H ^a	v ^a	H ^a	v ^a						
1-1, 29-31	0.3												
1-1, 49-51	1.5											11.53	
2-5, 48-51	7.5	1.491		1.35		80.6		1.42	69.5	50.0	2.12		
2-5, 86-89	7.9	1.482		1.21		89.0		1.41	77.9	56.5	2.09		
2-5, 100-101	8.0											11.53	
2-6, 71-74	9.2	1.492		1.32		82.4		1.41	75.5	54.7	2.10		2.213
2-6, 96-98	9.5											24.71	
3-1, 83-86	11.4	1.506		1.59		66.3		1.51	70.8	48.2	2.27		
3-3, 56-59	14											29.24	
3-4, 68-71	15.6	1.537		1.71		59.1		1.70	64.6	38.9	2.61		
3-4, 81-84	15.8											26.3	
4-1, 69-72	20.7	1.533		1.69		60.3		1.68	65.8	40.2	2.58		
4-4, 93-96	25.5	1.496		1.59		66.3		1.61	64.0	40.6	2.41		
4-4, 110	25.5												3.475
4-4, 123-126	25.7											47.7	
4-6, 84-87	28.3											39.53	
5-2, 7-10	31	1.559		1.73		57.9		1.63	64.1	40.2	2.54		
5-3, 70-72	33.2											78.24	
6-1, 63-65	39.6											37.47	
6-1, 68-70	39.7	1.537		1.66		62.1		1.66	60.9	37.6	2.55		
7-2, 109-112	51	1.514	1.541	1.72		58.5		1.67	63.2	38.9	2.57		
7-3, 53-56	52	1.535	1.536	1.58		66.9		1.68	62.1	37.9	2.56		
7-3, 82-86	52.3											42.83	
7-3, 117	52.5												3.119
7-6, 86-89	56.9											60.12	
8-1, 69-71	58.7	1.516	1.536	1.72		58.5		1.70	61.1	36.8	2.61		
8-1, 79-82	58.8											44.47	
8-4, 76-79	63.3											27.17	
8-5, 42-46	64.5	1.554	1.535	1.72		58.5		1.71	59.6	35.7	2.62		
8-7, 45-48	67.5											87.30	
8-7, 49-53	67.5	1.509	1.528	1.66		62.1		1.65	63.3	39.4	2.52		
9-2, 53-56	69.5											72.48	
9-4, 56-59	72.6											46.04	
9-6, 89-91	75.9	1.535	1.626	1.72		58.5		1.71	60.3	36.0	2.78		
10-1, 100-102	78.0											53.53	
10-2, 79-82	79.3	1.566	1.598	1.69		60.3		1.72	59.6	35.6	2.75		
10-3, 111	81.1												3.287
10-3, 117-118	81.2											49.83	
10-4, 50-53	82	1.550	1.539	1.75		56.7		1.69	61.2	37.0	2.60		
10-4, 60-63	82.1											64.24	
10-6, 129-131	85.8											70.83	
10-7, 16-19	86.2											45.71	
11-1, 90-93	87.4											57.65	
11-1, 99-102	87.5	1.562	1.568	1.76		56.1		1.71	60.2	36.0	2.68		
11-4, 54-57	91.5	1.591	1.598	1.79		54.3		1.77	57.1	33.0	2.83		
11-4, 74-77	91.7											72.89	
11-4, 111-113	92.1											80.30	
12-1, 110-113	97.1											90.60	
12-1, 118-122	97.2	1.561	1.581	1.85		50.8		1.79	56.3	32.1	2.83		
12-1, 133	97.3												3.924
12-2, 25-28	97.8											107.07	
12-7, 12-15	105.1	1.601	1.596	1.83		51.9		1.76	57.3	33.4	2.81		
12-7, 19-22	105.2											76.59	
13-1, 89-92	106.4	1.592	1.618	1.71		59.1		1.69	61.7	37.4	2.73		
13-1, 118-121	106.6											81.95	
13-3, 123-125	109.7											93.07	
13-5, 41-44	111.9	1.598	1.608	1.86		50.1		1.77	57.8	33.4	2.85		
13-5, 91-94	112.4											83.18	
13-7, 25-28	114.7	1.661	1.596	1.85		50.7		1.78	56.8	32.6	2.84		
14-1, 87-90	115.9											84.01	
14-3, 40-43	118.4	1.556	1.551	1.02	1.88	49.0		1.78	57.4	33.0	2.76		
14-5, 70-73	121.7	1.559	1.574	1.91	2.05	47.2	38.8	1.77	57.7	33.4	2.79		
14-5, 97-100	122											51.06	
15-1, 80-83	125.3	1.541	1.539	1.86	1.81	50.2	53.1	1.74	58.6	34.4	2.68		
15-3, 71-74	128.2											90.60	
15-5, 41-44	130.9	1.581	1.575	1.81	1.86	53.1	50.2	1.80	55.4	31.5	2.84		
15-5, 74-77	131.2											98.83	
15-2, 110	136.6												3.287
16-3, 58-60	137.6	1.581	1.589	1.43	1.83	75.8	51.9	1.81	55.1	31.2	2.88		
16-3, 68-71	137.7											>128.83	
16-5, 100-103	141											116.95	
16-6, 50-52	142	1.585	1.568	1.83	1.80	51.9	53.7	1.77	57.3	33.2	2.78		
17-2, 35-38	145.4	1.581	1.569	1.77	1.81	55.5	53.1	1.79	56.1	32.1	2.81		
17-2, 44-47	145.5											102.13	
17-4, 68-71	148.7											>125.19	
17-5, 85-88	150.4	1.617	1.563					1.73	59.0	35.0	2.70		
18-1, 97-100	154											121.89	
18-1, 108-111	154.1	1.572	1.545	1.89	1.72	48.4	58.5	1.68	61.6	37.6	2.60		

Table 3. (Continued).

Sample (core-section, interval in cm)	Sub-bottom depth (m)	Sonic velocity (km/s)		2-min. GRAPE				Gravimetric			Acoustic impedance ($\times 10^5$ g/cm ² s) V ^a	Shear strength (kPa)	Thermal conductivity [$\times 10^{-3}$ (cal/ cm · s · deg)]	
				Wet-bulk density (g/cm ³)		Porosity (%)		Wet-bulk density (g/cm ³)	Porosity (%)	Water (%)				
				H ^a	V ^a	H ^a	V ^a							
18-3, 113-116	157.1													
18-3, 122-126	157.2													
18-5, 106-109	160.1													
19-1, 83-85	163.3													
19-1, 89-92	163.4													
19-3, 41-44	165.9													
19-5, 56-59	169.1													
19-5, 64-67	169.2													
19-6, 90-93	170.9													
20-1, 62-64	172.6													
20-1, 76-79	172.8													
20-4, 33-36	176.9													
20-4, 39-43	176.9													
20-6, 28	179.8													
20-7, 8-11	181.1													
21-1, 67-70	182.2													
21-1, 72-76	182.2													
21-2, 46-49	183.5													
21-2, 51-54	183.5													
21, CC	191													
22-2, 21-24	192.7													
22-2, 28-30	192.8													
22-3, 49-52	194.5													
22-6, 91-94	199.4													
22-6, 119-122	199.7													
22-7, 21-24	200.2													
23-1, 47-50	201.													
23-1, 87-90	201.4													
23-1, 70-73	204.2													
23-5, 52-55	207.													
23-5, 61-63	207.1													
24-1, 52-55	210.5													
24-1, 69-72	210.7													
24-1, 80	210.8													
24-4, 58-60	215.1													
24-4, 66-69	215.2													
24-5, 80-82	216.8													
25-1, 101-104	220.5													
25-1, 107-110	220.6													
25-3, 54-57	223.													
25-3, 64-67	223.1													
25-7, 18-21	226.7													
25-7, 28-31	226.8													
26-2, 36-39	230.9													
26-2, 78-80	231.3													
26-2, 78-80	231.3													
26-2, 78-80	231.3													
26-4, 25-28	233.8													
26-4, 68-70	234.2													
26-4, 68-70	234.2													
26-4, 68-70	234.2													
27-1, 107-110	239.6													
27-1, 107-110	239.6													
27-1, 107-110	239.6													
27-2, 119-122	241.2													
27-5, 60-63	245.1													
27-5, 86-89	245.4													
28-1, 90-93	248.9													
28-2, 86-86	250.4													
28-4, 34-37	252.9													
28-5, 88-91	254.9													
28-5, 108-111	255.1													
29-2, 30-33	259.3													
29-2, 36-39	259.4													
29-4, 110-113	263.1													
29-4, 138-141	263.4													
29-6, 14-17	265.2													
30-1, 86-90	267.9													
30-2, 75-79	269.3													
30-2, 79	269.3													
30-2, 84-87	269.4													
30-5, 103-107	274.													
30-5, 129-131	274.3													
30-7, 36-39	276.4													
31-1, 125-127	277.8													
31-1, 130-133	277.8													
31-3, 119-121	280.7													
31-5, 98-100	283.5													

Table 3. (Continued).

Sample (core-section, interval in cm)	Sub-bottom depth (m)	Sonic velocity (km/s)		2-min. GRAPE				Gravimetric			Acoustic impedance ($\times 10^5$ g/cm ² s)	Shear strength (kPa)	Thermal conductivity [$\times 10^{-3}$ (cal/ cm · s · deg)]
				Wet-bulk density (g/cm ³)		Porosity (%)		Wet-bulk density (g/cm ³)	Porosity (%)	Water (%)			
				H ^a	V ^a	H ^a	V ^a						
31-6, 111-114	285.1	1.629	1.642	1.92	1.90	46.6	47.8	1.88	50.6	27.5	3.09		
31-6, 135-138	285.4												
32-1, 52-55	286.5	1.636	1.650	1.82	1.88	52.5	49.0	1.87	51.4	28.2	3.09		> 115.30
32-1, 60-63	286.6												> 125.19
32-3, 106-109	290.1												> 116.13
32-5, 28-31	292.3												130.95
32-5, 34-37	292.4	1.661	1.654	1.92	1.93	46.6	46.0	1.91	48.9	26.2	3.16		
32-6, 102-105	294.5												65.89
33-1, 98-101	296.5												122.72
33-1, 104-107	296.5	1.661	1.671					1.91	50.0	26.8	3.19		
33-4, 82-85	300.8												110.36
33-6, 106-109	304.1												124.36
33-7, 23-26	304.7												112.01
33-7, 31-34	304.7	1.716	1.727	1.85	1.95	50.7	44.8	1.92	48.2	25.7	3.32		
34-2, 75-77	307.3												107.07
34-2, 82-86	307.4	1.626	1.614	1.86	1.89	50.1	48.4	1.84	53.3	29.7	2.97		
34-2, 95	307.5												2.100
34-4, 103-105	310.5												47.77
34-6, 108-112	313.6	1.673	1.675	1.96	1.98	44.2	43.0	1.92	48.8	26.0	3.22		
34-6, 115-118	313.7												> 121.89
35-1, 99-101	315.5												113.66
35-4, 97-99	320.												> 121.89
35-4, 103-106	320.	1.655	1.625	1.90	1.90	47.8		1.87	52.1	28.6	3.04		
35-6, 25-28	322.3												> 112.83
35-6, 33-36	322.3	1.651	1.638	1.78	1.95	54.9	44.8	1.89	50.4	27.2	3.10		
35-7, 39-41	323.9												113.66
36-1, 40-45	324.4	1.691	1.657	1.87	1.89	49.6	48.4	1.92	49.1	26.2	3.14		
36-2, 29-34	325.8	1.694	1.690	1.90	1.93	47.8	46.0	1.89	49.9	27.0	3.19		
37-1, 125	334.7												3.287
37-1, 133-135	334.8												> 113.66
37-2, 138-142	334.9	1.700	1.692	2.12	1.98	34.6	43.0	1.97	50.6	26.3	3.33		
37-4, 81-83	337.8												36.24
37-5, 89-93	340.4	1.610	1.604	1.83	1.87	51.9	49.6	1.82	55.1	31.0	2.92		
37-5, 93-96	340.5												65.89
37-6, 81-84	341.8												105.42
38-1, 84-87	543.9	1.633	1.650	1.66	1.74	62.1	57.3	1.74	60.6	35.7	2.87		
38-1, 103-106	344.0												98.83
38-6, 36-39	350.9												28.00
38-6, 82-85	351.3												56.0
38-7, 5-8	352.	1.662	1.639	1.85	1.88	50.7	49.0	1.82	57.0	32.0	2.98		
39-5, 49-52	359.	1.638	1.628	1.73	1.77	57.9	55.5	1.73	61.7	36.6	2.82		
40-1, 40-43	362.4	1.678	1.708	1.62	1.77	64.5	55.5	1.72	61.2	36.4	2.94		
40-4, 65-68	367.2	1.686	1.662	1.89	1.88	48.4	49.0	1.78	59.2	34.1	2.96		
40-6, 50-53	370.												75.77
41-1, 107-110	372.6												88.95
41-3, 90-95	375.4	1.635	1.647	1.86	1.86	50.1		1.77	58.2	33.7	2.92		
41-4, 28-31	376.3												93.89
41-4, 36-39	376.4	1.669	1.671	1.94	1.96	45.4	44.2	1.89	50.0	27.1	3.16		
42-1, 12-16	381.1	1.623	1.663	1.77	1.86	55.5	50.1	1.76	60.0	35.0	2.93		
42-4, 72-78	386.3	1.685	1.689	1.79	1.76	54.3	56.1	1.71	62.0	37.1	2.89		
42-7, 10	390.3												2.966
42-7, 33	390.3												3.200
43-1, 107-112	391.6	1.670	1.682	1.85	1.79	50.7	54.3	1.82	55.8	31.4	3.06		
43-2, 58-61	392.6												105.42
43-4, 18-24	395.2	1.628						1.74	59.8	35.2	2.83		
43-5, 99-103	397.5	1.645	1.689	1.59	1.68	66.3	60.9	1.65	65.4	40.6	2.79		
44-4, 123-128	405.8	1.719	1.691	1.91	1.92	47.2	46.6	1.79	59.8	34.1	3.03		
44-7, 17-20	409.2	1.638	1.622	1.79	1.74	54.3	57.3	1.70	63.0	38.0	2.76		
45-1, 136-140	410.9	1.705	1.663	1.74	1.81	57.3	53.1	1.71	63.1	37.9	2.84		
45-3, 42-48	412.9	1.664	1.702	1.75	1.73	56.7	57.9	1.66	66.4	41.0	2.83		
47-1, 32-36	428.8	1.668	1.688	1.81	1.80	53.1	53.7	1.74	60.7	35.8	2.94		
47-2, 131-135	431.3	1.594	1.595	1.72	1.61	58.5	65.1	1.67	61.6	37.7	2.66		
48-1, 105-109	439.1	1.661	1.622	1.74	1.78	57.3	54.9	1.69	63.0	38.2	2.74		
48-3, 63-67	441.7	1.654	1.613	1.80	1.91	53.7	47.2	1.76	59.2	34.6	2.84		
48-5, 113	445.1												2.875
48-6, 121-125	446.7	1.701	1.635	1.75	1.79	56.7	54.3	1.75	57.9	34.0	2.86		
49-1, 84-87	448.3	1.702	1.674	1.81	1.79	53.1	54.3	1.71	61.8	37.0	2.86		
49-4, 2-5	452.0	1.700	1.658	1.74	1.73	57.3	57.9	1.73	59.0	35.0	2.87		
50-1, 67-70	457.7	1.663	1.651	1.71	1.72	59.1	58.5	1.72	58.2	34.7	2.84		

Note: Some shear strength measurements exceeded instrumentation limits and are indicated by a greater than (>) symbol. These values are not plotted in any figures and the values are considered below failure strength of the material.

^a H = horizontal, V = vertical.

sedimentary sections were cored with a 1-in. plastic sampling tube, the cylindrical axis of which is perpendicular to the surface of the split core (presumably parallel to bedding in the hole). Velocity measurements on soft sediment were attempted only in a direction parallel to the mini-cylinder core axis. More consolidated samples were cut into cubes from the split cores in such a way that one pair of faces on the cube are parallel to the core axis and the other pair of cube faces are perpendicular to the core axis. The orientation of the cubic sample to the core axis will be denoted as "perpendicular" and "parallel" (implicitly, to the geologic formation in the hole), respectively, hereafter. Ultrasonic velocity measurements were made through both orientations of the cubic samples.

The accuracy of the velocity measurements was calibrated using three standards provided on the ship. Eleven test measurements were run on each standard: lucite, brass, and aluminum blocks. Errors for each test run were 1.0, 0.8, and 0.2%, respectively. The maximum error in the Hamilton Frame system itself is estimated to be 1.5%. This figure is probably not applicable to samples that do not have completely parallel surfaces or a sufficiently large ratio of length to thickness, as is probably true for most hand-trimmed samples. The accuracy and reproducibility of the velocity measurements is approximately 2%.

Gravimetric Data: Wet-Bulk Density, Porosity, and Water Content

Gravimetric data, as well as gamma-ray (GRAPE) density measurements and carbonate content, were determined for all the samples tested for sonic velocities. The density data were obtained by weighing water-saturated samples. Porosity and water content were then calculated by weighing these samples after dehydrating at 110°C in an oven.

Gamma-Ray Technique (2-minute GRAPE)

The 2-minute gamma-ray technique (GRAPE) was also used to determine the corrected wet-bulk density of individual consolidated samples. From the corrected wet-bulk density, the true wet-bulk density and porosity were calculated (based upon certain assumptions on the grain density of quartz and the corrected grain densities determined from the gravimetric measurements). Also, continuous GRAPE measurements for all of the recovered cores at Site 541 were performed immediately after recovery except for Cores 23 to 37, when the GRAPE machine was inoperative.

Shear Strength

Shear strength of semiconsolidated sediment in split sections of the cores was measured using a Wykeham Farrance Vane Shear Frame (model 23500, serial 861) and a Lebow Torque Sensor (model 1102-50, serial 1081) supplied by the U.S. Geological Survey. Shear strength measurements were recorded on an analog strip-chart recorder (Soltec model S-4201, serial 60158). Samples (e.g., Section 541-10,CC) were collected from the site of

each shear strength measurement for later analyses of water and carbonate content.

Thermal Conductivity

Thermal conductivity of selected sedimentary cores was measured by using a needle probe (serial no. 27, DSDP). The thermal conductivity κ was calculated by the following formula:

$$\text{Needle Probe (no. 27)} \kappa = \frac{(0.8774 \times 10^{-3}) [\ln (t_2/t_1)]}{T_2 - T_1 \text{ (cal/cm} \cdot \text{s} \cdot \text{deg)}}$$

where t and T are time and temperature, respectively. Recovered cores were allowed to equilibrate to the ambient room temperature for at least 4 hr. (often as long as 12 hr.).

PHYSICAL PROPERTIES RESULTS

All the results of physical property measurements on cores from Site 541 are listed in Tables 3 and 4 and shown diagrammatically in Figures 7 to 10.

Sonic Velocities

On the average, two ultrasonic measurements were made on samples from each core (Table 3). One distinctive observation is that the variation in compressional velocity throughout the entire hole is extremely uniform and quite small (Fig. 7). The slowest velocity, measured near the top of the hole at a sub-bottom depth of 7.5 m, is 1.482 km/s (Table 3). The fastest velocity, measured in the lower part of the hole at a sub-bottom depth of 305 m, is 1.727 km/s. Thus the maximum difference in velocity throughout the drilled section is one 245 m/s (0.245 km/s) or about 16.5%. As can be seen in Figure 7, the increase in velocity down the hole is very slight, very gradual, and linear.

To investigate further the rather monotonous increase in velocity with depth for Site 541, the vertical components of the sonic velocities were converted to acoustic impedance (denoted z hereafter), defined as:

$$z = \rho \cdot V_p \text{ or (density} \times \text{vertical velocity)}$$

Because acoustic impedance varies with both density and velocity and because the velocity increased very gradually down the hole, we hoped to find impedance variation corresponding to density variations. However, as can be seen in Figure 8, the density values of the samples are distributed in a narrow and limited range. Thus the computed impedance values listed in Table 3 and shown on Figure 7 mimic the trend of the sonic velocity and density values. The impedance values increase gradually with depth, except for a slight decrease below a sub-bottom depth of 340 m, which corresponds to a slight decrease in density at the same depth (see section below).

In order to describe the variation in velocity with depth, we calculated mean velocities for given depth increments as well as for the entire hole, as shown in Table 4. As this table shows, the average velocities paral-

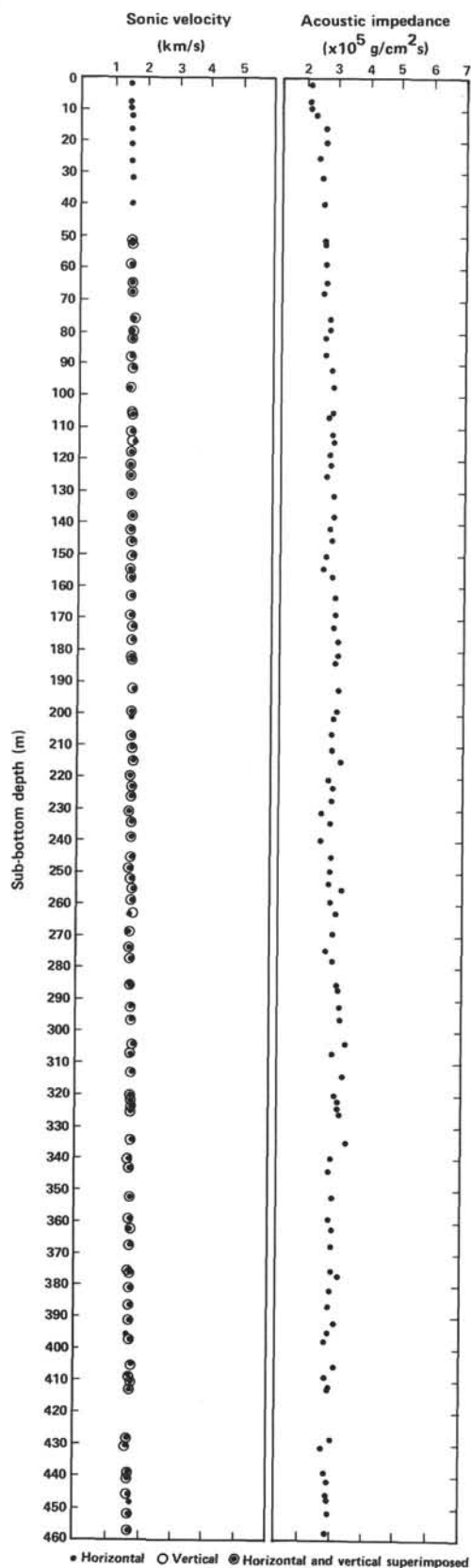


Figure 7. Plot of acoustic impedance and sonic velocity versus depth at Site 541. (Sonic velocities are calculated from recovered core samples and are *not* corrected to *in situ* values. Acoustic impedance values are also *not* corrected to *in situ* values.)

lel and perpendicular to the cores for the entire hole are virtually indistinguishable. This relationship suggests that core material from the site is acoustically isotropic.

In order to test whether samples from Site 541 are indeed acoustically isotropic, we computed relative anisotropy for each core sample from the relationship:

$$\text{Anisotropy } A_n (\%) = 100 \times (V_{\parallel} - V_{\perp}) / (V_{\parallel} + V_{\perp})$$

The results of these calculations are shown in Table 5. For all 88 computations, the average anisotropy, \bar{A}_n , is -0.05% with a standard deviation of 0.94% , which is statistically insignificant. If we exclude the last six calculations for Cores 48, 49, and 50, then the average anisotropy is -0.14% with a standard deviation of 0.90% , again a rather insignificant figure. If we now examine the six measurements for Cores 48 to 50, we find the average anisotropy is $+1.15\%$ with a standard deviation of 0.54% . This last figure of $+1.15\%$, albeit derived from a small population of 6, may be significant when correlated with lithologic and seismic reflection data from Site 541.

At a sub-bottom depth of 438 m at Site 541, the bit encountered a radiolarian-bearing, yellowish brown mudstone of the late early Miocene. These were the oldest beds as well as the only beds containing radiolarians recovered at Site 541. Although these beds do not differ significantly in terms of their velocity profile from the overlying sections, they are definitely anisotropic, unlike the rest of the hole.

To investigate further the acoustic and lithologic changes beginning at Core 48, we corrected the average velocities measured in the laboratory to *in situ* velocities. To correct the laboratory velocity values to *in situ*, we used the approach favored by Boyce (1976). According to Boyce, when sedimentary samples are brought from the subsurface to the ship, both the original *in situ* overburden pressure (p) and temperature (T) of the sample are changed to those of the laboratory. Using the empirical law given by Boyce (1976), correction factors used for obtaining *in situ* velocities are as follows:

- 1) 5% increase for sediment samples with porosities between 30% and 60%;
- 2) 3% increase for sediment samples with porosities between 20% and 30%;
- 3) no increase for porosities below 20%.

The average vertical velocity for Site 541, corrected for *in situ* conditions, is 1.693 km/s and was used in constructing the synthetic seismic-reflection profile shown in Figure 9. As this figure shows, there is an excellent correlation between a reflector observed on profile A1D across Site 541 (Figure 3) and the predicted lithologic change at a sub-bottom depth of 438 m (Core 48). Thus, to conclude, the section drilled at Site 541 is acoustically monotonous except for an anisotropic and lithologic boundary at a sub-bottom depth of 438 m (Core 48), a boundary where the oldest sedimentary section in the hole was recovered and a boundary that appears to correspond to a major reflection event on line A1D across the drilling site.

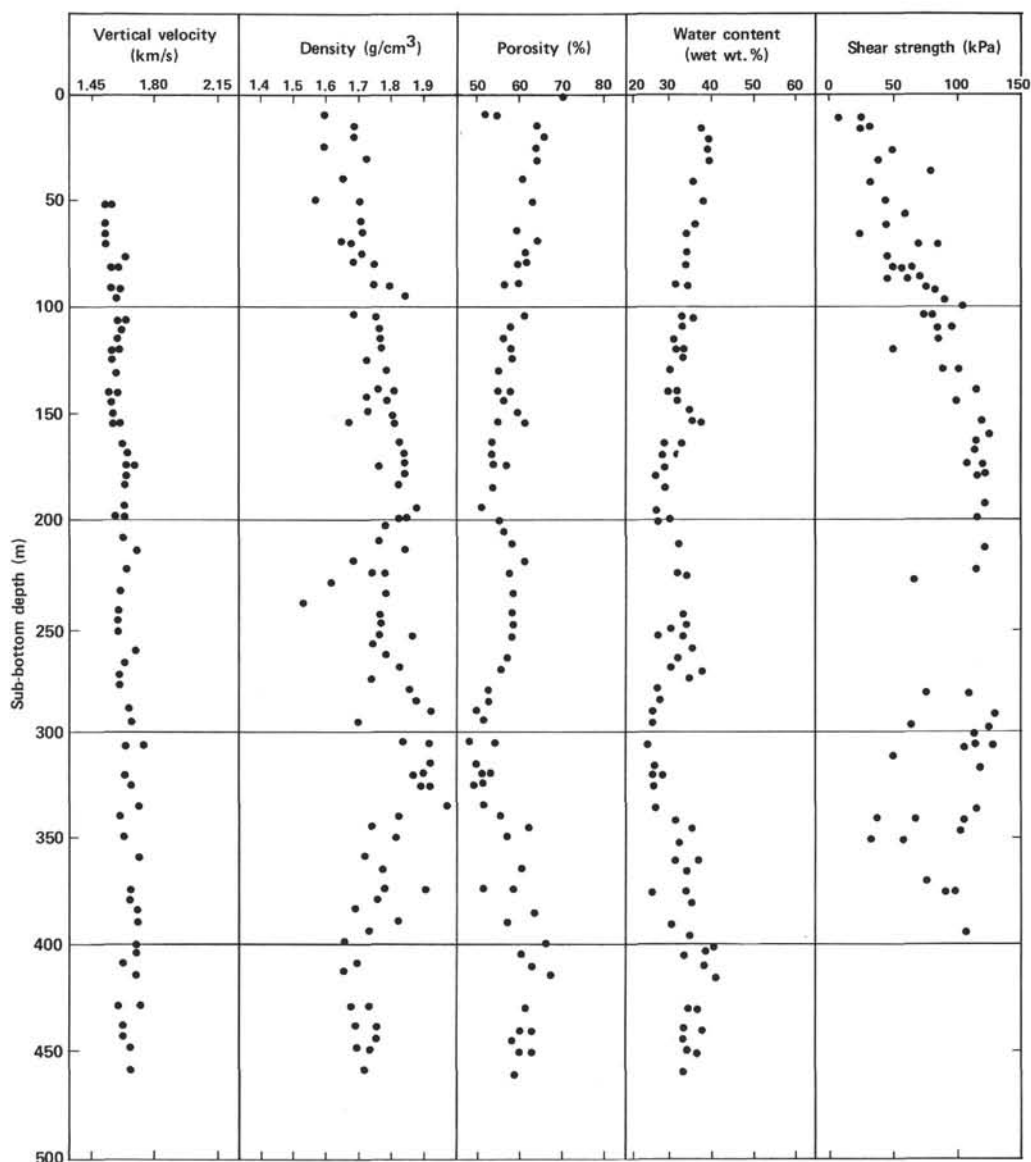


Figure 8. Plot of water content (wet wt. %), porosity (%), density (g/cm³), vertical velocity (km/s), and shear strength (kPa) values versus depth at Site 541.

Table 4. Average sonic velocities, Site 541.

Depth range m	\bar{V}_{\parallel}			\bar{V}_{\perp} ^a			
	(km/s)	S	N	(km/s)	S	N	
0-100	1.527	0.040	20	1.541	0.039	20	
100-200	1.597	0.031	22	1.595	0.032	22	
200-300	1.611	0.037	27	1.623	0.038	23	
300-400	1.661	0.029	21	1.663	0.032	20	
300-500	1.672	0.035	12	1.655	0.033	12	
Total	0-459	1.610	0.508	102	1.612	0.056	97

Note: \bar{V}_{\parallel} = average velocity presumed parallel to bedding and perpendicular to the core; \bar{V}_{\perp} = average velocity presumed perpendicular to bedding and parallel to the core; S = standard deviation; and N = number of samples.

^a Includes values of V_{\perp} in the upper 70 m of semiconsolidated material, where V_{\parallel} is assumed to be equal to V_{\perp} .

Porosity, Density, and Water Content

Porosity and density data were measured from selected core samples that were also analyzed for their acoustical properties using the Hamilton Frame device. Porosity and density analyses were made using gamma-ray techniques (2-min. GRAPE) and by gravimetric weighing. The difference between both methods is generally less than 5%, which is small enough to allow the use of the gamma-ray technique instead of gravimetric measurements for quick calculations. However, the gamma-ray method is based upon certain assumptions, and if these prerequisites were not satisfied, we found large deviations from the gravimetric data. The gravimetric results are used exclusively in the figure plots and subsequent calculations such as acoustic impedance.

Plots of water content, porosity, and density are shown in Figure 8. As noted earlier, density increases

Table 5. Calculated anisotropy values for individual core samples from Hole 541 (see text for derivation).

Sample (interval in cm)	Sub-bottom depth (m)	Anisotropy (%)	Sample (interval in cm)	Sub-bottom depth (m)	Anisotropy (%)
7-2, 109-112	51	-0.88	28-1, 90-93	249	-0.41
7-3, 53-56	52	-0.03	28-4, 34-37	253	-0.90
8-1, 69-71	59	-0.66	28-5, 108-111	255	-0.77
8-5, 42-46	65	0.62	29-2, 30-33	259	-0.34
8-7, 49-53	68	-0.63	29-4, 110-113	263	-4.13
9-6, 89-91	76	-2.90	30-2, 75-79	269	-1.38
10-2, 79-82	79	-1.01	30-5, 103-107	274	0.09
10-4, 50-53	82	0.36	31-1, 130-133	278	1.07
11-1, 99-102	88	-0.15	31-6, 111-114	285	-0.40
11-4, 54-57	92	-0.22	32-1, 52-55	287	-0.43
12-1, 118-122	97	-0.64	32-5, 34-37	292	0.21
12-7, 12-15	105	0.16	33-1, 104-107	297	-0.30
13-1, 89-92	106	-2.15	33-7, 31-34	305	-0.32
13-5, 41-44	112	-0.31	34-2, 87-86	307	0.37
13-7, 25-28	115	2.00	34-6, 108-112	314	-0.06
14-3, 40-43	118	0.16	35-4, 103-106	320	0.91
14-5, 70-73	122	-0.48	35-6, 33-36	322	0.40
15-1, 80-83	125	0.06	36-1, 40-45	324	1.02
15-5, 41-44	131	0.19	36-2, 29-34	326	0.12
16-3, 58-60	138	-0.25	37-1, 138-142	335	0.24
16-6, 50-52	142	0.54	37-5, 89-93	340	0.19
17-2, 35-38	145	0.38	38-1, 84-87	344	-0.52
17-5, 85-88	150	1.70	38-1, 5-8	352	0.70
18-1, 108-111	154	0.87	39-5, 49-52	359	0.31
18-3, 122-126	157	-0.25	40-1, 40-43	362	-0.89
19-1, 89-92	163	-0.50	40-4, 65-68	367	0.72
19-5, 64-67	169	-0.66	41-3, 90-95	375	-0.37
20-1, 76-79	173	-0.03	41-4, 36-39	376	-0.06
20-4, 39-43	177	-1.36	42-1, 12-16	381	-1.22
21-1, 72-76	182	-0.59	42-4, 72-78	386	-0.12
21-2, 51-54	184	-0.09	43-1, 107-112	392	-0.36
22-2, 21-24	193	-0.43	43-5, 99-103	398	-1.32
22-6, 91-94	199	-0.89	44-4, 123-128	406	0.82
23-1, 47-50	201	0.69	44-7, 17-20	409	0.49
23-5, 52-55	207	-0.06	45-1, 136-140	411	1.25
24-1, 69-72	211	-0.12	45-3, 42-48	413	-1.13
24-4, 66-69	215	-0.18	47-1, 32-36	429	-0.60
25-1, 101-104	221	-0.76	47-2, 131-135	431	-0.03
25-3, 54-57	223	0.37	48-1, 105-109	439	1.19
25-7, 28-31	227	-0.37	48-3, 63-67	442	1.26
26-2, 78-80	231	-0.03	48-6, 121-125	447	1.98
26-4, 68-70	234	1.28	49-1, 84-87	448	0.83
27-1, 107-110	240	-0.18	49-4, 2-5	452	1.25
27-5, 60-63	245	1.05	50-1, 67-70	458	0.36

gradually with depth until a sub-bottom depth of about 340 m, where the density decreases from 1.97 gm/cm³ to 1.74 gm/cm³ (a 12% decrease). Below 340 m sub-bottom the average density is nearly constant, about 1.75 gm/cm³, to the bottom of the hole.

The porosity and water content of samples from Site 541 decrease rapidly from near the seafloor to a sub-bottom depth about 15 m, and then the values decrease gradually to a depth near 150 m. At around 150 to 160 m below the seafloor, the porosity and water content exhibit a sharp increase and then sudden decrease, which may correspond to the Pliocene/Miocene boundary encountered in the hole at this depth. Below 160 m to the bottom of the hole, both the porosity and water content exhibit a cyclic increase and decrease in values over two cycles with a wave length of 120 to 140 m. This repetitious sinusoidal fluctuation in the two values may correspond to the stratigraphic repetition of Pliocene and Miocene sedimentary sequences across a major thrust fault near 276 meters sub-bottom (see the Lithology section, this chapter).

Shear Strength

Shear strength was measured for all but the lower few cores; the values are listed in Table 3 and are shown in Figures 4 and 8. Shear-strength measurements increase rapidly from the seafloor to a sub-bottom depth of

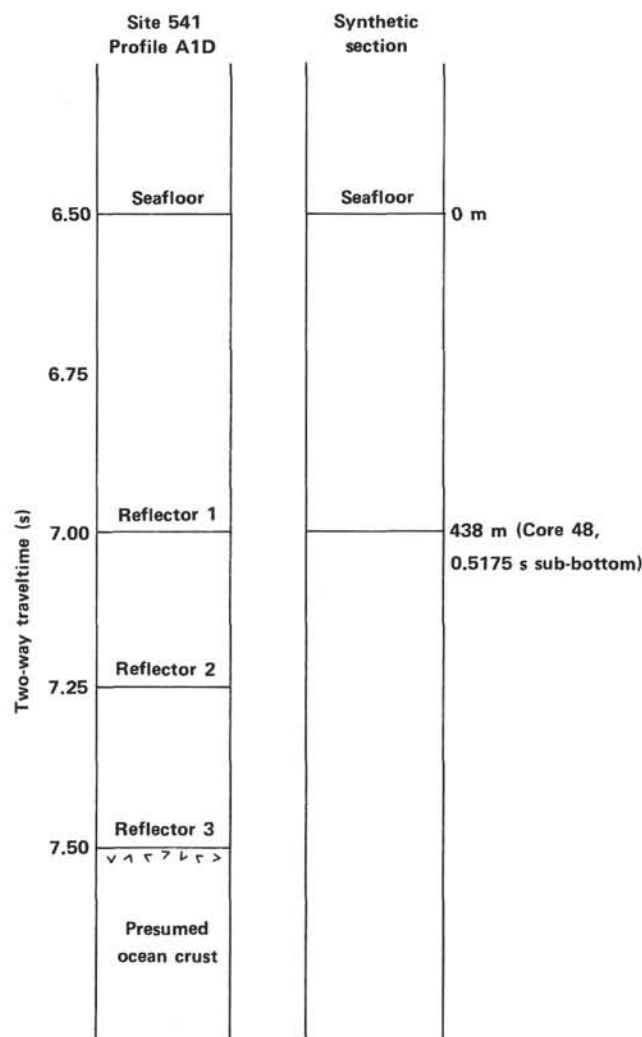


Figure 9. Interpretive seismic stratigraphy of Site 541 derived from seismic reflection profile A1D across the site compared to a synthetic profile based on physical properties of core samples from the site. (See text for explanation.)

about 140 m, although there is a great deal of scatter in the data from the upper cores (probably due to drilling disturbance). From 140 to 320 m shear-strength values are constant or decrease slightly. Below 280 m and a major reverse fault, the values are scattered but generally low. Note that the sudden change in shear-strength behavior occurs at a sub-bottom depth of 140 m, close to the boundary between the Pliocene and Miocene sedimentary sections. The fairly uniform values of shear strength from 140 to 320 m suggest that the cored strata in this interval have reached a maximum strength, perhaps due to consolidation from either overburden pressure or tectonic deformation or both.

Thermal Conductivity

A total of 14 conductivity measurements were made throughout the hole at Site 541. These values were used in conjunction with temperature readings measured by probe and logging techniques to calculate heat flow (see the Temperature Measurements section, this chapter;

and Davis et al., this volume). The conductivity of the semiconsolidated sedimentary strata with relatively high porosity (i.e., high water content) is low, around 2 to 3×10^{-3} cal/cm · s · deg. Near the Pleistocene/Pliocene boundary, conductivity values increase to a maximum reading of 3.924×10^{-3} cal/cm · s · deg. Values below this depth decrease slightly and average around 3.0×10^{-3} cal/cm · s · deg to the bottom of the hole. One interesting low value of 2.100×10^{-3} cal/cm · s · deg occurs about 307.5 m sub-bottom, just below a major thrust contact in the drilled sequence.

Continuous GRAPE (Gamma-Ray Measurement)

All cores except 32 to 37 were logged through GRAPE, and an uncorrected density data file was compiled on board ship. Before quantitative estimates of core density can be made, these data must be corrected for core diameter variation, lithology changes, material surrounding the core, and core alignment. Also, core disturbance, which is considerable in the upper muddy cores, may strongly influence GRAPE density.

Immediate qualitative comparison of core density may be made from the raw GRAPE density logs in semiconsolidated material. For cores of equal diameter, direct comparisons of varying lithologies can be made and density difference approximated. Breaks in the cores can be qualitatively eliminated and density-lithology comparisons made by comparing raw GRAPE logs with archive section photographs. Unfortunately, significant changes in lithology were not apparent either during vis-

ual inspection of the cores or in the density values from Site 541.

Some Related Findings

Figure 10 is a plot of porosity versus density measurements from cores taken at Site 541. Except for a few scattered points, most of the data plot as a linear function. Also shown is the empirically derived equation from DSDP relating density and porosity:

$$\rho_b = 2.70 - 1.675\phi \text{ (DSDP)}$$

where ρ_b = wet-bulk density of a sample and ϕ = porosity of a sample. As can be seen from the plot, the agreement is quite good between the observed data and the empirically derived relation. The implication, albeit speculative, is that the entire column of drilled strata is composed of mineralogically fairly uniform material without substantial change down the hole.

Discussion

The rather uniform nature of the physical properties measured at Site 541, including sonic velocities, densities, porosities, acoustic impedances, and so on, is rather surprising. Although lithologic and fossil data demonstrate that the site is underlain by repetitive stratigraphic sections in probable thrust contacts, the physical properties are remarkably uniform. If the hole at Site 541 did indeed penetrate an active convergence zone flanking the Lesser Antilles arc, then we are puzzled by

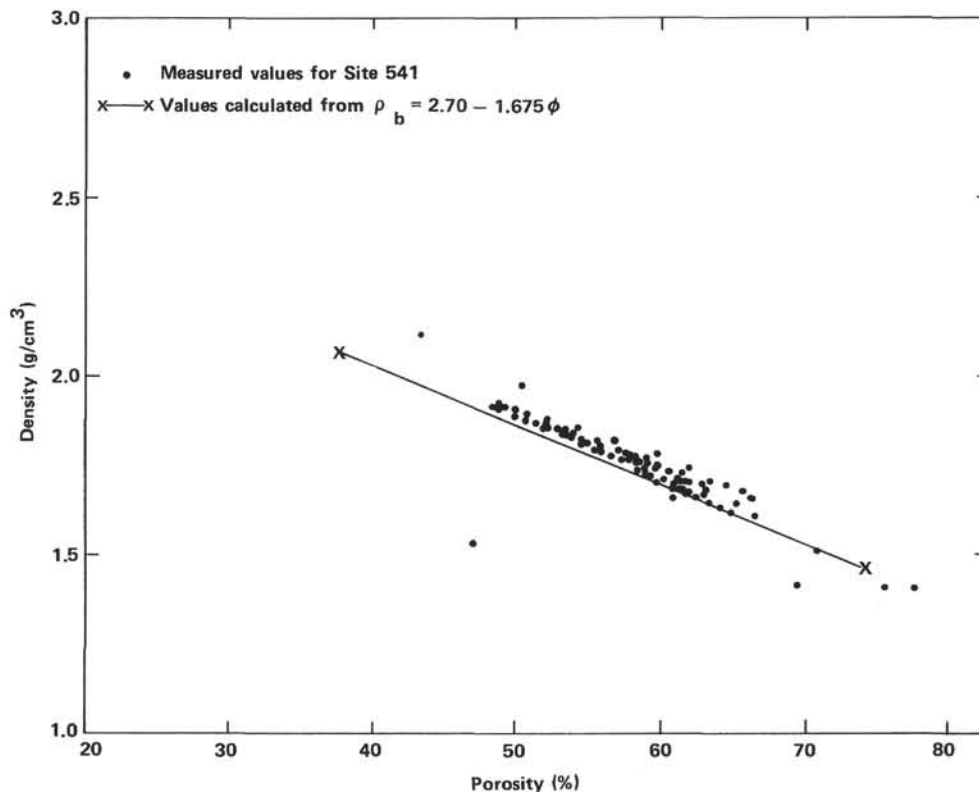


Figure 10. Plot of density versus porosity for core samples from Site 541. (See text for discussion.)

the lack of significant breaks in the physical properties of the cored material.

Perhaps the explanation for the uniform behavior of strata in what is thought to be a highly tectonized subduction zone lies in the *in situ*, interstitial pore fluids within the subduction complex. These fluids may be absorbing the tectonic "shock" of overburden pressure as well as lateral motion from the underthrusting Atlantic Plate. Mobilized, high-pressurized pore water may allow the sedimentary section to deform very uniformly with depth in the convergence zone, giving rise to the uniform physical properties measured in the recovered cores. Moreover, actual *in situ* variations may exist in the form of fracture porosity that would be impossible to measure on small shipboard samples.

PALEOMAGNETICS

Paleomagnetic sampling for Site 541 was carried out with two objectives: to help determine age by polarity stratigraphy; and to infer *in situ* structure with estimates of bed strikes. To avoid problems with drilling disturbance or rotation due to undetected tectonic tilting, samples were only taken at visible beds. Drilling and tectonic disturbance led to no samples being taken from the intervals 0 to 59 m, 209 to 289 m, and 341–376 m. Generally the sample interval was 1 to 2 m, with occasional gaps of several meters due to lack of recovery or the disturbed nature of the core. Because of the high sedimentation rate, this rather sparse sample interval was adequate for polarity stratigraphy over most of the hole.

In the less consolidated parts of the core, samples were taken by pressing at least one plastic cube ($2 \times 2 \times 1.5$ -cm) into each section. These cubes, scribed with arrows pointing upcore, were pried from the rest of the core. In the more consolidating regions, an upcore arrow was scribed directly on the core, and a sample of measurable size was sawn or drilled. The samples were measured on the shipboard Digico fluxgate spinner magnetometer, with alternating field demagnetization studies carried out using the Schoenstedt alternating-field demagnetizer. For some of the specimens, follow-up studies were done on the SCT (Superconducting Technology) two-axis cryogenic magnetometer with built-in alternating-field demagnetizer at Stanford University. For the shipboard measurements, the most straightforward procedure was to imagine an arrow on the top (upcore side) of each specimen pointing toward the upcore arrow scribed on the side of the sample. The hypothetical arrow corresponds to the fiducial line referred to in the Digico manual and allows the samples to be measured without using the time-consuming field or bedding corrections. The Digico convention defines the coordinate system for relative declinations: the direction normal to and away from the cut surface of the core is 0° , increasing clockwise looking downcore. In this coordinate system, the working half of the core is the "south" half. This same coordinate system was used to record strikes and dips of bedding for structural analysis. At each measurable bed, the core was sliced to give apparent dips in two different planes, defining the bedding plane.

The strike of the bed was taken to be the line in the bedding plane normal to the axis of the core. By convention, the strikes recorded are 90° counterclockwise from the down-dip direction. The magnetization directions are corrected for bedding by rotating the direction about the strike line by the amount of the dip.

Figure 11 shows the stable inclinations for the upper 210 m; refer to Wilson (this volume) for a complete presentation of the data. Site 541 latitude is 15° , which should be valid for the entire Neogene. This latitude predicts a di-pole inclination of 28° , which is far enough from horizontal for polarity interpretation, but shallow enough that some horizontal magnetizations should be expected from normal secular variation. Based on this information, a sample with a stable inclination greater than $+10^\circ$ was judged to be normal, and one with less than -10° , reversed.

The interval from 59 to 200 m (Cores 8–22) worked quite well for polarity stratigraphy (see Wilson, this volume; and Fig. 6). The first sample (59.4 m) is normal, corresponding to either the oldest Brunhes (0.7 Ma) or the Jaramillo event (0.91–0.97 Ma; ages are from Ness et al., 1980). Other recognizable markers are at 88 to 90 m (Core 11, Sections 2 and 3)—the Olduvai event (1.66–1.87 Ma); the Matuyama/Gauss transition (2.47 Ma) at 120.5 m (Core 14, Section 4); the Gauss/Gilbert

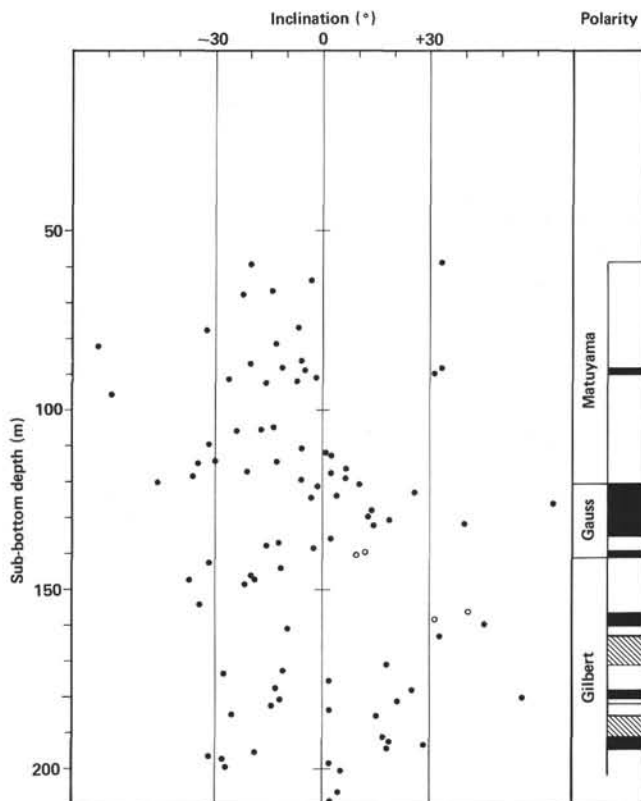


Figure 11. Stable magnetic inclination versus sub-bottom depth, and polarity interpretation. (Black areas indicate normal polarity; white areas show reversed polarity; cross-hatching shows polarity is uncertain or data are missing. Solid vertical lines at $+30^\circ$ and -30° give possible range of secular variation. Open circles represent data judged to be less reliable than that represented by filled circles.)

transition (3.40 Ma) at ~141 m (Core 16, Section 6); and the first normal event in the Gilbert epoch (3.86 Ma) at 156 m (Core 18, Section 3). If there is a fault at the base of Core 19, the polarity information would indicate about 20 m of repeated section, with the first normal event in the Gilbert occurring again at 178 m (Core 20, Section 5). This correlation is consistent with the two thick ash beds in Core 18 (541-18-1, 140 cm and 541-18-2, 135 cm) being the equivalent to the two thick beds in Core 20 (541-20-1, 119 cm and 541-20-3, 15 cm). The polarity transition at 195 m (Core 22, Section 3) probably corresponds to the last normal event in the Gilbert (4.79 Ma).

The samples from 289 to 340 m (Cores 32–37) have a high percentage of horizontally magnetized samples, and our few confident polarity determinations are too far apart for polarity stratigraphy. The samples from 382 to 419 m (Cores 42–44) at first looked promising. Fourteen of fifteen samples have inclinations between 21 and 38 (without tectonic correction), and all of these samples have very high intensities and show exceptional directional stability. However, applying the tectonic correction to the two samples from the overturned section in Core 43, Section 5 resulted in nearly horizontal magnetizations, strongly suggesting a postdeformational magnetization. This interpretation is supported by the failure to observe similar properties of intensity or stability in any samples that might be the same age at Site 543. The most likely candidate for resetting the magnetization is thermal or chemical changes associated with the warm water observed at the bottom of the hole.

The interpretation of *in situ* structure provided interesting results. Of the samples collected at dipping beds, twelve have very stable direction, and eight of these have unambiguous polarity. For the samples with clear polarity, true north was assumed to be the declination direction for normal samples, and declination minus 180° for reversed rocks. The apparent *in situ* strikes and down-dip directions in Table 6 and Figure 12 are relative to this north. For any one sample, the uncertainty in this technique is estimated to be about 40°. The eight samples

Table 6. Structural interpretation based on paleomagnetic data for Hole 541.

Sample (core-section, cm level)	Bedding (relative to core)		Magnetization (corrected)			Apparent <i>in situ</i>	
	Strike	Dip	Incl.	Decl.	Polarity ^a	Strike	Down-dip direction
18-1, 39	300°	20°	-17°	36°	R	84°	S
18-5, 133	0°	20°	45°	162°	N	198°	WNW
19-1, 77	130°	40°	32°	348°	N	142°	SW
19-6, 110	0°	10°	18°	210°	N	150°	SW
22-1, 64	150°	25°	17°	320°	N	190°	W
32-3, 29	210°	45°	-30°	315°	R	75°	SSE
37-3, 81	330°	25°	-37°	69°	R	81°	S
37-5, 78	0°	15°	21°	188°	N	172°	W
Polarity ambiguous						Strike (0–180°)	
23-1, 78	310°	15°	5°	46°		84°	
23-5, 78	150°	40°	4°	317°		13°	
33-6, 75	50°	45°	-4°	157°		13°	
34-1, 32	60°	30°	-6°	76°		164°	

^a R = reversed, N = normal.

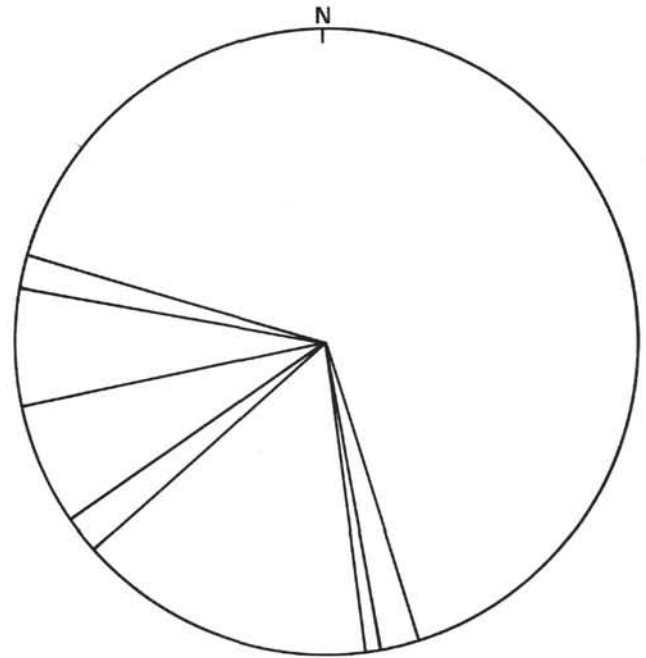


Figure 12. Projected down-dip directions for dipping beds (from Table 6).

with clear polarity scatter about dip directions to the southwest, and the samples with ambiguous polarity are not inconsistent with this. The best interpretation of these data seems to be that the regions of horizontal bedding are separated by bands of monoclinical folding.

TEMPERATURE MEASUREMENTS

Four temperature measurements were made at Site 541. Two were made in the mud at the bottom of the hole during pauses in the drilling process using the Tokyo T-probe (e.g., Uyeda and Horai, 1982), and two consisted of short excursions of the Gearhart-Owen logging tool past the end of the pipe. The high temperatures measured (roughly 15°C at less than 170 m sub-bottom) are consistent with rapid upward migration of warm water. For additional details, see Davis et al. (this volume).

SEISMIC STRATIGRAPHY

As described by Ngokwey et al. (this volume), Site 541 is near the intersection of lines A1D and A1E and the sequence recorded on the seismic reflection records consists of two seismic sequences:

1) 500 m/s of acoustically discontinuously reflective character without any coherent reflectors;

2) 500 m/s of an acoustically layered sequence resting on the deepest reflector (Reflector 3) that is presumed to be oceanic crust.

These two units are separated by a prominent reflector (Reflector 1), which can be followed in Figure 3 from beneath the Atlantic abyssal plain to the west for some 20 km beneath the eastern flank of the Barbados Ridge.

From 0 to 276 m (sub-bottom) the well-layered Pleistocene–Pliocene–upper Miocene sequence does not exhibit any major sharp lithologic boundaries that would

yield impedance contrasts and resultant seismic reflections. The poor reflectivity of this section is due to the lack of significant changes in the physical properties.

At 276 m a sharp fault contact was penetrated that separates upper Miocene clays (above) from nannofossil-foraminifer oozes of the lower upper Pliocene (below). This tectonic-stratigraphic inversion is not observed in processed seismic reflection records. The lack of a reflection event at this boundary is probably due to the fact that we found no significant contrasts in velocity or density in the recovered cores from this depth. However, even though reverse faults were observed in Core 30 (near and on the contact itself), the fault discontinuity could be parallel to regional bedding, that is, relatively flat, and not appear as a significant reflector.

From 276 m to the total depth (459 m) drilled, the lithological changes are again very gradual; shearing, development of scaly foliation, and brecciation do not correspond to any major change in physical properties of the cores. From velocity calculations (Fig. 7), Reflector 1, which seismically defines the bottom of the discontinuously reflective sequence, should coincide with the deformation zone at the base of the hole. Sheared yellowish brown radiolarian oozes encountered in this deformation zone (between 438 and 459 m) may correspond to Reflector 1 and hence to the top of the underthrust sedimentary section. Reflector 1 also corresponds to the anisotropic fabric in the lowermost cores of Site 541 (see Physical Properties section, this chapter).

SUMMARY AND CONCLUSIONS

At Site 541 we cored 459 m and recovered seven lithologic units ranging in age from Quaternary to early Miocene. A major reverse fault occurs at 276 m, as documented by repetition of units. Smaller-scale repetitions occur at 75 to 80 m, 172 m, and 263 m. Repetitions at 172 m, 263 m, and 276 m are associated with stratal disruption and/or significant displacements, hence are probably of tectonic origin. The small (~6 m) displacement and soft consistency of the sediments at 75 to 80 m possibly suggests slump origin of this repetition. A zone of stratal disruption at the base of the hole suggests proximity to a major fault.

Unit 1, of the Quaternary (Cores 1–8; 0–65 m), consists of nannofossil mud with common ash layers, whereas Unit 2 (Quaternary–lower Pliocene; Cores 9–15; 65–135 m) is composed of marly nannofossil ooze and marly foraminifer ooze with rare ash layers. Unit 3 (Cores 16–25, Section 3, 50 cm); 135–215 m; lower Pliocene–upper Miocene), composed of nannofossil mud with ash layers, overlies mud of Unit 4 (Core 25, Section 3, 50 cm to Core 30, Section 6, 215–276 m; upper Miocene), which in turn is faulted against the ashy nannofossil mud of Unit 5 (Core 30, Section 6–Core 37; 276–340 m; upper Pliocene–upper Miocene). Unit 6 (Cores 37–47, Section 2, 50 cm; 340–340 m), upper Miocene mudstone, is succeeded downsection by lower Miocene radiolarian mud of Unit 7 (Core 47, Section 2, 50 cm–Core 50; 430–459 m). Lithologic Units 1 to 4 make up Tectonic Unit A, which overlies Tectonic Unit B (Lithologic Units 5–7) along the major reverse fault at 276 m.

Overall, the deposits cored at Site 541 accumulated in a hemipelagic to pelagic setting at a modest sedimentation rate (see the Accumulation Rates chapter, Wright, this volume), interrupted only by the occasional influx of ash beds and the downslope transport of foraminifer-rich turbidites. The clay mineralogy, as determined by X-ray diffraction, indicates mixed volcanic and continental terrigenous sources. The lack of terrigenous turbidites suggests that the section at Site 541 accumulated on a high, possibly the Tiburon Rise. Each Tectonic Unit A and B at Site 541 exhibits a downsection transition from a paleoenvironment at or near the lysocline in the Pliocene to one respectively at or below the CCD in the late Miocene. Time correlative rocks in Unit A accumulated in slightly shallower water than those in Unit B. Temporal variations in the CCD recorded in both units may principally stem from its Miocene shallowing (Berger, 1977), though independent vertical tectonic motions cannot be discounted.

The ash beds in cores from Site 541 provide an historical record of arc volcanism and a precise correlation tool. The temporal frequency of ash beds suggests a climax in eruptive activity in the early Pliocene, followed by a lull in the late Pliocene, culminating with a renewed burst of activity in the Quaternary. The repetition of a distinctive ash-bed sequence from Cores 18, 20, and 34 supports reverse faulting at 172 and 263 to 276 m.

Small-scale structural fabrics occur at both the base of the hole and in association with the documented reverse faults at 263 and 276 m. Inclined beds occur below 125 m with true dips of up to 45°. The stratal disruption and scaly fabrics characteristic of mudstones above the major reverse fault contrast with the general lack of pervasive fabrics in subjacent nannofossil mud. Fracturing, intense scaly foliation, and stratal disruption characterize cores that locally resemble fault gouge within 100 m of the base of Hole 451. This concentrated deformation zone may reflect proximity to a décollement separating offscraped and subducted rocks. High concentrations of smectite distinguish both this basal shear zone and the beds near the reverse fault at 172 m, and a deformed zone above the major reverse fault at 276 m.

Seismic reflection profiles through Site 541 reveal a discontinuously reflective unit overlying an acoustically layered sequence. Shipboard velocity measurements suggest penetration just through the discontinuously reflective unit. The sheared radiolarian mudstone below 450 m at Site 541 may correspond to a prominent reflector at the top of the acoustically layered sequence. Velocity-density data reveal no impedance contrasts across the faults at 172 and 276 m.

Extremely low levels of hydrocarbon gases (parts per billion) occur in cores from Site 541. Most samples show a full range of C₂ to C₆ hydrocarbons and C₁:C₂ ratios varying from 10 to 20:1, suggesting *in situ* thermogenic generation of the hydrocarbons. The rate of increase of C₂ to C₆ with depth suggests a moderate geothermal gradient. Similarly heat probe and downhole temperature logs indicate anomalously high temperatures at shallow depths.

Penetration of biostratigraphically defined reverse faults in a modern subduction zone is the most significant

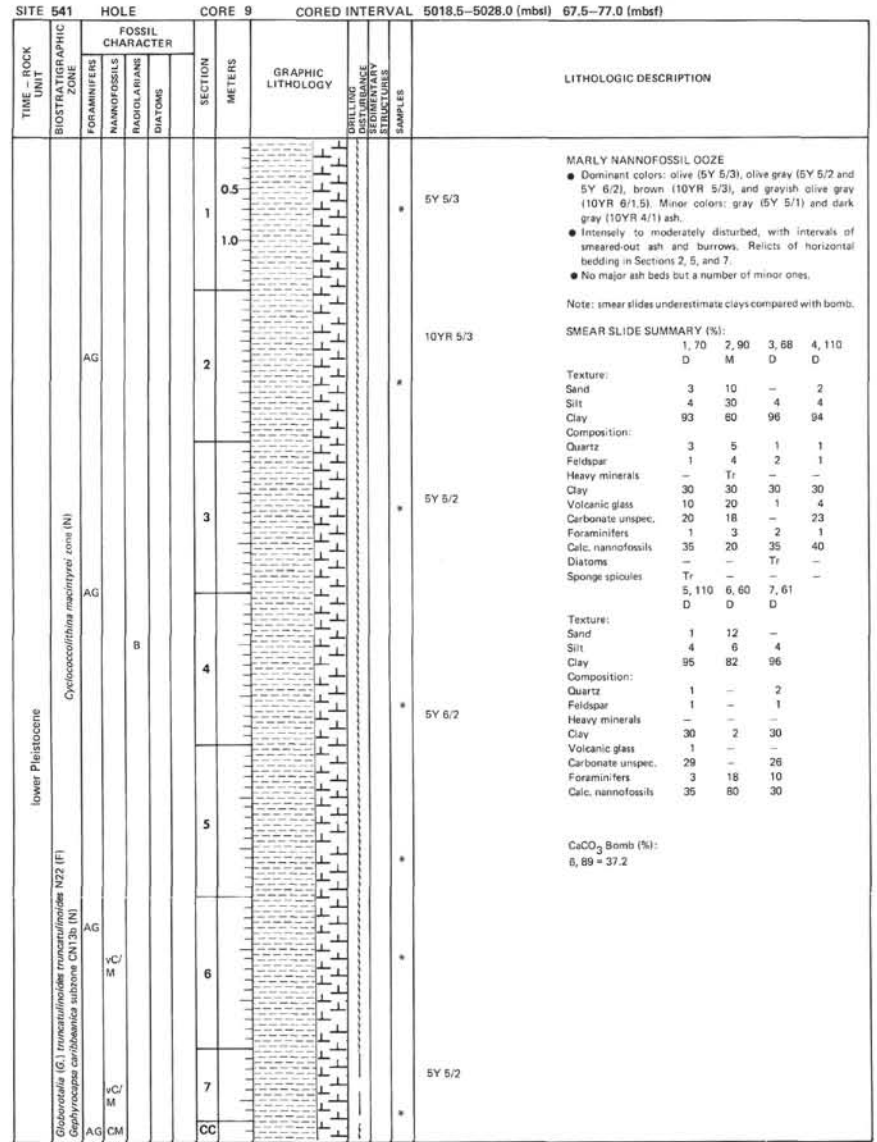
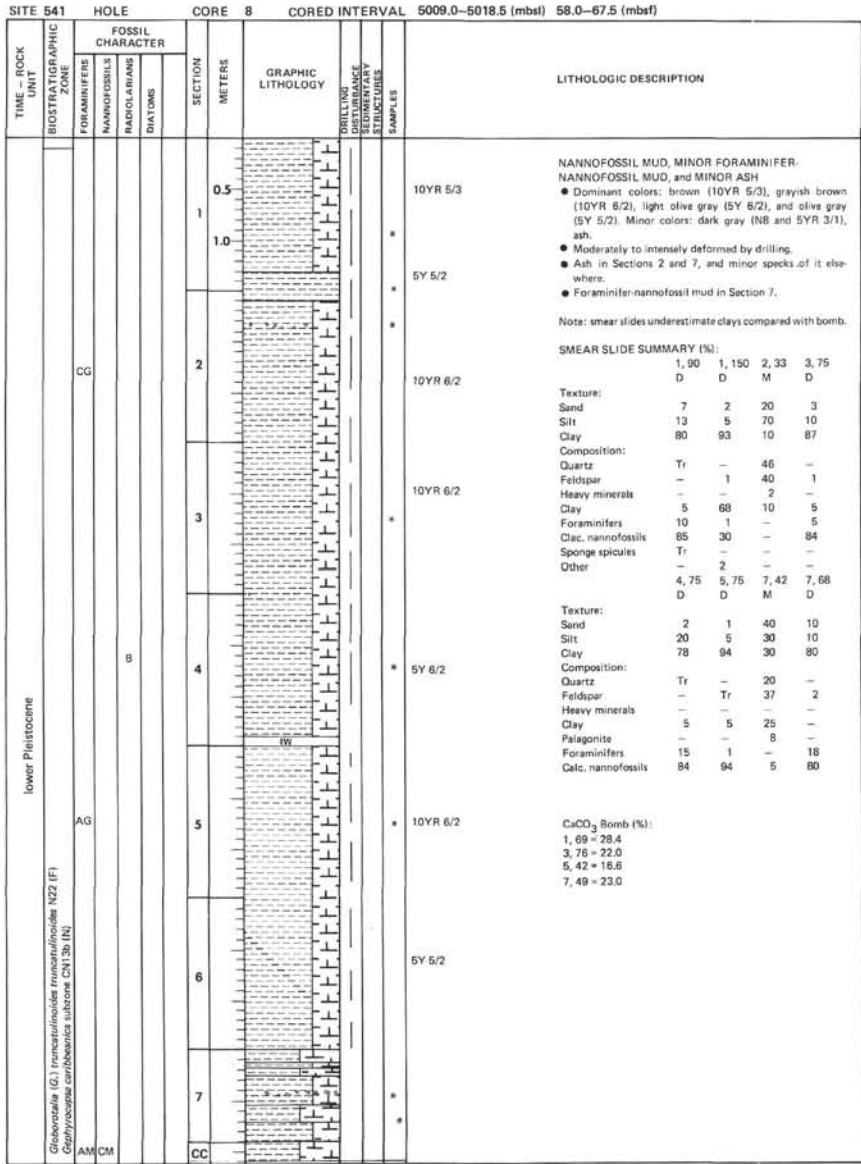
result of drilling at this site. Although the exact origin of this imbricated sequence remains in doubt, the basal transition to radiolarian mudstone favors oceanic origin and hence offscraping. Faulting must postdate the early late Pliocene, the age of the youngest rocks of the lower plate. The lack of a documented middle Miocene section at the base of the hole could be due to structural attenuation in the basal shear zone or a hiatus or a condensed section.

REFERENCES

- Bé, A. W. H., 1980. Gametogenic calcification in a spinose planktonic foraminifer, *Globigerinoides sacculifer* (Brady). *Mar. Micropaleontol.*, 5:283-310.
- Berger, W. H., 1968. Planktonic foraminifera: selective solution and paleoclimatic interpretation. *Deep-Sea Res.*, 15:31-43.
- , 1970. Planktonic foraminifera: selective solution and the lysocline. *Mar. Geol.*, 8:111-138.
- , 1977. Carbon dioxide excursion and the deep-sea record: aspects of the problem. In Anderson, N. R., and Malahoff, A. (Eds.), *The Fate of Fossil Fuel CO₂ in the Oceans*: New York (Plenum Press), pp. 505-542.
- , 1979. Preservation of foraminifera. In *Foraminiferal Ecology and Paleocology*, Soc. Econ. Paleontol. Mineral. Short Course, 6:105-155.
- Berggren, W. A., 1973. The Pliocene time scale: calibration of planktonic foraminiferal and calcareous nannoplankton zones. *Nature*, 243:391-397.
- Blow, W. H., 1969. Late middle Eocene to recent planktonic biostratigraphy. In Bronnimann, P., and Renz, H. H. (Eds.), *Proc. First Int. Conf. Planktonic Microfossils, Geneva, 1967*, 1:199-422.
- Boyce, R. E., 1976. Definitions and laboratory techniques of compressional sound velocity parameters and wet-water content, wet bulk density and porosity parameters by gravimetric and gamma-ray attenuation techniques. In Schlanger, S., Jackson, E. D., et al., *Init. Repts. DSDP*, 33: Washington (U.S. Govt. Printing Office), 931-957.
- Bukry, D., and Okada, H., 1980. Supplementary modification and introduction of code numbers to the low-latitude Cocolith biostratigraphic zonation. *Mar. Micropaleontol.* 5:321-325.
- Carey, S. N., and Sigurdsson, H., 1980. The Roseau ash: deep-sea tephra deposits from a major eruption on Dominica, Lesser Antilles arc, *J. Volcanol. Geotherm. Res.*, 7:67-86.
- Carroll, D., 1970. Clay minerals: a guide to their X-ray identification. *Geol. Soc. Am. Spec. Pap.* 126.
- Cowan, D. S., 1982. Origin of "vein structure" in slope sediments of the inner slope of the Middle America Trench off Guatemala. In Aubouin, J., von Huene, R., et al., *Init. Repts. DSDP*, 67: Washington (U.S. Govt. Printing Office), 645-650.
- Ekdale, A. A., 1974. Geologic history of the abyssal benthos: evidence from trace fossils in Deep Sea Drilling Project cores (Ph.D. dissert.). Rice University, Houston, Texas.
- Gartner, S., 1977. Calcareous nannofossil biostratigraphy and revised zonation of the Pleistocene. *Mar. Micropaleontol.*, 2:1-25.
- Gartner, S., and Bukry, D., 1975. Morphology and phylogeny of the Cocolithophyceae family, Ceratolithaceae. *J. Res. U.S. Geol. Surv.*, 3:451-469.
- Lundberg, N., and Moore, J. C., 1982. Structural features of the Middle America trench slope off southern Mexico, Deep Sea Drilling Project Leg 66. In Watkins, J. S., Moore, J. C., et al., *Init. Repts. DSDP*, 66: Washington (U.S. Govt. Printing Office), 793-814.
- Ness, G., Levi, S., and Couch, R., 1980. Marine magnetic anomaly time scales for the Cenozoic and Late Cretaceous: a precis, critique, and synthesis. *Rev. Geophys. Space Phys.*, 18:753-770.
- Parker, F. L., and Berger, W. H., 1971. Faunal and solution patterns of planktonic foraminifera in surface sediments of the South-Pacific. *Deep-Sea Res.*, 18:73-107.
- Riedel, W. R., and Sanfilippo, A., 1978. Stratigraphy and evolution of tropical Cenozoic radiolarians. *Micropaleontology*, 23:61-69.
- Sanfilippo, A., and Riedel, W. R., in press. Revision of the radiolarian genera *Theocotyle*, *Theocotylissa*, and *Thyrsoctyrtis*. *Micropaleontology*.
- Schnitker, D., 1979. Cenozoic deep water benthic foraminifers, Bay of Biscay. In Montadert, L., Roberts, D. G., et al., *Init. Repts. DSDP*, 48: Washington (U.S. Govt. Printing Office), 377-414.
- Sparks, R. S. J., Sigurdsson, H., and Garey, S. N., 1980. The entrance of pyroclastic flows into the sea, I. Oceanographic and geologic evidence from Dominica, Lesser Antilles. *J. Volcanol. Geotherm. Res.*, 7:87-96.
- Thunell, R. C., and Honjo, S., 1981. Calcite dissolution and the modification of planktonic foraminiferal assemblages. *Mar. Micropaleontol.*, 6:169-182.
- Uyeda, S., and Horai, K., 1982. Heat flow measurements on Deep Sea Drilling Project Leg 60. In Hussong, D. M., Uyeda, S., et al., *Init. Repts. DSDP*, 60: Washington (U.S. Govt. Printing Office), 789-800.

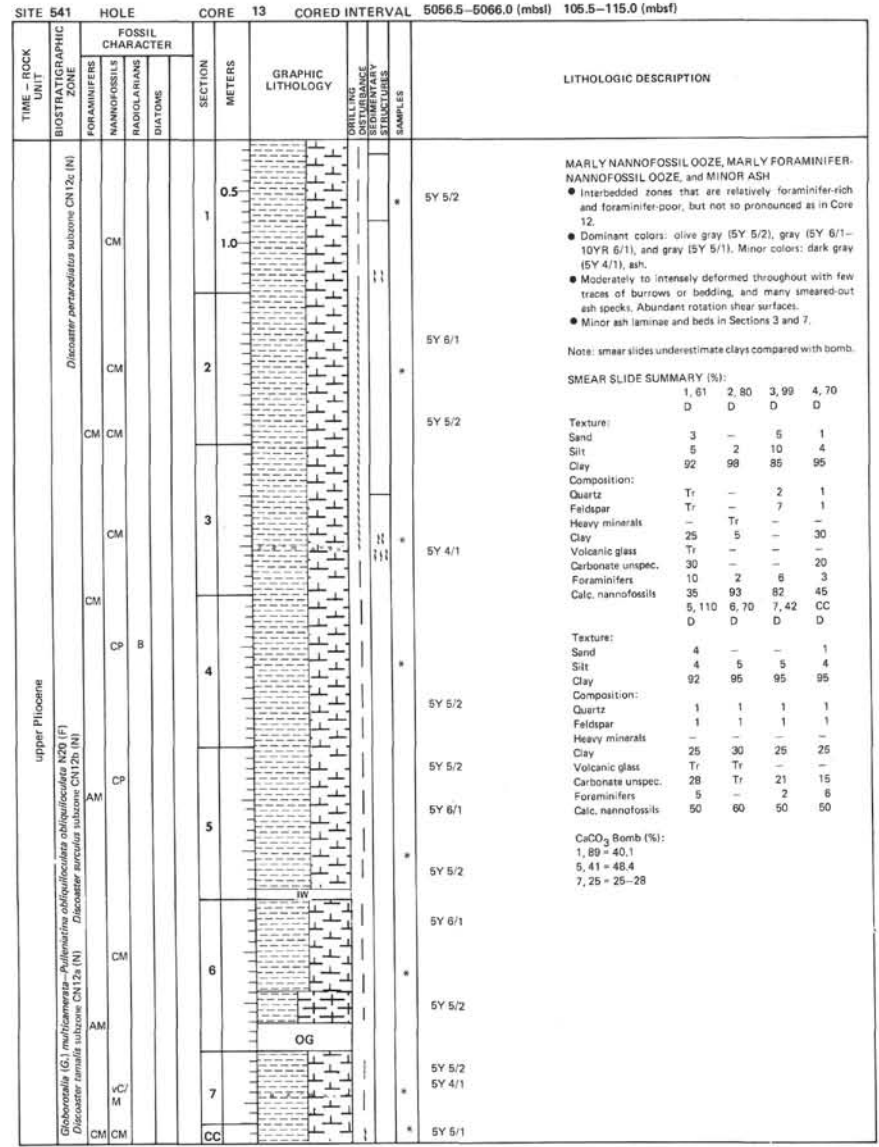
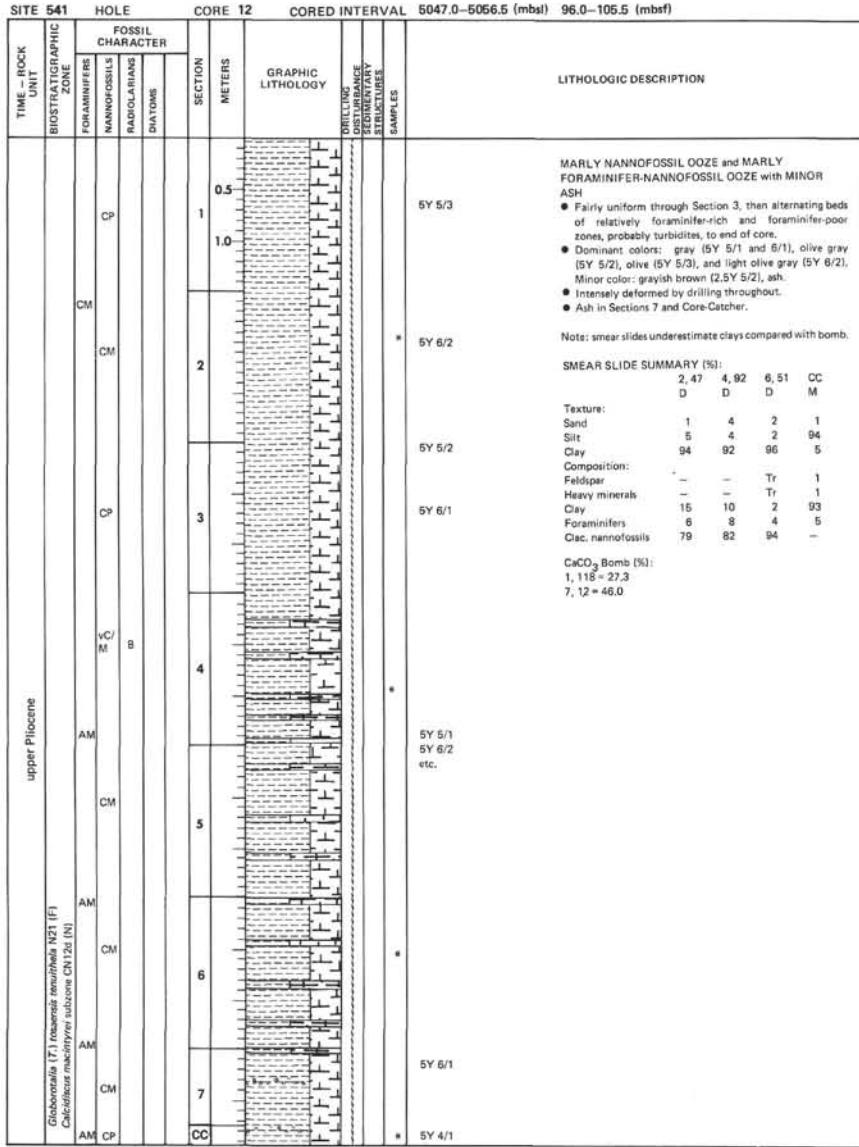
SITE 541		HOLE		CORE 3		CORED INTERVAL		4961.5-4971.0 (mbsf) 10.5-20.0 (mbsf)										
TIME - ROCK UNIT	BIOSTRATIGRAPHIC ZONE	FOSSIL CHARACTER			SECTION METERS	GRAPHIC LITHOLOGY	DRILLING DISTURBANCE	SEMI-QUANTITATIVE STRATIGRAPHIC SAMPLES	LITHOLOGIC DESCRIPTION									
		FORAMINIFERS	NANNOFOSSILS	RADIOLARIANS						DIATOMS								
lower-upper Pleistocene	Emiliana ovata subzone CN14a (N)	AG	CM		1		* * * * * * * * *	NANNOFOSSIL MUD with MINOR MUD and VOLCANIC ASH • Dominant colors: olive gray (5Y 5/2) and olive (5Y 5/3), with lesser gray (5Y 6/1) and gray (10YR 6/6) (ashy). • Core is intensely disturbed by drilling and has rust particles upper 15 cm. • Grayer intervals due to ash, now distorted by drilling. SMEAR SLIDE SUMMARY (%): <table border="1"> <tr> <td></td> <td>1, 10</td> <td>1, 104</td> <td>2, 80</td> <td>3, 73</td> </tr> <tr> <td></td> <td>D</td> <td>M</td> <td>D</td> <td>D</td> </tr> </table> Texture: Sand Tr 10 1 Tr Silt 5 75 5 Tr Clay 75 15 94 100 Composition: Quartz 5 10 1 1 Feldspar 5 15 2 2 Heavy minerals Tr Tr - Tr Clay 20 5 25 - Volcanic glass - 70 - - Carbonate unsp. 35 - 38 45 Foraminifers Tr - 1 - Calc. nannofossils 35 - 30 30 Diatoms Tr - - - Radiolarians - - 2 - 4, 55 CC, 5 D D		1, 10	1, 104	2, 80	3, 73		D	M	D	D
			1, 10	1, 104	2, 80				3, 73									
			D	M	D				D									
		AG	CM		2				5Y 5/3	5Y 5/3	5Y 5/3							
		AG	VC/M		3				5Y 5/3	5Y 5/3	5Y 5/3							
		AG	CM		4				5Y 5/3	5Y 5/3	5Y 5/3							
		AG	VC/M		CC				5Y 6/1	5Y 5/2	5Y 5/2							
		AG	CM															
		AG	CM															
		AG	CM															
AG	CM																	
AG	CM																	

SITE 541		HOLE		CORE 4		CORED INTERVAL		4971.0-4980.5 (mbsf) 20.0-29.5 (mbsf)												
TIME - ROCK UNIT	BIOSTRATIGRAPHIC ZONE	FOSSIL CHARACTER			SECTION METERS	GRAPHIC LITHOLOGY	DRILLING DISTURBANCE	SEMI-QUANTITATIVE STRATIGRAPHIC SAMPLES	LITHOLOGIC DESCRIPTION											
		FORAMINIFERS	NANNOFOSSILS	RADIOLARIANS						DIATOMS										
lower-upper Pleistocene	Emiliana ovata subzone CN14a (N)	AG	VC/M		1		* * * * * * * * *	NANNOFOSSIL MUD with MINOR ASH • Dominant colors: olive gray (5Y 5/2) and olive (5Y 5/3), with dark gray (10YR 4/1) ash and streaks of light brownish gray (2.5YR 6/2) ash. • Core is intensely disturbed throughout. Recovery (9.81 m) exceeded core interval (9.5 m) because of squeeze-up. Deformation less in Section 6 where there is a horizontal bedding plane. SMEAR SLIDE SUMMARY (%): <table border="1"> <tr> <td></td> <td>1, 70</td> <td>2, 70</td> <td>3, 100</td> <td>3, 136</td> <td>4, 100</td> </tr> <tr> <td></td> <td>D</td> <td>D</td> <td>D</td> <td>M</td> <td>D</td> </tr> </table> Texture: Sand 1 1 1 30 2 Silt 2 2 2 50 3 Clay 97 97 97 20 95 Composition: Quartz Tr Tr 1 30 1 Feldspar - - 1 40 2 Heavy minerals - - Tr Tr Clay 35 40 35 10 30 Volcanic glass - - 2 20 4 Carbonate unsp. 25 29 26 - 33 Foraminifers Tr Tr - - - Calc. nannofossils 40 30 45 - 30 Radiolarians Tr 1 - - - 5, 100 6, 130 6, 140 7, 53 7, 66 D D D M D		1, 70	2, 70	3, 100	3, 136	4, 100		D	D	D	M	D
			1, 70	2, 70	3, 100				3, 136	4, 100										
			D	D	D				M	D										
		AG	VC/M		2				5Y 5/3	5Y 5/3	5Y 5/3									
		AG	VC/M		3				5Y 5/3	5Y 5/3	5Y 5/3									
		AG	VC/M		4				5Y 5/2	5Y 5/2	5Y 5/2									
		AG	VC/M		5				5Y 5/2	5Y 5/2	5Y 5/2									
		AG	VC/M		6				5Y 5/2	5Y 5/2	5Y 5/2									
		AG	VC/M		7				5Y 5/2	5Y 5/2	5Y 5/2									
		AG	VC/M																	
AG	VC/M																			



SITE 541		HOLE		CORE 10		CORED INTERVAL		5028.0-5037.5 (mbsl) 77.0-86.5 (mbsf)																																																			
TIME - ROCK UNIT	BIOSTRATIGRAPHIC ZONE	FOSSIL CHARACTER			SECTION METERS	GRAPHIC LITHOLOGY	DISTURBANCE STRUCTURES	SAMPLES	LITHOLOGIC DESCRIPTION																																																		
		FORAMINIFERS	NANNOFOSSILS	RADIOLARIANS						DIALONES																																																	
lower Pleistocene	<i>Globorotalia</i> (G.) <i>truncatulinoides</i> truncatulinoides N22 (F) <i>Gephyrocapsa</i> <i>caribbaeensis</i> subzone CN13b (N)	VC	M			0.5			5Y 5/2	<p>MARLY NANNOFOSSIL OOZE with MINOR ASH</p> <ul style="list-style-type: none"> ● Dominant colors: olive (5Y 5/2) and gray (5Y 5/1). Minor colors: olive (10YR 4/2) and olive brown (10YR 5/2) thin beds and laminae; gray (5Y 5/1) ash. ● Moderately deformed with some arching of beds and horizontal rotation shear surfaces. ● Thin ash bed in Section 1. ● Traces of horizontal bedding and burrowing. <p>Note: smear slides underestimate clays compared with bomb.</p>																																																	
		AG				1.0			5Y 5/1																																																		
		VC	M			2			5Y 5/2																																																		
		VC	M							5Y 5/2	<p>SMEAR SLIDE SUMMARY (%):</p> <table border="1"> <tr> <td></td> <td>1, 70</td> <td>2, 85</td> <td>3, 120</td> <td>4, 32</td> <td>4, 87</td> </tr> <tr> <td>D</td> <td>D</td> <td>D</td> <td>D</td> <td>D</td> <td>D</td> </tr> </table> <p>Texture:</p> <table border="1"> <tr> <td>Sand</td> <td>Tr</td> <td>2</td> <td>-</td> <td>-</td> <td>Tr</td> </tr> <tr> <td>Silt</td> <td>3</td> <td>10</td> <td>4</td> <td>3</td> <td>4</td> </tr> <tr> <td>Clay</td> <td>97</td> <td>88</td> <td>96</td> <td>97</td> <td>96</td> </tr> </table> <p>Composition:</p> <table border="1"> <tr> <td>Feldspar</td> <td>Tr</td> <td>Tr</td> <td>-</td> <td>-</td> <td>Tr</td> </tr> <tr> <td>Heavy minerals</td> <td>-</td> <td>-</td> <td>-</td> <td>-</td> <td>Tr</td> </tr> <tr> <td>Clay</td> <td>5</td> <td>3</td> <td>40</td> <td>12</td> <td>15</td> </tr> </table>		1, 70	2, 85	3, 120	4, 32	4, 87	D	D	D	D	D	D	Sand	Tr	2	-	-	Tr	Silt	3	10	4	3	4	Clay	97	88	96	97	96	Feldspar	Tr	Tr	-	-	Tr	Heavy minerals	-	-	-	-	Tr	Clay	5	3	40	12	15
			1, 70	2, 85	3, 120	4, 32	4, 87																																																				
		D	D	D	D	D	D																																																				
		Sand	Tr	2	-	-	Tr																																																				
Silt	3	10	4	3	4																																																						
Clay	97	88	96	97	96																																																						
Feldspar	Tr	Tr	-	-	Tr																																																						
Heavy minerals	-	-	-	-	Tr																																																						
Clay	5	3	40	12	15																																																						
VC	M							5Y 5/2																																																			
AM								5Y 5/1																																																			
VC	M							GAS																																																			
AG								OG																																																			
VC	M							5Y 5/2	<p>SMEAR SLIDE SUMMARY (%):</p> <table border="1"> <tr> <td></td> <td>1, 70</td> <td>2, 85</td> <td>3, 120</td> <td>4, 32</td> <td>4, 87</td> </tr> <tr> <td>D</td> <td>D</td> <td>D</td> <td>D</td> <td>D</td> <td>D</td> </tr> </table> <p>Texture:</p> <table border="1"> <tr> <td>Sand</td> <td>2</td> <td>Tr</td> <td>1</td> <td>-</td> <td>-</td> </tr> <tr> <td>Silt</td> <td>10</td> <td>3</td> <td>4</td> <td>9</td> <td>3</td> </tr> <tr> <td>Clay</td> <td>88</td> <td>97</td> <td>95</td> <td>97</td> <td>97</td> </tr> </table> <p>Composition:</p> <table border="1"> <tr> <td>Feldspar</td> <td>Tr</td> <td>-</td> <td>-</td> <td>-</td> <td>-</td> </tr> <tr> <td>Heavy minerals</td> <td>Tr</td> <td>Tr</td> <td>Tr</td> <td>Tr</td> <td>-</td> </tr> <tr> <td>Clay</td> <td>40</td> <td>20</td> <td>12</td> <td>40</td> <td>20</td> </tr> </table>		1, 70	2, 85	3, 120	4, 32	4, 87	D	D	D	D	D	D	Sand	2	Tr	1	-	-	Silt	10	3	4	9	3	Clay	88	97	95	97	97	Feldspar	Tr	-	-	-	-	Heavy minerals	Tr	Tr	Tr	Tr	-	Clay	40	20	12	40	20		
	1, 70	2, 85	3, 120	4, 32	4, 87																																																						
D	D	D	D	D	D																																																						
Sand	2	Tr	1	-	-																																																						
Silt	10	3	4	9	3																																																						
Clay	88	97	95	97	97																																																						
Feldspar	Tr	-	-	-	-																																																						
Heavy minerals	Tr	Tr	Tr	Tr	-																																																						
Clay	40	20	12	40	20																																																						
VC	M							5Y 5/2																																																			
AG								5Y 5/1																																																			
VC	M							5Y 5/1																																																			
AG								5Y 5/1																																																			
VC	M							5Y 5/1-5Y 5/2																																																			
AG								5Y 5/1-5Y 5/2																																																			

SITE 541		HOLE		CORE 11		CORED INTERVAL		5037.5-5047.0 (mbsl) 86.5-96.0 (mbsf)																																																								
TIME - ROCK UNIT	BIOSTRATIGRAPHIC ZONE	FOSSIL CHARACTER			SECTION METERS	GRAPHIC LITHOLOGY	DISTURBANCE STRUCTURES	SAMPLES	LITHOLOGIC DESCRIPTION																																																							
		FORAMINIFERS	NANNOFOSSILS	RADIOLARIANS						DIALONES																																																						
lower Pleistocene	<i>Globorotalia</i> (G.) <i>truncatulinoides</i> truncatulinoides N22 (F) <i>Emiliana</i> <i>annula</i> subzone CN13a (N)	VC	M			0.5			5Y 5/3	<p>MARLY NANNOFOSSIL OOZE with MINOR ASH</p> <ul style="list-style-type: none"> ● Dominant colors: olive (5Y 5/3), gray (5Y 6/1 and 5/1), light olive gray (5Y 6/2), and light brownish gray (2.5Y 6/2). Minor color: light brownish gray (2.5Y 6/2). ● Intensely to moderately deformed with smeared out burrows and minor ash throughout. ● Thin ash bed in Section 3. ● Traces of horizontal bedding preserved in places. <p>Note: smear slides underestimate clays compared with bomb.</p>																																																						
		AG				1.0			2.5Y 6/2																																																							
		VC	M							5Y 5/1																																																						
		AG								5Y 6/2																																																						
upper Pliocene	<i>Globorotalia</i> (G.) <i>truncatulinoides</i> truncatulinoides N21 (F) <i>Emiliana</i> <i>annula</i> subzone CN120 (N)	VC	M						5Y 6/1	<p>SMEAR SLIDE SUMMARY (%):</p> <table border="1"> <tr> <td></td> <td>1, 80</td> <td>2, 80</td> <td>3, 25</td> <td>3, 80</td> <td>4, 80</td> </tr> <tr> <td>D</td> <td>D</td> <td>D</td> <td>M</td> <td>D</td> <td>D</td> </tr> </table> <p>Texture:</p> <table border="1"> <tr> <td>Sand</td> <td>1</td> <td>3</td> <td>15</td> <td>5</td> <td>3</td> </tr> <tr> <td>Silt</td> <td>10</td> <td>10</td> <td>20</td> <td>10</td> <td>10</td> </tr> <tr> <td>Clay</td> <td>89</td> <td>87</td> <td>65</td> <td>85</td> <td>87</td> </tr> </table> <p>Composition:</p> <table border="1"> <tr> <td>Quartz</td> <td>-</td> <td>-</td> <td>20</td> <td>1</td> <td>Tr</td> </tr> <tr> <td>Feldspar</td> <td>Tr</td> <td>-</td> <td>15</td> <td>Tr</td> <td>1</td> </tr> <tr> <td>Heavy minerals</td> <td>1</td> <td>-</td> <td>1</td> <td>Tr</td> <td>Tr</td> </tr> <tr> <td>Clay</td> <td>-</td> <td>-</td> <td>59</td> <td>-</td> <td>-</td> </tr> </table> <p>Carbonate unspec. Tr - - - - - Foraminifers 5 13 - - - - - Calc. nannofossils 94 87 5 85 87</p> <p>CaCO₃ Bomb (%): 1, 99 = 36.7 4, 54 = 35.7</p>		1, 80	2, 80	3, 25	3, 80	4, 80	D	D	D	M	D	D	Sand	1	3	15	5	3	Silt	10	10	20	10	10	Clay	89	87	65	85	87	Quartz	-	-	20	1	Tr	Feldspar	Tr	-	15	Tr	1	Heavy minerals	1	-	1	Tr	Tr	Clay	-	-	59	-	-
			1, 80	2, 80	3, 25	3, 80	4, 80																																																									
		D	D	D	M	D	D																																																									
		Sand	1	3	15	5	3																																																									
Silt	10	10	20	10	10																																																											
Clay	89	87	65	85	87																																																											
Quartz	-	-	20	1	Tr																																																											
Feldspar	Tr	-	15	Tr	1																																																											
Heavy minerals	1	-	1	Tr	Tr																																																											
Clay	-	-	59	-	-																																																											
AG								5Y 6/1																																																								
VC	M							5Y 6/1																																																								
AG								5Y 6/1																																																								



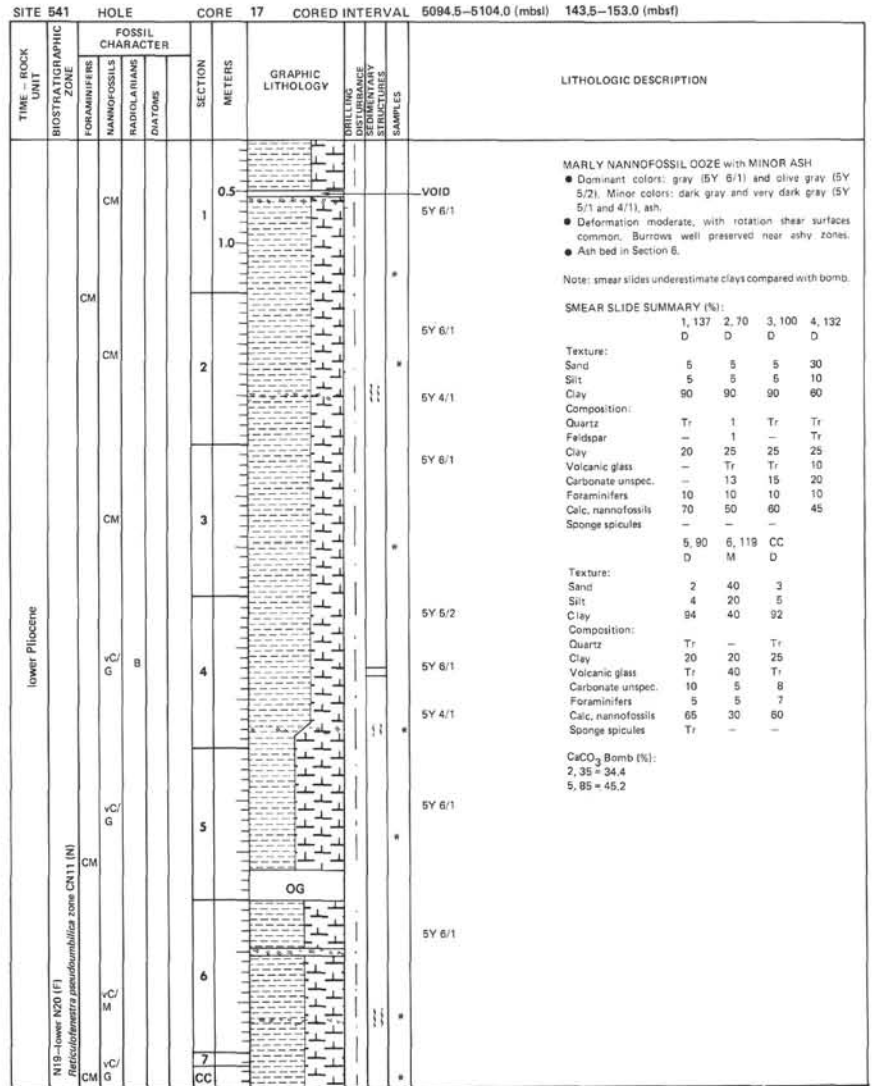
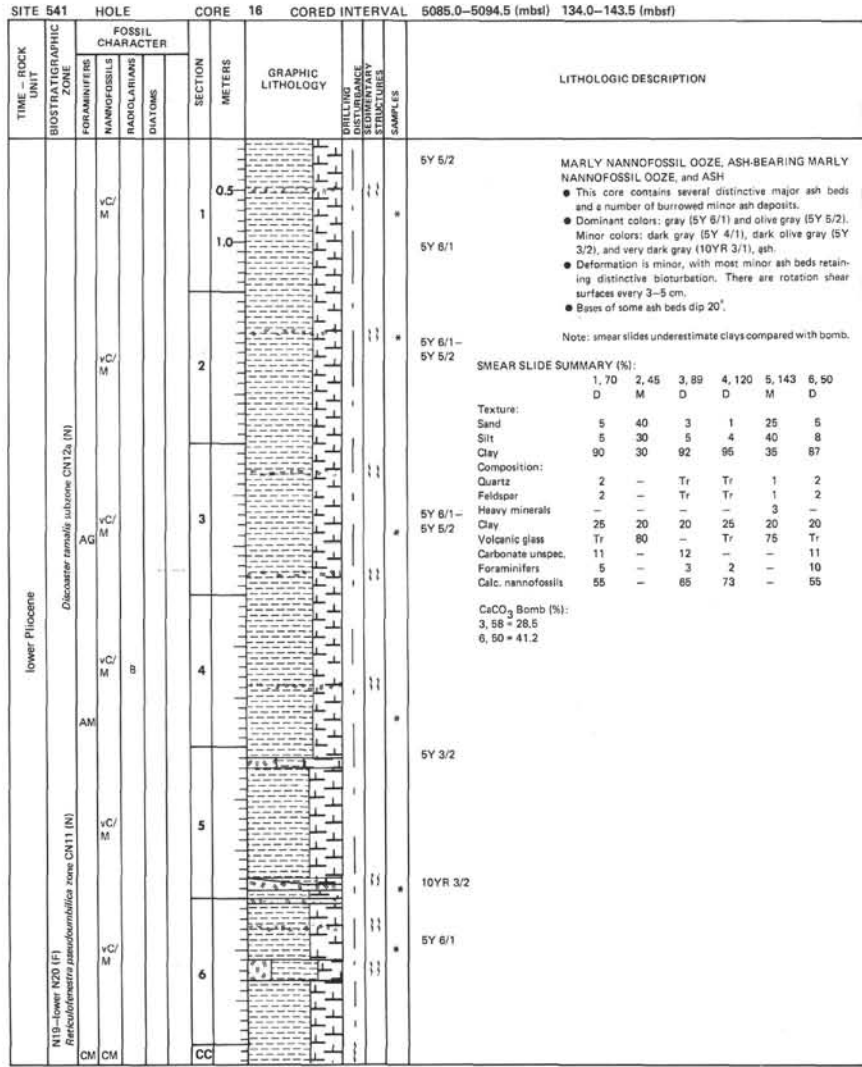
SITE 541		HOLE		CORE 14		CORED INTERVAL		5066.0-5075.5 (mbsf)		115.0-124.5 (mbsf)			
TIME - ROCK UNIT	BIOSTRATIGRAPHIC ZONE	FOSSIL CHARACTER			SECTION	METERS	GRAPHIC LITHOLOGY	DRILLING DISTURBANCE	STRUCTURE	SAMPLES	LITHOLOGIC DESCRIPTION		
		FORAMINIFERS	NANNOFOSSILS	RADIOLARIANS								DIATOMS	
upper Pliocene	<i>Globorotalia</i> (G.) <i>multicarinata</i> - <i>Puffinbergeria obliquifurcata obliquifurcata</i> N20 (F) <i>Discosaster tanaisalis</i> subzone CN12a (N)	vC/M				0.5					5Y 5/2	MARLY NANNOFOSSIL OOZE and MARLY FORAMINIFER-NANNOFOSSIL OOZE ● Sections 1-3 relatively uniform. Sections 4-Core Catcher contain rhythmic beds of relatively foraminifer-poor and foraminifer-rich material, probably turbidites. ● Dominant colors: olive gray (5Y 5/2) and gray (5Y 6/1). ● Deformation moderate; rotation shear surfaces common. ● There are only specks of ash in this core. Note: smear slides underestimate clays compared with bomb.	
		M				1.0					5Y 6/1		
		AG											
		CM					2						5Y 5/2
		vC/M											5Y 5/2
		M											5Y 5/2
		B											5Y 6/1
AG										5Y 6/1-5Y 5/2			
AM											5Y 5/2		
CM											5Y 6/1-5Y 5/2		
CP											5Y 5/2		
CM											5Y 5/2		
AM											5Y 5/2		
CM											5Y 5/2		
AM											5Y 5/2		
CM											5Y 5/2		
CC											5Y 5/2		

SITE 541		HOLE		CORE 15		CORED INTERVAL		5075.5-5085.0 (mbsf)		124.5-134.0 (mbsf)				
TIME - ROCK UNIT	BIOSTRATIGRAPHIC ZONE	FOSSIL CHARACTER			SECTION	METERS	GRAPHIC LITHOLOGY	DRILLING DISTURBANCE	STRUCTURE	SAMPLES	LITHOLOGIC DESCRIPTION			
		FORAMINIFERS	NANNOFOSSILS	RADIOLARIANS								DIATOMS		
lower-upper Pliocene	<i>Sphaerostoma obliquifurcata obliquifurcata</i> N20 (F) <i>Discosaster tanaisalis</i> subzone CN12a (N)	CM				0.5					5Y 5/2	MARLY NANNOFOSSIL OOZE, MARLY FORAMINIFER-NANNOFOSSIL OOZE, and MINOR ASH ● Dominant colors: olive gray (5Y 5/2), and gray (5Y 5/1). ● Mainly uniform ooze, but with some zones relatively rich in foraminifers. Deformation moderate to slight. Burrowing faint except near thin ash zones. ● Ash bed in Section 5. Note: smear slides underestimate clays compared with bomb.		
		AM				1.0								
		vC/M											5Y 5/2	
		M												5Y 5/2
		FP												5Y 5/2
		vC/M												5Y 5/2
M											5Y 5/2			
CM											5Y 5/1			
B											5Y 5/2			
CM											5Y 5/2			
OG											5Y 5/2			
vC/M											5Y 5/2			
M											5Y 5/2			
vC/M											5Y 5/1			
M											5Y 5/1			
CC											5Y 5/1			

SMEAR SLIDE SUMMARY (%):

	1,90	2,35	3,90	4,70	5,119	5,143
	D	D	D	D	M	D
Texture:						
Sand	2	30	3	2	25	5
Silt	4	20	5	6	15	5
Clay	94	50	92	92	60	90
Composition:						
Quartz	1	1	1	2	1	1
Feldspar	1	1	1	2	1	2
Clay	20	15	20	20	20	20
Volcanic glass	-	2	Tr	2	30	Tr
Zeolite	13	-	-	-	-	-
Carbonate unsp. spec.	-	10	18	11	18	12
Foraminifers	5	30	5	3	-	10
Calc. nannofossils	60	40	55	60	30	55

CaCO₃ Bomb (%):
1, 80 = 31.4
5, 41 = 30.4



SITE 541		HOLE		CORE 20		CORED INTERVAL		5123.0-5132.5 (mbsl) 172.0-181.5 (mbst)																																						
TIME - ROCK UNIT	BIOSTRATIGRAPHIC ZONE	FOSSIL CHARACTER			SECTION METERS	GRAPHIC LITHOLOGY	DRILLING DISTURBANCE	SECONDARY STRUCTURES	SAMPLES	LITHOLOGIC DESCRIPTION																																				
		FORAMINIFERS	NANNOFOSSILS	RADIOLARIANS							DIAZONIA																																			
lower Pliocene	N17-N18 (F) Ceratolithus rugosus subzone CN11a (N)	CM	M	B	1	0.5				5Y 5/2	<p>MARLY NANNOFOSSIL OOZE and MINOR ASH</p> <ul style="list-style-type: none"> ● Dominant colors: olive gray (5Y 5/2), gray (5Y 6/1), olive (5Y 5/3). Minor colors: dark gray (5Y 4/1), gray (5Y 5/1), black (5Y 2.5/1) (ash), light greenish gray (5GY 6/1) (alteration next to ash). ● Abundance of ash contributes to grayer colors than in Core 19. ● Major ash beds in Sections 2, 3, and 6. ● Deformation moderate; rotation shear surfaces every 2-6 cm. Burrows intact especially near ashy zones. <p>Note: smear slides underestimate clays compared with bomb.</p> <p>SMEAR SLIDE SUMMARY (%):</p> <table border="1"> <tr><td>1, 106</td><td>4, 60</td></tr> <tr><td>M</td><td>D</td></tr> </table> <p>Texture:</p> <table border="1"> <tr><td>Sand</td><td>1</td><td>1</td></tr> <tr><td>Silt</td><td>86</td><td>4</td></tr> <tr><td>Clay</td><td>14</td><td>95</td></tr> </table> <p>Composition:</p> <table border="1"> <tr><td>Quartz</td><td>5</td><td>-</td></tr> <tr><td>Feldspar</td><td>81</td><td>-</td></tr> <tr><td>Heavy Minerals</td><td>Tr</td><td>-</td></tr> <tr><td>Clay</td><td>11</td><td>25</td></tr> <tr><td>Foraminifers</td><td>-</td><td>5</td></tr> <tr><td>Calc. nannofossils</td><td>3</td><td>70</td></tr> </table> <p>CaCO₃ Bomb (%):</p> <table border="1"> <tr><td>1, 76</td><td>37.8</td></tr> <tr><td>4, 39</td><td>27.5</td></tr> </table>	1, 106	4, 60	M	D	Sand	1	1	Silt	86	4	Clay	14	95	Quartz	5	-	Feldspar	81	-	Heavy Minerals	Tr	-	Clay	11	25	Foraminifers	-	5	Calc. nannofossils	3	70	1, 76	37.8	4, 39	27.5
					1, 106	4, 60																																								
					M	D																																								
					Sand	1	1																																							
					Silt	86	4																																							
					Clay	14	95																																							
					Quartz	5	-																																							
Feldspar	81	-																																												
Heavy Minerals	Tr	-																																												
Clay	11	25																																												
Foraminifers	-	5																																												
Calc. nannofossils	3	70																																												
1, 76	37.8																																													
4, 39	27.5																																													
2	1.0				VOID				5Y 2.5/1																																					
3									10YR 2.5/1																																					
4									5Y 5/2																																					
5									5Y 5/3																																					
6									5Y 5/3																																					
7									5Y 5/2																																					
									5Y 4/1																																					
									5Y 6/1																																					

SITE 541		HOLE		CORE 21		CORED INTERVAL		5132.5-5142.0 (mbsl) 181.5-191.0 (mbst)																																						
TIME - ROCK UNIT	BIOSTRATIGRAPHIC ZONE	FOSSIL CHARACTER			SECTION METERS	GRAPHIC LITHOLOGY	DRILLING DISTURBANCE	SECONDARY STRUCTURES	SAMPLES	LITHOLOGIC DESCRIPTION																																				
		FORAMINIFERS	NANNOFOSSILS	RADIOLARIANS							DIAZONIA																																			
lower Pliocene	N17-N18 (F) Ceratolithus rugosus subzone CN10c (N)	VC/M	M	B	1	0.5				5Y 5/3	<p>MARLY NANNOFOSSIL OOZE, NANNOFOSSIL MUD, and MINOR ASH</p> <ul style="list-style-type: none"> ● Dominant colors: brownish gray (2.5Y 6/2 and 5/2) or olive (5Y 5/3) alternating with light olive gray (5Y 6/2), gray (5Y 5/1) or light brownish gray (2.5Y 6/2). Minor colors: black (5Y 2.5/1) black (10YR 2.5/1) (ash). ● Deformation minor; rotation shear surfaces every 3-5 cm. Bioturbation prominent. ● No major ash beds. <p>Note: smear slides underestimate clays compared with bomb.</p> <p>SMEAR SLIDE SUMMARY (%):</p> <table border="1"> <tr><td>1, 100</td><td>3, 100</td></tr> <tr><td>D</td><td>D</td></tr> </table> <p>Texture:</p> <table border="1"> <tr><td>Sand</td><td>5</td><td>Tr</td></tr> <tr><td>Silt</td><td>20</td><td>20</td></tr> <tr><td>Clay</td><td>75</td><td>70</td></tr> </table> <p>Composition:</p> <table border="1"> <tr><td>Quartz</td><td>1</td><td>Tr</td></tr> <tr><td>Feldspar</td><td>2</td><td>Tr</td></tr> <tr><td>Clay</td><td>30</td><td>30</td></tr> <tr><td>Volcanic glass</td><td>1</td><td>-</td></tr> <tr><td>Carbonate unspcc.</td><td>1</td><td>10</td></tr> <tr><td>Calc. nannofossils</td><td>65</td><td>60</td></tr> </table> <p>CaCO₃ Bomb (%):</p> <table border="1"> <tr><td>1, 72</td><td>23.1</td></tr> <tr><td>2, 51</td><td>30.0</td></tr> </table>	1, 100	3, 100	D	D	Sand	5	Tr	Silt	20	20	Clay	75	70	Quartz	1	Tr	Feldspar	2	Tr	Clay	30	30	Volcanic glass	1	-	Carbonate unspcc.	1	10	Calc. nannofossils	65	60	1, 72	23.1	2, 51	30.0
					1, 100	3, 100																																								
					D	D																																								
					Sand	5	Tr																																							
					Silt	20	20																																							
					Clay	75	70																																							
					Quartz	1	Tr																																							
Feldspar	2	Tr																																												
Clay	30	30																																												
Volcanic glass	1	-																																												
Carbonate unspcc.	1	10																																												
Calc. nannofossils	65	60																																												
1, 72	23.1																																													
2, 51	30.0																																													
2	1.0								5Y 6/1-5Y 6/2																																					
3									5Y 5/3																																					
4									5Y 5/2																																					
5									2.5Y 6/2																																					
6									2.5Y 5/2																																					
7									2.5Y 5/2-5Y 6/2																																					
									10YR 5/3																																					

SITE 541		FOSSIL CHARACTER		CORE 22		CORED INTERVAL 5142.0-5151.5 (mbsl) 191.0-200.5 (mbcf)	
TIME - ROCK UNIT	BIOSTRATIGRAPHIC ZONE	FOSSIL CHARACTER		SECTION METERS	GRAPHIC LITHOLOGY	DRILLING DISTURBANCE SEGMENTARY STRUCTURES	SAMPLES
		FORAMMIFERS	NANNOFOSSILS				
upper Miocene—lower Pliocene	N17-N18 (F) <i>Ceratolithus acutus</i> subzone CN10a (N)	CM		1			5Y 6/1
		CM		2			5Y 5/2 5Y 5/1 5Y 5/2
		VC/M		3	IW		5Y 5/3 5G 6/1 5Y 5/2
		VC/M		4			5Y 5/2
		VC		5			5Y 5/2 5Y 6/1
		B		6			10YR 5/2
		F		7			10YR 4/3
CC							

LITHOLOGIC DESCRIPTION

NANNOFOSSIL MUD, MARLY NANNOFOSSIL OOZE, and MINOR ASH

- Alternating dark zones, comparatively rich in clay and/or ash, and light zones, comparatively rich in carbonate.
- Dominant colors: gray (5Y 6/1-5/1) alternating with olive gray (5Y 5/2-4/2), olive (5Y 5/3), grayish brown (10YR 5/2) and dark brown (10YR 4/3). Minor colors: gray and dark gray (2.5Y 5/1-4/1), and medium gray (N5), ash; greenish gray (5G 6/1) - altered mud next to ash.
- Deformation minor, but rotation shear surfaces every 3-5 cm. Bioturbation marked.
- Ash in Sections 1, 3, and 4.

Note: smear slides underestimate clays compared with bomb.

SMEAR SLIDE SUMMARY (%):

	1, 30	3, 69	5, 122	6, 95
D	M	D	D	

Texture:

Sand	5	7	-	-
Silt	1	88	12	4
Clay	96	25	88	96

Composition:

Quartz	-	Tr	-	-
Feldspar	3	73	12	1
Heavy minerals	Tr	2	-	-
Clay	5	23	67	25
Carbonate unspc.	2	-	1	3
Calc. nannofossils	89	2	20	71

CaCO₃ Bomb (%):
2, 21 = 24.6
6, 91 = 24.1

SITE 541		FOSSIL CHARACTER		CORE 23		CORED INTERVAL 5151.5-5161.0 (mbsl) 200.5-210.0 (mbcf)	
TIME - ROCK UNIT	BIOSTRATIGRAPHIC ZONE	FOSSIL CHARACTER		SECTION METERS	GRAPHIC LITHOLOGY	DRILLING DISTURBANCE SEGMENTARY STRUCTURES	SAMPLES
		FORAMMIFERS	NANNOFOSSILS				
upper Miocene	N17-N18 (F) <i>Ammobaculites primus</i> subzone CN8b (N)	CP		1			10YR 5/2 10YR 5/6
		CM		2			5G 6/1 10YR 5/2 10YR 6/2
		VC/M		3	IW		5B 7/1 5B 7/1
		CP		4			10YR 5/3
		CM		5			10YR 6/3
		B		6			10YR 5/2 N4
		FP		7			10YR 5/2 2.5Y 5/2 5Y 5/1-5Y 5/2
CC							

LITHOLOGIC DESCRIPTION

MARLY NANNOFOSSIL OOZE changing downward to NANNOFOSSIL MUD, with MINOR ASH

- Dominant colors: grayish brown (10YR 5/2), brown (10YR 5/3), grayish brown (2.5Y 5/2), pale brown (10YR 6/3), gray (5Y 5/1), and olive (5Y 5/2), generally darker downward. Minor colors: black (N4), brownish black (5YR 2/1) ash and greenish gray (5G 6/1) and light bluish gray (5B 7/1), altered ash.
- Core disturbance moderate through Section 6, 85 cm, extensive below. Rotation shear surfaces every 3-5 cm in least disturbed sections.
- Bioturbation strong, especially marked at light/dark transitions.
- Minor ash throughout, ash bed in Section 6, several intervals of bluish or greenish alteration due to ash.

Note: smear slides underestimate clays compared with bomb.

SMEAR SLIDE SUMMARY (%):

	1, 70	5, 62
D	D	

Texture:

Sand	1	-
Silt	4	3
Clay	96	97

Composition:

Feldspar	5	Tr
Clay	8	5
Carbonate unspc.	-	3
Calc. nannofossils	87	93

CaCO₃ Bomb (%):
1, 47 = 27.0
5, 52 = 4.4

SITE 541		HOLE		CORE 24		CORED INTERVAL		5161.0-5170.5 (mbsl) 210.0-219.5 (mbst)	
TIME - ROCK UNIT	BIOSTRATIGRAPHIC ZONE	FOSSIL CHARACTER			SECTION METERS	GRAPHIC LITHOLOGY	DRILLING DISTURBANCE	SEMI-QUANTITATIVE SAMPLES	LITHOLOGIC DESCRIPTION
		FORAMINIFERS	NANNOFOSSILS	RADIOLARIANS					
upper Miocene	N17-N18 (F) <i>Ammobaculites primus</i> subzone CNR (N)	RP			1				5Y 5/2
					0.5			5Y 4/1	
		FP			2			5Y 5/1	
					1.0			5Y 5/2	
								5Y 5/1	
								5Y 5/2-5Y 5/3	
								5Y 5/1	
								5Y 5/2	
								5Y 5/1-5Y 5/2	
								5Y 5/1	
								5Y 5/2	
								5Y 5/2	

LITHOLOGIC DESCRIPTION

NANNOFOSSIL MUD, CLAY and traces of ASH

- Carbonate content dwindles to almost nothing in this core.
- Dominant colors: olive gray (5Y 5/2-4/2), dark gray (5Y 4/1), and gray (5Y 5/1). Minor colors: very dark gray (2.5Y 4/1) ash, and dark greenish gray (5G 4/1), altered ashy mud.
- Bioturbation extensive throughout. Deformation minor, drilling rotation shear surfaces every 3-5 cm.
- Some slickensides present.

Note: smear slides underestimate clays compared with bomb.

SMEAR SLIDE SUMMARY (%):

	1, 110	2, 86	4, 58
	D	D	D

Texture:

Silt	3	15	-
Clay	97	85	100

Composition:

Feldspar	2	14	Tr
Heavy minerals	-	1	-
Clay	40	85	80
Carbonate unspec.	1	-	Tr
Calc. nannofossils	57	-	20

CaCO₃ Bomb (%):
1, 69 = 3.4
4, 86 = 1.5

SITE 541		HOLE		CORE 25		CORED INTERVAL		5170.5-5180.0 (mbsl) 219.5-229.0 (mbst)	
TIME - ROCK UNIT	BIOSTRATIGRAPHIC ZONE	FOSSIL CHARACTER			SECTION METERS	GRAPHIC LITHOLOGY	DRILLING DISTURBANCE	SEMI-QUANTITATIVE SAMPLES	LITHOLOGIC DESCRIPTION
		FORAMINIFERS	NANNOFOSSILS	RADIOLARIANS					
upper Miocene	B				1				5Y 5/1
					0.5			5Y 5/2	
					1.0			5Y 5/2	
								5Y 5/1	
								5Y 5/2	
								5Y 5/1-5Y 4/1	
								5Y 5/2	
								5Y 5/1	
								N4	
								5Y 5/1	
								5Y 5/1	
								5Y 5/1-5Y 5/2	

LITHOLOGIC DESCRIPTION

CLAY with MINOR ASH

- Internally fractured and slickensided.
- Dominant colors: gray (5Y 5/1), olive gray (5Y 5/2), and dark gray (5Y 4/1). Minor color: gray ash (N4).
- Drilling disturbance minor. Rotation shear surfaces every 3-5 cm, accentuated by pre-existing fracturing and slickensides in core.
- Ash bed top of Section 4.
- Some bioturbation in least fractured intervals.

SMEAR SLIDE SUMMARY (%):

	1, 60	2, 60	3, 60	4, 60
	M	D	D	D

Texture:

5Y 5/2	60	1	1	2
Silt	30	10	2	15
Clay	10	89	97	83

Composition:

Quartz	1	-	-	-
Feldspar	Tr	2	1	Tr
Clay	10	97	97	83
Volcanic glass	89	1	Tr	17
Carbonate unspec.	-	-	2	-

CaCO₃ Bomb (%):
5, 60
6, 60
7, 60
D D D

Texture:

5Y 5/1	-	3	1
Sand	3	5	6
Silt	97	92	93
Clay	97	92	93

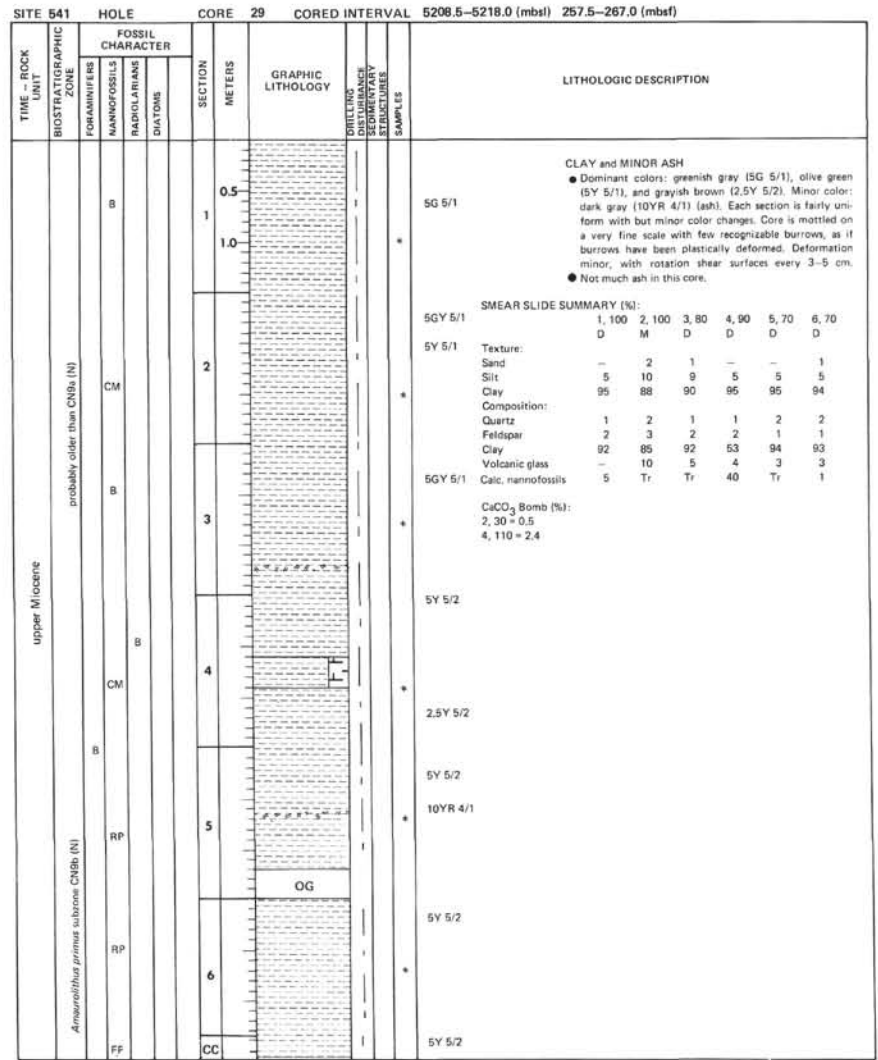
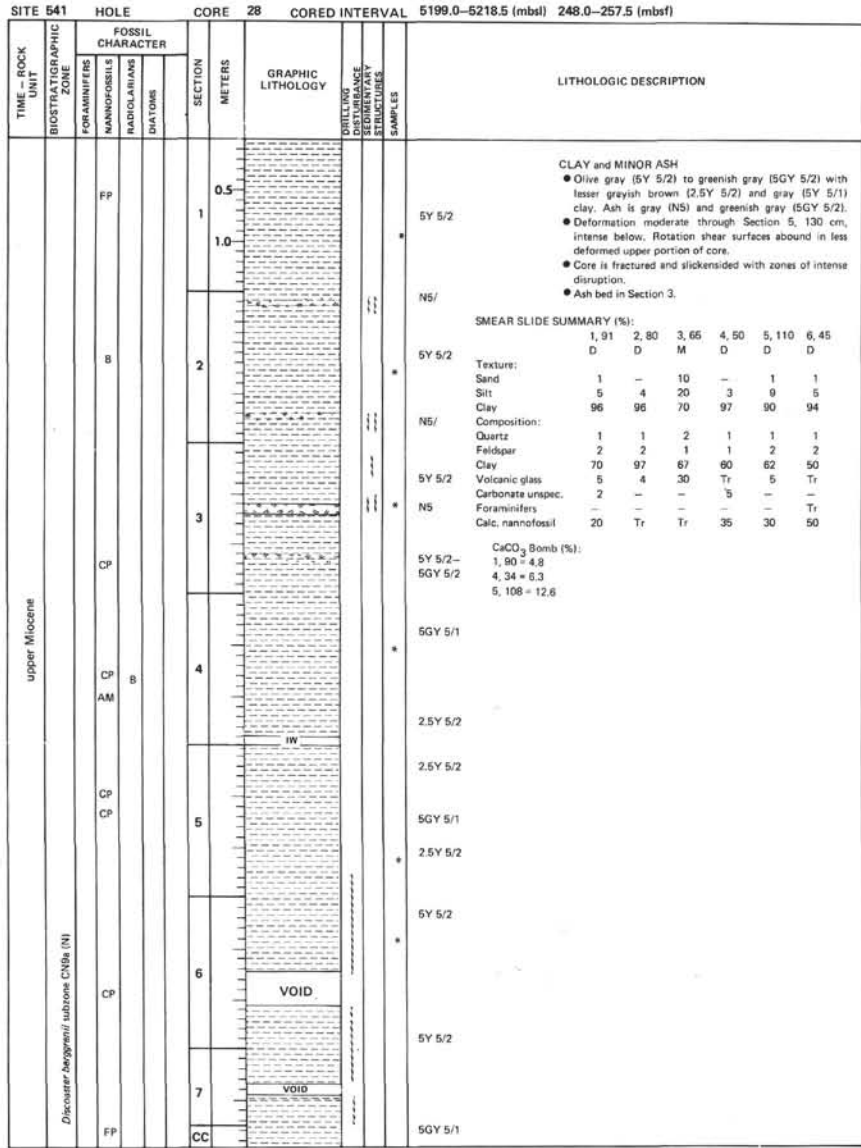
Composition:

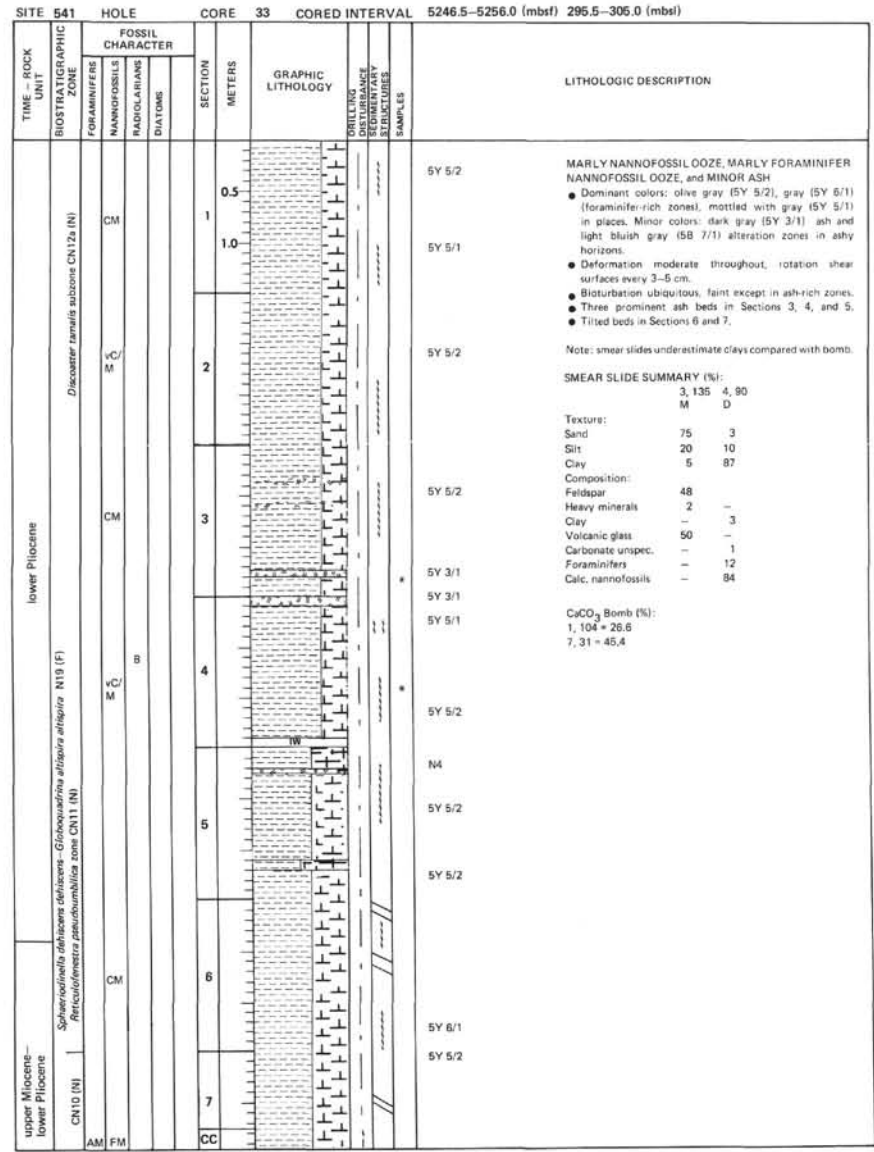
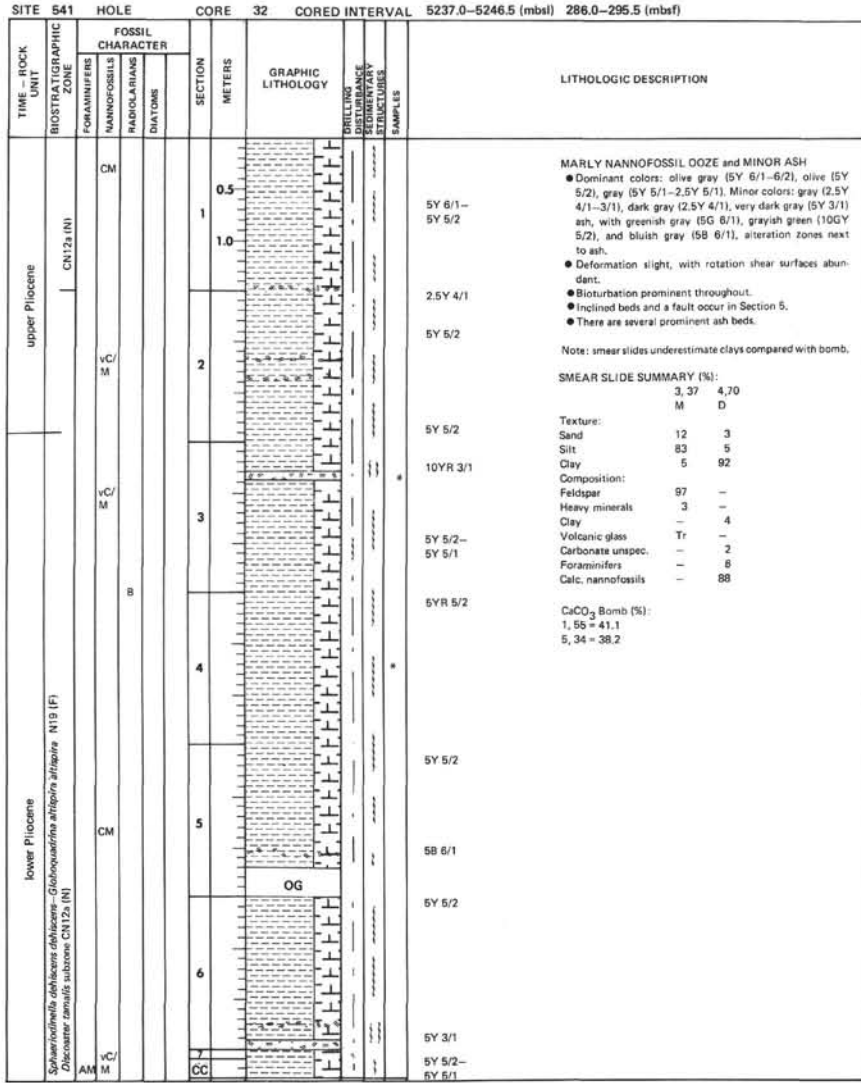
Quartz	Tr	-	-
Feldspar	1	1	1
Heavy minerals	-	Tr	Tr
Clay	97	92	96
Volcanic glass	2	7	2
Carbonate unspec.	-	-	3

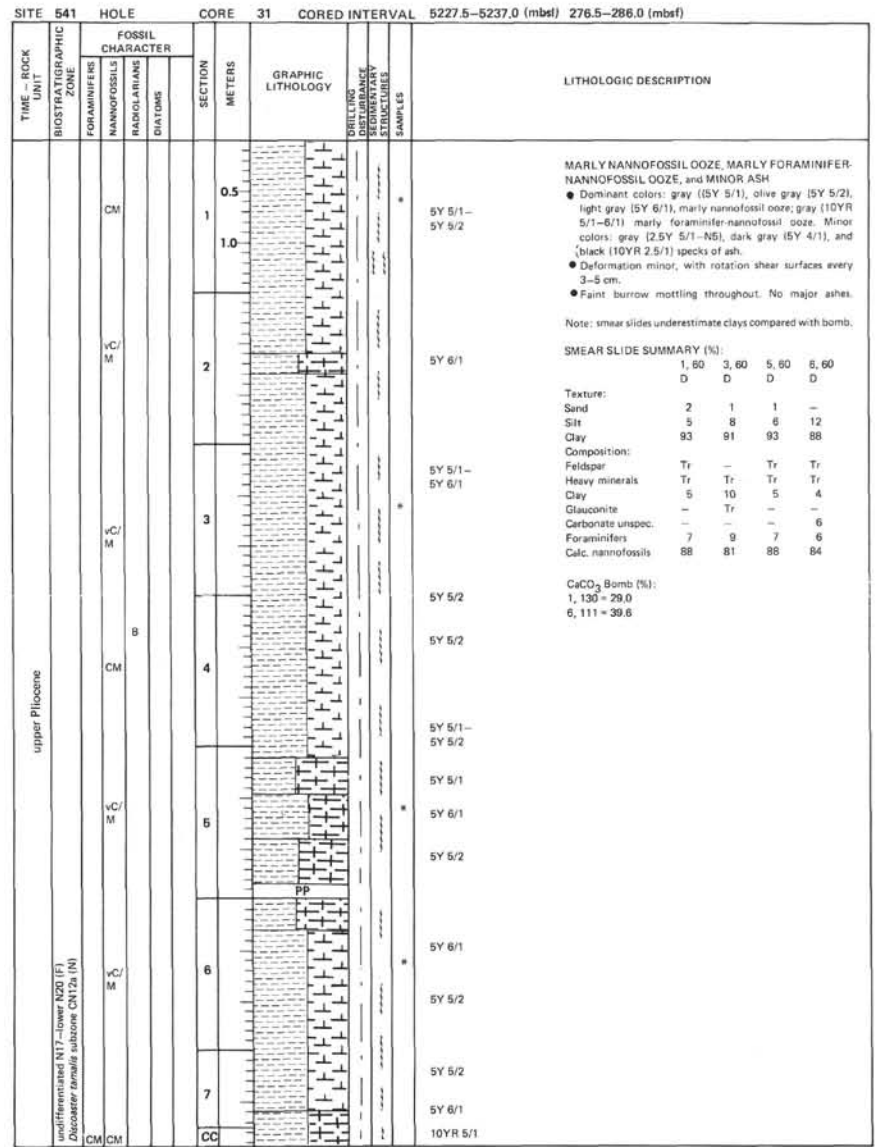
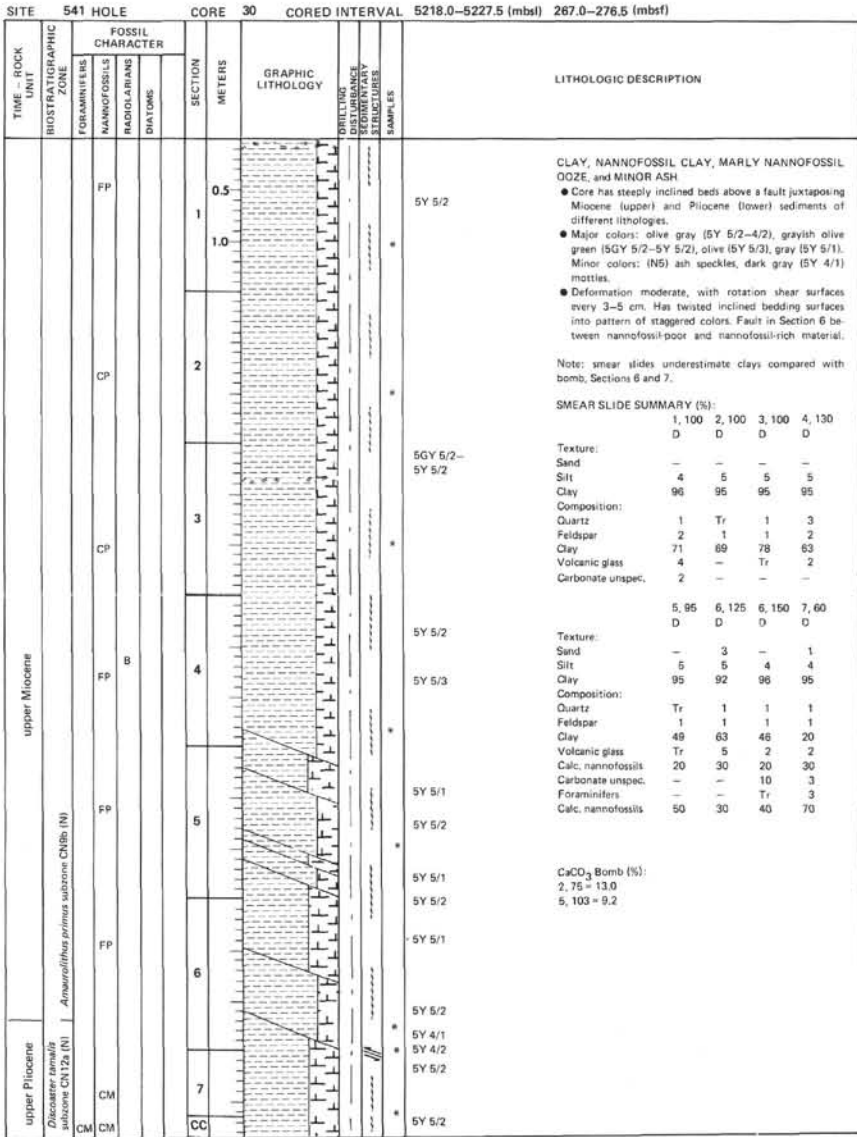
CaCO₃ Bomb (%):
1, 101 = 1.5
3, 54 = 1.5
7, 28 = 0.0

SITE 541		HOLE		CORE 26		CORED INTERVAL		5180.0-5189.5 (mbsl) 229.0-238.5 (mbst)																																																																																										
TIME - ROCK UNIT	BIOSTRATIGRAPHIC ZONE	FOSSIL CHARACTER			SECTION METERS	GRAPHIC LITHOLOGY	DRILLING DISTURBANCE	SEDIMENTARY STRUCTURES	SAMPLES	LITHOLOGIC DESCRIPTION																																																																																								
		FORAMINIFERS	MAMMOFOSILS	RADOLIARIANS							DIATOMS																																																																																							
Upper Miocene	B B				0.5					<p>CLAY and MINOR ASH</p> <ul style="list-style-type: none"> Internally fractured and slickensided uniform greenish gray (5GY 5/1) to olive gray (5G 5/2) clay, with local medium gray (N5) bioturbated ash. Drilling disturbance minor, but rotation shear surfaces occur every 3-5 cm. Material stiff enough to have allowed surface disruption by splitting with plano wire. <p>SMEAR SLIDE SUMMARY (%):</p> <table border="1"> <tr> <td></td> <td>1,90</td> <td>2,40</td> <td>3,110</td> <td>4,125</td> <td>5,65</td> <td>6,28</td> </tr> <tr> <td>D</td> <td>D</td> <td>D</td> <td>D</td> <td>D</td> <td>D</td> <td>D</td> </tr> </table> <p>Texture:</p> <table border="1"> <tr> <td>Sand</td> <td>-</td> <td>-</td> <td>-</td> <td>-</td> <td>-</td> <td>2</td> </tr> <tr> <td>Silt</td> <td>3</td> <td>4</td> <td>5</td> <td>5</td> <td>3</td> <td>4</td> </tr> <tr> <td>Clay</td> <td>97</td> <td>96</td> <td>95</td> <td>95</td> <td>97</td> <td>94</td> </tr> </table> <p>Composition:</p> <table border="1"> <tr> <td>Quartz</td> <td>Tr</td> <td>Tr</td> <td>1</td> <td>1</td> <td>1</td> <td>1</td> </tr> <tr> <td>Feldspar</td> <td>2</td> <td>2</td> <td>2</td> <td>2</td> <td>2</td> <td>2</td> </tr> <tr> <td>Heavy minerals</td> <td>-</td> <td>Tr</td> <td>Tr</td> <td>-</td> <td>-</td> <td>-</td> </tr> <tr> <td>Clay</td> <td>95</td> <td>93</td> <td>90</td> <td>92</td> <td>94</td> <td>93</td> </tr> <tr> <td>Volcanic glass</td> <td>3</td> <td>3</td> <td>5</td> <td>3</td> <td>3</td> <td>4</td> </tr> <tr> <td>Carbonate unsp. spec.</td> <td>-</td> <td>2</td> <td>2</td> <td>2</td> <td>-</td> <td>-</td> </tr> <tr> <td>Calc. nanofossils</td> <td>-</td> <td>Tr</td> <td>Tr</td> <td>Tr</td> <td>-</td> <td>-</td> </tr> </table> <p>CaCO₃ Bomb (%):</p> <table border="1"> <tr> <td>5GY 5/1-</td> <td>2, 78 = 0</td> </tr> <tr> <td>5GY 5/2</td> <td>4, 68 = 1,0</td> </tr> </table>		1,90	2,40	3,110	4,125	5,65	6,28	D	D	D	D	D	D	D	Sand	-	-	-	-	-	2	Silt	3	4	5	5	3	4	Clay	97	96	95	95	97	94	Quartz	Tr	Tr	1	1	1	1	Feldspar	2	2	2	2	2	2	Heavy minerals	-	Tr	Tr	-	-	-	Clay	95	93	90	92	94	93	Volcanic glass	3	3	5	3	3	4	Carbonate unsp. spec.	-	2	2	2	-	-	Calc. nanofossils	-	Tr	Tr	Tr	-	-	5GY 5/1-	2, 78 = 0	5GY 5/2	4, 68 = 1,0
			1,90	2,40	3,110	4,125	5,65	6,28																																																																																										
		D	D	D	D	D	D	D																																																																																										
		Sand	-	-	-	-	-	2																																																																																										
		Silt	3	4	5	5	3	4																																																																																										
		Clay	97	96	95	95	97	94																																																																																										
Quartz	Tr	Tr	1	1	1	1																																																																																												
Feldspar	2	2	2	2	2	2																																																																																												
Heavy minerals	-	Tr	Tr	-	-	-																																																																																												
Clay	95	93	90	92	94	93																																																																																												
Volcanic glass	3	3	5	3	3	4																																																																																												
Carbonate unsp. spec.	-	2	2	2	-	-																																																																																												
Calc. nanofossils	-	Tr	Tr	Tr	-	-																																																																																												
5GY 5/1-	2, 78 = 0																																																																																																	
5GY 5/2	4, 68 = 1,0																																																																																																	
				1.0																																																																																														
				2																																																																																														
				3																																																																																														
				4																																																																																														
				5																																																																																														
				6																																																																																														

SITE 541		HOLE		CORE 27		CORED INTERVAL		5189.5-5199.0 (mbsl) 238.5-248.0 (mbst)																																																																										
TIME - ROCK UNIT	BIOSTRATIGRAPHIC ZONE	FOSSIL CHARACTER			SECTION METERS	GRAPHIC LITHOLOGY	DRILLING DISTURBANCE	SEDIMENTARY STRUCTURES	SAMPLES	LITHOLOGIC DESCRIPTION																																																																								
		FORAMINIFERS	MAMMOFOSILS	RADOLIARIANS							DIATOMS																																																																							
Upper Miocene	B B				0.5					<p>CLAY and MINOR ASH</p> <ul style="list-style-type: none"> Internally fractured and slickensided greenish gray (5GY 5/2) clay mottled with dark greenish gray (5GY 4/1) and gray (N5) burrows. Some intervals of dark greenish gray (5GY 4/1). Moderately deformed with rotation shear surfaces common. No major ash beds. <p>SMEAR SLIDE SUMMARY (%):</p> <table border="1"> <tr> <td></td> <td>1,88</td> <td>2,96</td> <td>3,100</td> <td>4,95</td> <td>5,57</td> <td>7,30</td> </tr> <tr> <td>D</td> <td>M</td> <td>D</td> <td>D</td> <td>D</td> <td>D</td> <td>D</td> </tr> </table> <p>Texture:</p> <table border="1"> <tr> <td>Sand</td> <td>-</td> <td>2</td> <td>1</td> <td>4</td> <td>1</td> <td>1</td> </tr> <tr> <td>Silt</td> <td>3</td> <td>8</td> <td>9</td> <td>7</td> <td>4</td> <td>5</td> </tr> <tr> <td>Clay</td> <td>97</td> <td>90</td> <td>90</td> <td>89</td> <td>95</td> <td>94</td> </tr> </table> <p>Composition:</p> <table border="1"> <tr> <td>Quartz</td> <td>1</td> <td>1</td> <td>1</td> <td>2</td> <td>1</td> <td>2</td> </tr> <tr> <td>Feldspar</td> <td>1</td> <td>1</td> <td>1</td> <td>1</td> <td>1</td> <td>2</td> </tr> <tr> <td>Clay</td> <td>96</td> <td>78</td> <td>93</td> <td>87</td> <td>96</td> <td>86</td> </tr> <tr> <td>Volcanic glass</td> <td>2</td> <td>20</td> <td>5</td> <td>10</td> <td>2</td> <td>5</td> </tr> <tr> <td>Calc. nanofossils</td> <td>-</td> <td>-</td> <td>Tr</td> <td>-</td> <td>Tr</td> <td>5</td> </tr> </table> <p>CaCO₃ Bomb (%):</p> <table border="1"> <tr> <td>1, 107 = 0.5</td> </tr> <tr> <td>5, 60 = 0.6</td> </tr> </table>		1,88	2,96	3,100	4,95	5,57	7,30	D	M	D	D	D	D	D	Sand	-	2	1	4	1	1	Silt	3	8	9	7	4	5	Clay	97	90	90	89	95	94	Quartz	1	1	1	2	1	2	Feldspar	1	1	1	1	1	2	Clay	96	78	93	87	96	86	Volcanic glass	2	20	5	10	2	5	Calc. nanofossils	-	-	Tr	-	Tr	5	1, 107 = 0.5	5, 60 = 0.6
			1,88	2,96	3,100	4,95	5,57	7,30																																																																										
		D	M	D	D	D	D	D																																																																										
		Sand	-	2	1	4	1	1																																																																										
		Silt	3	8	9	7	4	5																																																																										
		Clay	97	90	90	89	95	94																																																																										
		Quartz	1	1	1	2	1	2																																																																										
		Feldspar	1	1	1	1	1	2																																																																										
Clay	96	78	93	87	96	86																																																																												
Volcanic glass	2	20	5	10	2	5																																																																												
Calc. nanofossils	-	-	Tr	-	Tr	5																																																																												
1, 107 = 0.5																																																																																		
5, 60 = 0.6																																																																																		
				1.0																																																																														
				2																																																																														
				3																																																																														
				4																																																																														
				5																																																																														
				6																																																																														
				7																																																																														
				CC																																																																														







SITE 541		HOLE		CORE 34		CORED INTERVAL		5256.0-5265.5 (msl) 306.0-314.5 (msf)		
TIME - ROCK UNIT	BIOSTRATIGRAPHIC ZONE	FOSSIL CHARACTER			SECTION METERS	GRAPHIC LITHOLOGY	DRILLING DISTURBANCE BY STRUCTURES	SAMPLES	LITHOLOGIC DESCRIPTION	
		FORAMINIFERS	NANNOFOSSILS	RADIOLARIANS						DIATOMS
upper Miocene-lower Pliocene	N17-lower N20 (F) <i>Reticulofenestra pseudobumbilica</i> zone CN11 (N)	CM	CM	vC/M	0.5				5Y 6/1	
					1.0				5Y 4/1	
					2				5Y 6/1	
		CM	CP	B	3					5Y 5/1
					4					5Y 6/1
					5					5Y 5/2
		CM	CM	B	6					2.5Y 6/2
					5Y 4/1					
					2.5Y 6/2					
		CM	CM	B	5					5Y 2.5/1
					6					5Y 5/2
					7					5Y 2.5/1
CM	CM	B	6					5Y 5/1		
			7					5Y 5/1		
			8					5Y 5/3		

LITHOLOGIC DESCRIPTION

MARLY NANNOFOSSIL OOZE and several prominent ASH BEDS

- Dominant colors: gray (5Y 6/1) darkening downward
- through light brownish gray (2.5Y 6/2), olive gray (5Y 5/2), and olive (5Y 5/3). Minor colors: black (5Y 2.5/1), gray (5Y 4/1), brownish gray (5YR 4/1) ash, and gray (5Y 5/1), olive gray (5Y 5/2) ashy ooze.
- Deformation moderate, with rotation shear surfaces every 3-5 cm. Several prominent ash beds in this core with sharp lower contacts and bioturbated upper zones.
- Bioturbation throughout, especially pronounced near ash beds.
- Tilted ash lower contacts Sections 5 and 6.

Note: smear slides underestimate clays compared with bomb.

SMEAR SLIDE SUMMARY (%):

	1, 60	5, 73
	D	M

Texture:

Sand	2	60
Silt	20	30
Clay	78	10

Composition:

Quartz	-	5
Feldspar	-	40
Heavy minerals	-	2
Clay	10	10
Volcanic glass	-	43
Carbonate unspec.	Tr	-
Foraminifers	15	-
Calc. nannofossils	75	-

CaCO₃ Bomb (%):

2, 82 = 33.3
6, 106 = 31.4

SITE 541		HOLE		CORE 35		CORED INTERVAL		5247.5-5275.0 (msl) 314.5-324.0 (msf)		
TIME - ROCK UNIT	BIOSTRATIGRAPHIC ZONE	FOSSIL CHARACTER			SECTION METERS	GRAPHIC LITHOLOGY	DRILLING DISTURBANCE BY STRUCTURES	SAMPLES	LITHOLOGIC DESCRIPTION	
		FORAMINIFERS	NANNOFOSSILS	RADIOLARIANS						DIATOMS
upper Miocene-lower Pliocene	N17-lower N20 (F) <i>Cheridofusus rugosus</i> CN10c (N)	FP	CM	vC/M	0.5				2.5Y 6/2	
					1.0				5Y 5/2	
					2				5Y 5/3	
		FP	CM	vC/M	3					5Y 6/1
					4					5Y 5/2
					5					5Y 5/1
		FP	CM	vC/M	6					5Y 5/2
					7					5Y 5/2
					8					5Y 5/2
		FP	CM	vC/M	9					2.5Y 5/2-2.5Y 6/2
					10					2.5Y 5/2
					11					5Y 4/1
FP	CM	vC/M	12					2.5Y 5/2		
			13					2.5Y 6/2		
			14					2.5Y 5/2		
FP	CM	vC/M	15					2.5Y 6/2		
			16					2.5Y 6/2		
			17					2.5Y 6/2		

LITHOLOGIC DESCRIPTION

NANNOFOSSIL MUD alternating with MUD lower in the core; MINOR ASH

- Dominant colors: light brownish gray (2.5Y 6/2), gray (5Y 6/1), olive (5Y 5/3), gray (5Y 5/1), becoming darker downward to olive gray (5Y 5/2) alternating with grayish brown (2.5Y 5/2). Minor colors: ashes are olive gray (5Y 5/2), medium dark gray (N4), and gray (5Y 4/1). Alteration near ashes is light bluish gray (5B 7/1).
- Deformation slight throughout, with rotation shear surfaces abundant.
- Bioturbation distinctive, especially near ash zones.
- Several prominent ash beds in core.
- Some dipping burrows, Section 6.

Note: smear slides underestimate clays compared with bomb.

SMEAR SLIDE SUMMARY (%):

	2, 80	6, 60
	D	D

Texture:

Sand	3	Tr
Silt	10	15
Clay	87	85

Composition:

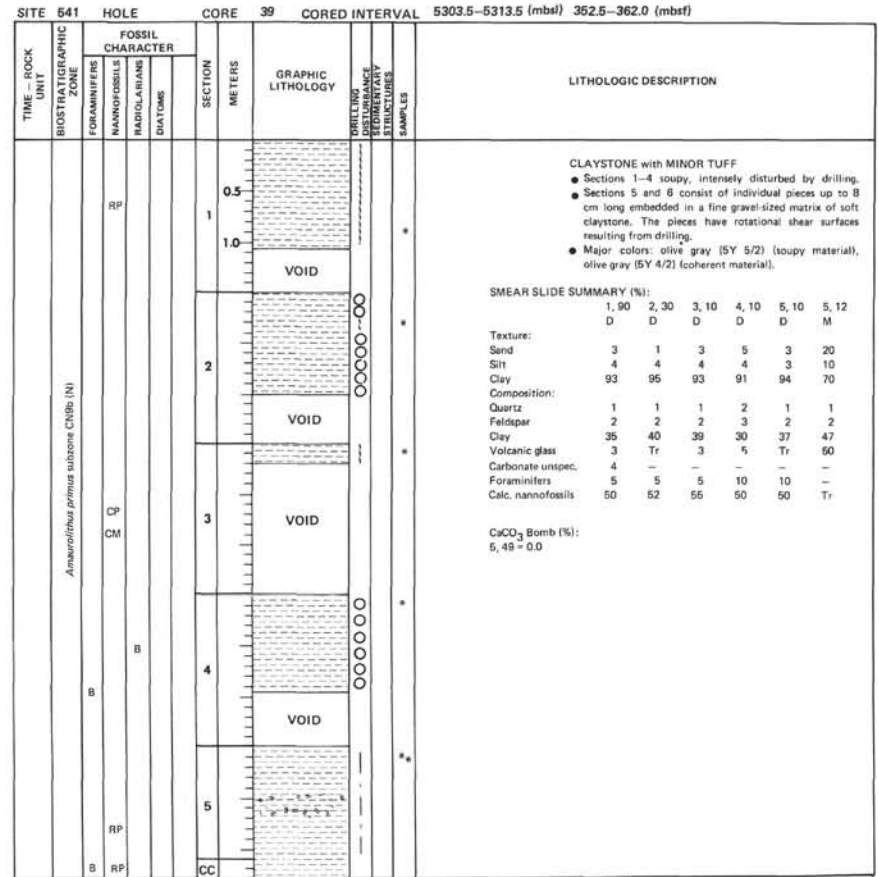
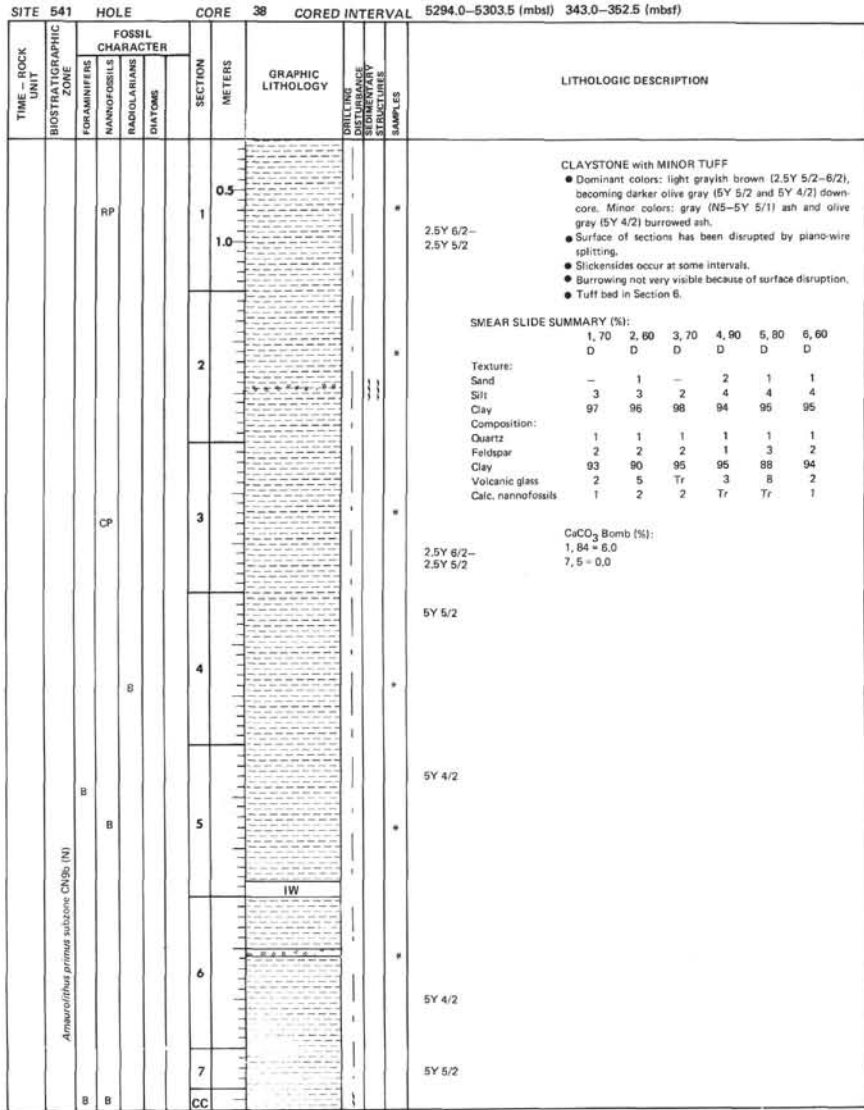
Feldspar	Tr	-
Clay	20	25
Volcanic glass	5	-
Foraminifers	2	Tr
Calc. nannofossils	73	75

CaCO₃ Bomb (%):

4, 103 = 24.2
6, 33 = 38.6

SITE 541		HOLE		CORE 36		CORED INTERVAL 5275.0–5284.5 (mbsl) 324.0–333.5 (mbsf)	
TIME – ROCK UNIT	BIOSTRATIGRAPHIC ZONE	FOSSIL CHARACTER			SECTION METERS	GRAPHIC LITHOLOGY	LITHOLOGIC DESCRIPTION
		FORAMINIFERS	NANNOFOSSILS	RADIOLARIANS			
N17–N19 (F) <i>Cretolittorax acutus</i> subzone CN10b (IN)	RP	CP			0.5		2.5Y 6/2 10YR 4/3
					1.0		
N17–N19 (F) <i>Cretolittorax acutus</i> subzone CN10b (IN)	CP	B			2		10YR 5/3 2.5Y 5/2
							<p>NANNOFOSSIL MUDSTONE</p> <ul style="list-style-type: none"> This core came from a badly damaged, bent, and twisted core liner. Bioturbation is intense. There are no ash beds. Deformation due to drilling and coring is intense. There are horizontal zones of intense drill-induced shear up to 1 cm thick. Chondrites, planolites, cylindrichnus and composite burrows occur. Colors are light brownish gray (2.5Y 6/2), brown (10YR 4/3 and 5/3), and brownish gray (2.5Y 5/2). <p>CaCO₃ Bomb (%): 1, 40 = 25.1 2, 29 = 25.1</p>

SITE 541		HOLE		CORE 37		CORED INTERVAL 5284.5–5294.0 (mbsl) 333.5–343.0 (mbsf)																																																																		
TIME – ROCK UNIT	BIOSTRATIGRAPHIC ZONE	FOSSIL CHARACTER			SECTION METERS	GRAPHIC LITHOLOGY	LITHOLOGIC DESCRIPTION																																																																	
		FORAMINIFERS	NANNOFOSSILS	RADIOLARIANS				DIATOMS																																																																
N17–N19 (F) <i>Cretolittorax acutus</i> subzone CN10b (IN)	RP	CP			0.5		CLAYSTONE, NANNOFOSSIL CLAYSTONE and MINOR ASH																																																																	
					1.0																																																																			
N17–N19 (F) <i>Cretolittorax acutus</i> subzone CN10b (IN)	CP	B			2		<ul style="list-style-type: none"> Dominant colors: pale brown (10YR 6/3), brown (10YR 5/3), grayish brown (10YR 5/2), light brownish gray (2.5Y 6/2), olive gray (5Y 5/2), and gray (5Y 5/1). Minor colors: gray (N4), greenish gray (5G 6/1), and olive black (5Y 2/1) ash, plus pale greenish gray (5GY 6/1), altered ashy claystone. Deformation moderate, with rotation shear surfaces every 3–5 cm. Bioturbation occurs sporadically. Locally foraminifer-bearing. Prominent ash beds in Sections 4 and 5. <p>Note: smear slides underestimate clays compared with bomb.</p> <p>SMEAR SLIDE SUMMARY (%):</p> <table border="1"> <thead> <tr> <th></th> <th>1, 43</th> <th>4, 49</th> <th>4, 80</th> <th>5, 75</th> </tr> <tr> <th></th> <th>D</th> <th>D</th> <th>M</th> <th>M</th> </tr> </thead> <tbody> <tr> <td>Texture:</td> <td></td> <td></td> <td></td> <td></td> </tr> <tr> <td>Sand</td> <td>1</td> <td>–</td> <td>60</td> <td>50</td> </tr> <tr> <td>Silt</td> <td>10</td> <td>3</td> <td>10</td> <td>15</td> </tr> <tr> <td>Clay</td> <td>89</td> <td>97</td> <td>30</td> <td>35</td> </tr> </tbody> </table> <p>Composition:</p> <table border="1"> <thead> <tr> <th></th> <th>–</th> <th>–</th> <th>Tr</th> <th>–</th> </tr> </thead> <tbody> <tr> <td>Quartz</td> <td>–</td> <td>–</td> <td>Tr</td> <td>–</td> </tr> <tr> <td>Feldspar</td> <td>Tr</td> <td>Tr</td> <td>1</td> <td>3</td> </tr> <tr> <td>Heavy minerals</td> <td>Tr</td> <td>–</td> <td>–</td> <td>–</td> </tr> <tr> <td>Clay</td> <td>40</td> <td>93</td> <td>25</td> <td>35</td> </tr> <tr> <td>Volcanic glass</td> <td>6</td> <td>Tr</td> <td>69</td> <td>60</td> </tr> <tr> <td>Calc, nannofossils</td> <td>54</td> <td>6</td> <td>5</td> <td>2</td> </tr> </tbody> </table> <p>CaCO₃ Bomb (%): 1, 138 = 4.8 5, 89 = 11.1</p>		1, 43	4, 49	4, 80	5, 75		D	D	M	M	Texture:					Sand	1	–	60	50	Silt	10	3	10	15	Clay	89	97	30	35		–	–	Tr	–	Quartz	–	–	Tr	–	Feldspar	Tr	Tr	1	3	Heavy minerals	Tr	–	–	–	Clay	40	93	25	35	Volcanic glass	6	Tr	69	60	Calc, nannofossils	54	6	5	2
			1, 43	4, 49	4, 80			5, 75																																																																
	D	D	M	M																																																																				
Texture:																																																																								
Sand	1	–	60	50																																																																				
Silt	10	3	10	15																																																																				
Clay	89	97	30	35																																																																				
	–	–	Tr	–																																																																				
Quartz	–	–	Tr	–																																																																				
Feldspar	Tr	Tr	1	3																																																																				
Heavy minerals	Tr	–	–	–																																																																				
Clay	40	93	25	35																																																																				
Volcanic glass	6	Tr	69	60																																																																				
Calc, nannofossils	54	6	5	2																																																																				
N17–N19 (F) <i>Cretolittorax acutus</i> subzone CN10b (IN)	CP	B			3		<p>5GY 6/1 N4</p>																																																																	
N17–N19 (F) <i>Cretolittorax acutus</i> subzone CN10b (IN)	CP	B			4																																																																			
N17–N19 (F) <i>Cretolittorax acutus</i> subzone CN10b (IN)	CP	B			5																																																																			
N17–N19 (F) <i>Cretolittorax acutus</i> subzone CN10b (IN)	CP	B			6		OG																																																																	
N17–N19 (F) <i>Cretolittorax acutus</i> subzone CN10b (IN)	CP	B			7																																																																			



SITE 541		HOLE CORE 40		CORED INTERVAL 5313.0-5322.5 (mbsl) 362.0-371.5 (mbsf)																																																																																		
TIME - ROCK UNIT	BIOSTRATIGRAPHIC ZONE	FOSSIL CHARACTER			SECTION METERS	GRAPHIC LITHOLOGY	DRILLING DISTURBANCE STRUCTURES	SAMPLES	LITHOLOGIC DESCRIPTION																																																																													
		FORAMINIFERS	NANNOFOSSILS	RADIOLARIANS						DIATOMS																																																																												
					0.5			*	<p>CLAYSTONE and MINOR TUFF</p> <ul style="list-style-type: none"> Greenish gray (5GY 5/1) with bits and specks of darker ash. Very uniform. Core has appearance of coherent chunks up to 10 cm long embedded in a broken-up brecciated claystone matrix. Rotational shear surfaces are abundant. Core has faintly mottled appearance, possibly burrows rearranged by plastic deformation in a fault zone. <p>SMEAR SLIDE SUMMARY (%):</p> <table border="1"> <tr> <td></td> <td>1,36</td> <td>1,58</td> <td>2,64</td> <td>3,63</td> </tr> <tr> <td></td> <td>M</td> <td>D</td> <td>D</td> <td>M</td> </tr> </table> <p>Texture:</p> <table border="1"> <tr> <td>Sand</td> <td>5</td> <td>2</td> <td>-</td> <td>30</td> </tr> <tr> <td>Silt</td> <td>5</td> <td>4</td> <td>5</td> <td>50</td> </tr> <tr> <td>Clay</td> <td>90</td> <td>94</td> <td>95</td> <td>20</td> </tr> </table> <p>Composition:</p> <table border="1"> <tr> <td>Quartz</td> <td>2</td> <td>2</td> <td>1</td> <td>-</td> </tr> <tr> <td>Feldspar</td> <td>3</td> <td>3</td> <td>4</td> <td>-</td> </tr> <tr> <td>Clay</td> <td>75</td> <td>90</td> <td>85</td> <td>30</td> </tr> <tr> <td>Volcanic glass</td> <td>20</td> <td>5</td> <td>10</td> <td>70</td> </tr> </table> <p>5,97 6,100 7,50 D D D</p> <p>Texture:</p> <table border="1"> <tr> <td>Sand</td> <td>-</td> <td>1</td> <td>1</td> </tr> <tr> <td>Silt</td> <td>2</td> <td>4</td> <td>3</td> </tr> <tr> <td>Clay</td> <td>98</td> <td>95</td> <td>96</td> </tr> </table> <p>Composition:</p> <table border="1"> <tr> <td>Quartz</td> <td>-</td> <td>1</td> <td>Tr</td> </tr> <tr> <td>Feldspar</td> <td>-</td> <td>3</td> <td>2</td> </tr> <tr> <td>Clay</td> <td>75</td> <td>94</td> <td>90</td> </tr> <tr> <td>Volcanic glass</td> <td>1</td> <td>2</td> <td>8</td> </tr> <tr> <td>Calc. nanofossils</td> <td>20</td> <td>Tr</td> <td>-</td> </tr> </table> <p>CaCO₃ Bomb (%): 1,40 = 0.5 4,65 = 1.0</p>		1,36	1,58	2,64	3,63		M	D	D	M	Sand	5	2	-	30	Silt	5	4	5	50	Clay	90	94	95	20	Quartz	2	2	1	-	Feldspar	3	3	4	-	Clay	75	90	85	30	Volcanic glass	20	5	10	70	Sand	-	1	1	Silt	2	4	3	Clay	98	95	96	Quartz	-	1	Tr	Feldspar	-	3	2	Clay	75	94	90	Volcanic glass	1	2	8	Calc. nanofossils	20	Tr	-
	1,36	1,58	2,64	3,63																																																																																		
	M	D	D	M																																																																																		
Sand	5	2	-	30																																																																																		
Silt	5	4	5	50																																																																																		
Clay	90	94	95	20																																																																																		
Quartz	2	2	1	-																																																																																		
Feldspar	3	3	4	-																																																																																		
Clay	75	90	85	30																																																																																		
Volcanic glass	20	5	10	70																																																																																		
Sand	-	1	1																																																																																			
Silt	2	4	3																																																																																			
Clay	98	95	96																																																																																			
Quartz	-	1	Tr																																																																																			
Feldspar	-	3	2																																																																																			
Clay	75	94	90																																																																																			
Volcanic glass	1	2	8																																																																																			
Calc. nanofossils	20	Tr	-																																																																																			
					1.0			*																																																																														
					2			*																																																																														
					3			*																																																																														
					4			*																																																																														
					5			*																																																																														
					6			*																																																																														
					7			*																																																																														
					CC			*																																																																														

SITE 541		HOLE CORE 41		CORED INTERVAL 5322.5-5332.0 (mbsl) 371.5-381.0 (mbsf)																																																																																		
TIME - ROCK UNIT	BIOSTRATIGRAPHIC ZONE	FOSSIL CHARACTER			SECTION METERS	GRAPHIC LITHOLOGY	DRILLING DISTURBANCE STRUCTURES	SAMPLES	LITHOLOGIC DESCRIPTION																																																																													
		FORAMINIFERS	NANNOFOSSILS	RADIOLARIANS						DIATOMS																																																																												
					0.5			*	<p>CLAYSTONE, NANNOFOSSIL CLAYSTONE and MINOR TUFF</p> <ul style="list-style-type: none"> Dominant colors: greenish gray (5GY 5/1), olive gray (5Y 5/2), and grayish green (5GY 5/2). Core has appearance of coherent chunks embedded in an intensely sheared or broken-up matrix. Probably sheared zones represent penetrative deformation. Rotational shear surfaces occur in matrix. Bioturbation is preserved locally but generally the core has a mottled appearance, suggesting pre-drilling burrow deformation. Gray (N4) tuff with horizontal green streak occurs in Section 3. Local carbonate-enriched zones occur not evident from core color variation. <p>SMEAR SLIDE SUMMARY (%):</p> <table border="1"> <tr> <td></td> <td>1,60</td> <td>2,41</td> <td>3,24</td> <td>4,58</td> <td>5,66</td> <td>6,35</td> </tr> <tr> <td></td> <td>D</td> <td>D</td> <td>M</td> <td>D</td> <td>D</td> <td>D</td> </tr> </table> <p>Texture:</p> <table border="1"> <tr> <td>Sand</td> <td>-</td> <td>1</td> <td>20</td> <td>1</td> <td>1</td> <td>3</td> </tr> <tr> <td>Silt</td> <td>2</td> <td>4</td> <td>20</td> <td>4</td> <td>5</td> <td>4</td> </tr> <tr> <td>Clay</td> <td>98</td> <td>95</td> <td>50</td> <td>95</td> <td>94</td> <td>93</td> </tr> </table> <p>Composition:</p> <table border="1"> <tr> <td>Quartz</td> <td>1</td> <td>2</td> <td>5</td> <td>1</td> <td>2</td> <td>2</td> </tr> <tr> <td>Feldspar</td> <td>2</td> <td>3</td> <td>10</td> <td>3</td> <td>3</td> <td>3</td> </tr> <tr> <td>Clay</td> <td>95</td> <td>93</td> <td>45</td> <td>42</td> <td>92</td> <td>39</td> </tr> <tr> <td>Volcanic glass</td> <td>2</td> <td>2</td> <td>40</td> <td>3</td> <td>3</td> <td>1</td> </tr> <tr> <td>Foraminifers</td> <td>-</td> <td>-</td> <td>-</td> <td>1</td> <td>-</td> <td>5</td> </tr> <tr> <td>Calc. nanofossils</td> <td>Tr</td> <td>-</td> <td>-</td> <td>50</td> <td>-</td> <td>50</td> </tr> </table> <p>CaCO₃ Bomb (%): 3,90 = 1.0 4,36 = 24.4</p>		1,60	2,41	3,24	4,58	5,66	6,35		D	D	M	D	D	D	Sand	-	1	20	1	1	3	Silt	2	4	20	4	5	4	Clay	98	95	50	95	94	93	Quartz	1	2	5	1	2	2	Feldspar	2	3	10	3	3	3	Clay	95	93	45	42	92	39	Volcanic glass	2	2	40	3	3	1	Foraminifers	-	-	-	1	-	5	Calc. nanofossils	Tr	-	-	50	-	50
	1,60	2,41	3,24	4,58	5,66	6,35																																																																																
	D	D	M	D	D	D																																																																																
Sand	-	1	20	1	1	3																																																																																
Silt	2	4	20	4	5	4																																																																																
Clay	98	95	50	95	94	93																																																																																
Quartz	1	2	5	1	2	2																																																																																
Feldspar	2	3	10	3	3	3																																																																																
Clay	95	93	45	42	92	39																																																																																
Volcanic glass	2	2	40	3	3	1																																																																																
Foraminifers	-	-	-	1	-	5																																																																																
Calc. nanofossils	Tr	-	-	50	-	50																																																																																
					1.0			*																																																																														
					2			*																																																																														
					3			*																																																																														
					4			*																																																																														
					5			*																																																																														
					6			*																																																																														
					CC			*																																																																														

SITE 541 HOLE		CORE 42		CORED INTERVAL 5332.0-5341.5 (mbsl) 381.0-390.5 (mbsf)																																																
TIME - ROCK UNIT	BIOSTRATIGRAPHIC ZONE	FOSSIL CHARACTER			SECTION METERS	GRAPHIC LITHOLOGY	DISTURBANCE STRUCTURES	LITHOLOGIC DESCRIPTION																																												
		FORAMINIFERS	NANNOFOSSILS	RADIOLARIANS					DIAZONES																																											
					0.5			<p>CLAYSTONE and NANNOFOSSIL CLAYSTONE, very MINOR TUFF</p> <ul style="list-style-type: none"> ● Dominant colors: greenish gray (5G 5/1), light greenish gray (5G 6/1), and olive gray (5Y 5/2). Minor colors: greenish gray (5G 5/1) and dark greenish gray (5G 4/1) mottles. ● Upper part of core has coherent chunks in crumbly matrix. Lower part has coherent chunks blending with highly fractured and sheared matrix. ● Part of shearing due to drilling rotation. Rest probably original tectonic fabric. ● Some chunks have healed microfractures. ● Burrows prominent. <p>SMEAR SLIDE SUMMARY (%):</p> <table border="1"> <tr> <td></td> <td>1, 92</td> <td>2, 60</td> <td>6, 50</td> </tr> <tr> <td>D</td> <td></td> <td>M</td> <td>D</td> </tr> </table> <p>Texture:</p> <table border="1"> <tr> <td>Sand</td> <td>-</td> <td>1</td> <td>-</td> </tr> <tr> <td>Silt</td> <td>1</td> <td>8</td> <td>Tr</td> </tr> <tr> <td>Clay</td> <td>99</td> <td>91</td> <td>100</td> </tr> </table> <p>Composition:</p> <table border="1"> <tr> <td>Feldspar</td> <td>1</td> <td>Tr</td> <td>Tr</td> </tr> <tr> <td>Heavy minerals</td> <td>Tr</td> <td>-</td> <td>Tr</td> </tr> <tr> <td>Clay</td> <td>94</td> <td>70</td> <td>95</td> </tr> <tr> <td>Carbonate unspc.</td> <td>-</td> <td>10</td> <td>1</td> </tr> <tr> <td>Foraminifers</td> <td>-</td> <td>5</td> <td>-</td> </tr> <tr> <td>Calc. nannofossils</td> <td>5</td> <td>15</td> <td>4</td> </tr> </table> <p>CaCO₃ Bomb (%):</p> <p>1, 12 = 1.0 4, 72 = 16.4</p>		1, 92	2, 60	6, 50	D		M	D	Sand	-	1	-	Silt	1	8	Tr	Clay	99	91	100	Feldspar	1	Tr	Tr	Heavy minerals	Tr	-	Tr	Clay	94	70	95	Carbonate unspc.	-	10	1	Foraminifers	-	5	-	Calc. nannofossils	5	15	4
	1, 92	2, 60	6, 50																																																	
D		M	D																																																	
Sand	-	1	-																																																	
Silt	1	8	Tr																																																	
Clay	99	91	100																																																	
Feldspar	1	Tr	Tr																																																	
Heavy minerals	Tr	-	Tr																																																	
Clay	94	70	95																																																	
Carbonate unspc.	-	10	1																																																	
Foraminifers	-	5	-																																																	
Calc. nannofossils	5	15	4																																																	
				1.0																																																
	FP			2			5G 5/1-5G 6/1																																													
	RP			3			5G 5/1-5G 6/1																																													
	B			4			5G 5/1																																													
	CM			5			5G 5/1-5Y 5/2																																													
	B			6			5G 5/1																																													
	RP			7			5G 5/1																																													

SITE 541 HOLE		CORE 43		CORED INTERVAL 5341.5-5351.0 (mbsl) 390.5-400.0 (mbsf)																															
TIME - ROCK UNIT	BIOSTRATIGRAPHIC ZONE	FOSSIL CHARACTER			SECTION METERS	GRAPHIC LITHOLOGY	DISTURBANCE STRUCTURES	LITHOLOGIC DESCRIPTION																											
		FORAMINIFERS	NANNOFOSSILS	RADIOLARIANS					DIAZONES																										
					0.5			<p>CLAYSTONE and MINOR TUFF</p> <ul style="list-style-type: none"> ● Dominant colors: greenish gray (5GY 5/1), grayish brown (2.5Y 5/2), grayish brown (10YR 4/2), dark grayish brown (2.5Y 4/2), and olive gray (5Y 5/2). Minor colors: dark brown (10YR 4/3), black (5Y 2/1), and dark gray (2.5Y 4/1) tuff. ● Top 40 cm of Section 1 has lumps that probably fell down the hole. Rest has appearance of extensively sheared, tectonically disrupted material. ● Sections 4 and 5 have coherent lumps of material in crumbly matrix. Sections 2, 3, and 6 are pervasively fractured. Upside-down ash Section 6. ● Burrows are prominent on coherent chunks. ● Rotation shear surfaces are abundant and complicate interpretation of original tectonic features. <p>SMEAR SLIDE SUMMARY (%):</p> <table border="1"> <tr> <td></td> <td>2, 60</td> <td>5, 97</td> </tr> <tr> <td>D</td> <td></td> <td>D</td> </tr> </table> <p>Texture:</p> <table border="1"> <tr> <td>Sand</td> <td>Tr</td> <td>Tr</td> </tr> <tr> <td>Silt</td> <td>5</td> <td>Tr</td> </tr> <tr> <td>Clay</td> <td>95</td> <td>100</td> </tr> </table> <p>Composition:</p> <table border="1"> <tr> <td>Quartz</td> <td>2</td> <td>Tr</td> </tr> <tr> <td>Feldspar</td> <td>3</td> <td>Tr</td> </tr> <tr> <td>Heavy minerals</td> <td>Tr</td> <td>-</td> </tr> <tr> <td>Clay</td> <td>95</td> <td>100</td> </tr> </table> <p>CaCO₃ Bomb (%):</p> <p>4, 123 = 2.0 7, 17 = 1.0</p>		2, 60	5, 97	D		D	Sand	Tr	Tr	Silt	5	Tr	Clay	95	100	Quartz	2	Tr	Feldspar	3	Tr	Heavy minerals	Tr	-	Clay	95	100
	2, 60	5, 97																																	
D		D																																	
Sand	Tr	Tr																																	
Silt	5	Tr																																	
Clay	95	100																																	
Quartz	2	Tr																																	
Feldspar	3	Tr																																	
Heavy minerals	Tr	-																																	
Clay	95	100																																	
				1.0																															
				2			10YR 4/2																												
				3			5Y 5/2																												
	B	B	B	4			2.5Y 4/2																												
				5			5GY 5/1																												
				6			5Y 5/2																												
				7			2.5Y 4/1																												
				8			5Y 5/2																												
	B			9			5Y 5/2																												
				10			5Y 5/2																												
				11			5Y 5/2																												
				12			5Y 5/2																												
				13			5Y 5/2																												
				14			5Y 5/2																												
				15			5Y 5/2																												
				16			5Y 5/2																												
				17			5Y 5/2																												
				18			5Y 5/2																												
				19			5Y 5/2																												
				20			5Y 5/2																												
				21			5Y 5/2																												
				22			5Y 5/2																												
				23			5Y 5/2																												
				24			5Y 5/2																												
				25			5Y 5/2																												
				26			5Y 5/2																												
				27			5Y 5/2																												
				28			5Y 5/2																												
				29			5Y 5/2																												
				30			5Y 5/2																												
				31			5Y 5/2																												
				32			5Y 5/2																												
				33			5Y 5/2																												
				34			5Y 5/2																												
				35			5Y 5/2																												
				36			5Y 5/2																												
				37			5Y 5/2																												
				38			5Y 5/2																												
				39			5Y 5/2																												
				40			5Y 5/2																												
				41			5Y 5/2																												
				42			5Y 5/2																												
				43			5Y 5/2																												
				44			5Y 5/2																												
				45			5Y 5/2																												
				46			5Y 5/2																												
				47			5Y 5/2																												
				48			5Y 5/2																												
				49			5Y 5/2																												
				50			5Y 5/2																												
				51			5Y 5/2																												
				52			5Y 5/2																												
				53			5Y 5/2																												
				54			5Y 5/2																												
				55			5Y 5/2																												
				56			5Y 5/2																												
				57			5Y 5/2																												
				58			5Y 5/2																												
				59			5Y 5/2																												
				60			5Y 5/2																												
				61			5Y 5/2																												
				62			5Y 5/2																												
				63			5Y 5/2																												
				64			5Y 5/2																												
				65			5Y 5/2																												
				66			5Y 5/2																												
				67			5Y 5/2																												
				68			5Y 5/2																												
				69			5Y 5/2																												
				70			5Y 5/2																												
				71			5Y 5/2																												
				72			5Y 5/2																												
				73			5Y 5/2																												
				74			5Y 5/2																												
				75			5Y 5/2																												
				76			5Y 5/2																												
				77			5Y 5/2																												
				78			5Y 5/2																												
				79			5Y 5/2																												
				80			5Y 5/2																												
				81			5Y 5/2																												
				82			5Y 5/2																												
				83			5Y 5/2																												
				84			5Y 5/2																												
				85			5Y 5/2																												
				86			5Y 5/2																												
				87			5Y 5/2																												
				88			5Y 5/2																												
				89			5Y 5/2																												
				90			5Y 5/2																												
				91			5Y 5/2																												
				92			5Y 5/2																												
				93			5Y 5/2																												
				94			5Y 5/2																												
				95			5Y 5/2																												
				96			5Y 5/2																												
				97			5Y 5/2																												
				98			5Y 5/2																												
				99			5Y 5/2																												
				100			5Y 5/2																												

SITE 541		HOLE		CORE 44		CORED INTERVAL 5351.0-5360.5 (mbsl) 400.0-409.5 (mbst)		
TIME - ROCK UNIT	BIOSTRATIGRAPHIC ZONE	FOSSIL CHARACTER			SECTION METERS	GRAPHIC LITHOLOGY	CORRELATION DISTURBANCE SEDIMENTARY STRUCTURES SAMPLES	LITHOLOGIC DESCRIPTION
		FORAMINIFERS	MAMMOFOSILS	RADIOLARIANS				
					0.5			CLAYSTONE <ul style="list-style-type: none"> • Dominant colors: grayish green (5GY 5/1), olive gray (5Y 4/2), dark brown (10YR 3/3), dark olive gray (5Y 3/2), dark greenish gray (5GY 4/1), gray to dark gray (5GY 4/2-5/2), olive (5Y 5/3), olive gray (5Y 5/2), gray (5Y 6/1-5/1), and dark gray (5Y 4/1). Minor color: dark green (5G 4/2) spots. • Core has appearance of coherent lumps embedded in sheared matrix with pervasive scaly penetrative deformation. • Nicely burrowed in places.
					1.0		*	SGY 3/1
					2			5Y 4/2
					3			10YR 3/3
					4			5Y 4/2
					5			5GY 4/1
					6			5Y 4/2-5Y 5/2
					7			5Y 5/2
					CC			5Y 5/2 5Y 4/3 5Y 3/1 5Y 4/2
								CaCO ₃ Bomb (%): 4, 123 = 0.5 7, 17 = 1.0
								SMEAR SLIDE SUMMARY (%): 1, 80 8, 47 D D
								Texture: Silt 2 3 Clay 98 97
								Composition: Quartz 1 3 Feldspar 1 Tr Heavy minerals - Tr Clay 98 97 Carbonate unsp. - Tr

SITE 541		HOLE		CORE 45		CORED INTERVAL 5360.0-5370.0 (mbsl) 409.5-419.0 (mbst)		
TIME - ROCK UNIT	BIOSTRATIGRAPHIC ZONE	FOSSIL CHARACTER			SECTION METERS	GRAPHIC LITHOLOGY	CORRELATION DISTURBANCE SEDIMENTARY STRUCTURES SAMPLES	LITHOLOGIC DESCRIPTION
		FORAMINIFERS	MAMMOFOSILS	RADIOLARIANS				
					0.5			CLAYSTONE and MINOR TUFFACEOUS CLAYSTONE <ul style="list-style-type: none"> • Dominant colors: gray (5GY 5/1), olive gray (5Y 4/2), olive gray (5Y 5/2), grayish olive (10Y 4/2), olive (5Y 5/3), dark grayish brown (2.5Y 4/2), and light olive brown (2.5Y 5/3). • Upper part of Section 1 probably is fill in the hole. • Rest of core is divided between sections with coherent chunks in a crumbly matrix and less coherent pieces blending in with pervasively sheared scaly claystone. • Rotation shear surfaces induced by coring have locally disturbed original tectonic fabric. • Bioturbation was originally extensive.
					1.0			5GY 5/1
					2		*	5GY 5/1
					3			5Y 4/2
					4			5GY 5/1
					5			10Y 4/2 5Y 5/2
					6			5Y 4/1
					7			5Y 5/1
					CC			2.5Y 4/2 2.5Y 5/4 10Y 4/2 5Y 5/3 10Y 4/2 5Y 5/3 5GY 5/1 5GY 5/1
								CaCO ₃ Bomb (%): 1, 136 = 0.5 3, 32 = 0.5
								SMEAR SLIDE SUMMARY (%): 2, 60 4, 24 M D
								Texture: Sand 3 1 Silt 20 3 Clay 77 96
								Composition: Quartz - Tr Feldspar 1 1 Heavy minerals - Tr Clay 77 96 Volcanic glass 22 3

SITE 541 HOLE CORE 46 CORED INTERVAL

TIME - ROCK UNIT	BIOSTRATIGRAPHIC ZONE				SECTION METERS	GRAPHIC LITHOLOGY	DRILLING DISTURBANCE SEDIMENTARY STRUCTURES	SAMPLES	LITHOLOGIC DESCRIPTION
	FORAMINIFERS	NANNOFOSSILS	RADIOLARIANS	DIAZONES					
	B	B	B		1			CLAYSTONE ● Drilling breccia. Shattered mudstone, olive gray (5Y 4/2). Largest piece 5 cm long.	
	B			0.5	CC				

SITE 541 HOLE CORE 47 CORED INTERVAL

TIME - ROCK UNIT	BIOSTRATIGRAPHIC ZONE				SECTION METERS	GRAPHIC LITHOLOGY	DRILLING DISTURBANCE SEDIMENTARY STRUCTURES	SAMPLES	LITHOLOGIC DESCRIPTION
	FORAMINIFERS	NANNOFOSSILS	RADIOLARIANS	DIAZONES					
			B		0.5			CLAYSTONE and MINOR RADIOLARIAN MUDSTONE ● Cavings from top of core to Section 2, 45 cm. Below that, brecciated and silty yellowish brown (10YR 5/4) radiolarian mudstone with dark brown (10YR 3/3) and yellowish brown (10YR 5/4) mudstone. Distinction between claystone and radiolarian mudstone difficult to make based on visual appearance.	
				1.0					
	B	B			2			SMEAR SLIDE SUMMARY (%): 2, 82 D Texture: Silt 3 Clay 97 Composition: Quartz 1 Feldspar 2 Heavy minerals Tr Clay 97 CaCO ₃ Bomb (%): 1, 32 = 0.5 2, 131 = 0.0	
	B		VR/ VP	3	CC				

SITE 541 HOLE CORE 48 CORED INTERVAL

TIME - ROCK UNIT	BIOSTRATIGRAPHIC ZONE				SECTION METERS	GRAPHIC LITHOLOGY	DRILLING DISTURBANCE SEDIMENTARY STRUCTURES	SAMPLES	LITHOLOGIC DESCRIPTION
	FORAMINIFERS	NANNOFOSSILS	RADIOLARIANS	DIAZONES					
early Miocene					0.5			2.5Y 5/2 5Y 4/1 6GY 5/1	CLAYSTONE, RADIOLARIAN CLAYSTONE, and MINOR ASH ● Dominant colors: brown (10YR 4/3), dusky yellow green (5GY 5/2), grayish brown (2.5Y 5/2), light yellowish brown (10YR 6/4), gray (5GY 5/1), yellowish brown (10YR 5/4), dark grayish brown (2.5Y 4/2), greenish gray (5Y 5/1), grayish green (10GY 5/2), gray (5YR 5/1), and olive (5Y 5/3). Minor colors: dark gray (5Y 4/1) (ash), and brown (7.5YR 5/2) and light yellowish brown (10YR 6/4) (burrows). In summary, variegated. ● Core appears as coherent lumps (grayish and greenish) in pervasively sheared-out matrix. Radiolarians more abundant in lower sections where colors are more to yellows and olives.
					1.0				
					2	VOID		2.5Y 5/2	
					3	VOID		10YR 5/4	
				VR/ VP	4	PP		5Y 5/1	
				B	5	IW		2.5Y 5/4	
Calocyclotza contrast zone Riedel and Santilippo 1978			B	6			10YR 6/4		
			B	7			2.5Y 5/2		
				8			5Y 5/2		
				9			2.5Y 5/4		
			AM	10			5Y 5/3		
			AM	11			10YR 6/4		
			AM	12					
			CC	13					

SMEAR SLIDE SUMMARY (%):
1, 30 D
1, 130 D
3, 77 D
4, 93 D
Texture:
Sand 1 10 3 10
Silt 5 10 5 20
Clay 94 80 92 70
Composition:
Quartz 2 3 2 1
Feldspar 5 5 3 2
Clay 63 32 75 66
Calc. nannofossils - - - -
Radiolarians - - - - 1
5, 20 D
6, 95 D
CC, 20 D

Texture:
Sand 2 - 1
Silt 8 5 3
Clay 90 95 96
Composition:
Quartz 1 1 2
Feldspar 2 3 3
Clay 70 91 80
Volcanic glass 25 5 5
Calc. nannofossils - - Tr
Radiolarians 2 Tr 10

CaCO₃ Bomb (%):
1, 105 = 0.5
3, 63 = 0.0

